Student thesis series INES nr 362

Analysis of NDVI variation and snowmelt around Zackenberg station, Greenland with comparison of ground data and remote sensing

Georgios-Konstantinos Lagkas

2015
Department of
Physical Geography and Ecosystems Science
Lund University
Sölvegatan 12
S-223 62 Lund
Sweden

Georgios-Konstantinos Lagkas (2015). ***Analysis of NDVI variation and snowmelt around Zackenberg station, Greenland with comparison of ground data and remote sensing***
Master degree thesis, 30 credits in *Geomatics*
Department of Physical Geography and Ecosystems Science, Lund University

Level: Master of Science (MSc)

Course duration: *January 2015* until *June 2015*

Disclaimer

This document describes work undertaken as part of a program of study at the University of Lund. All views and opinions expressed herein remain the sole responsibility of the author, and do not necessarily represent those of the institute.

Analysis of NDVI variation and snowmelt around Zackenberg station, Greenland with comparison of ground data and remote sensing

---

Georgios-Konstantinos Lagkas

Master thesis, 30 credits, in *Geomatics*

Supervisor Andreas Persson, PhD Associate professor
Department of Physical Geography and Ecosystem Science

Exam committee:
Lars Eklundh, PhD Professor
Department of Physical Geography and Ecosystem Science

Margareta Johansson, PhD Researcher
Department of Physical Geography and Ecosystem Science

In loving memory of my brother Vasilis,
whom I will always respect, admire and miss

ABSTRACT

Snow and permafrost are significant climatic factors affecting the climate in high latitudes and especially in arctic regions. Moreover, results of conducted scientific studies have shown that snow is crucial for photosynthetic activity and therefore vegetation vigor and growing season in arctic environments.

This master thesis aims to investigate the changes in photosynthetic activity in Zackenberg, located in the eastern coast of Greenland with estimation of the fluctuation of the normalized vegetation index (NDVI) from satellite images and the changes in snowmelt and active layer thickness with the study of ground data obtained by scientific measurements conducted in the established research station of Zackenberg.

Moreover, this study tries to relate the variations in photosynthetic activity expressed by the vegetation index with snow depth and length of snow season, as well as with properties of permafrost, like the thickness of the active layer. The time period for which this study is conducted includes the last 10 years, between 2005 and 2014. Analysis is performed with the help of statistics and by using principles of regression analysis.

Results show fluctuations in photosynthetic activity as well as in the duration of the growing season. Furthermore, correlations between snow depth and time of snowmelt (expressed by snow cover percentage) and photosynthetic activity are detected from the regression analysis, showing that snow depth and time of snowmelt affect the seasonal vegetation activity and enhancing the argument on the importance of snow for the high northern latitudes. On the other hand, results from the regression analysis show that photosynthetic activity is not affecting the active layer thickness.

Keywords: geography, physical geography, Greenland, Zackenberg, NDVI, growing period, snow, active layer, statistical analysis, regression analysis

FOREWORD – ACKNOWLEDGMENTS

The current master thesis elaborates as part of my studies in the Department of Physical Geography and Ecosystem Science, Lund University, finalizing my master program in Geomatics and I would like to acknowledge Lars Eklundh for initially suggesting the thesis topic.

As I complete my studies in Lund University I would like to take the opportunity to thank the professors of the department and the laboratory assistants for their help throughout my studies. Especially I would like to thank my supervisor, Andreas Persson for his guidance, advice and comments on my work.

Special acknowledgment goes to GeoBasis program for data and metadata that were used in this master thesis. Additional data from the Greenland Ecosystem Monitoring Program were provided by the Department of Bioscience, Aarhus University, Denmark in collaboration with Department of Geosciences and Natural Resource Management, Copenhagen University, Denmark.

More in particular, I acknowledge Magnus Lund and Kirstine Skov at the Department of Bioscience, Aarhus University Denmark for their collaboration and for providing useful additional data and information.

In addition, I would like to take the opportunity to thank my classmates for the collaboration and exchange of opinions regarding our studies as well as mutual exchange of cultures, flavors and ideas.

Moreover, I want to thank my parents and sister for their support and last but not least I would like to express my gratitude to "Bakalas foundation" in my home country Greece, for financially supporting and granting my studies in Sweden with a scholarship.

Georgios-Konstantinos Lagkas

August 2015

CONTENTS

LIST OF TABLES

LIST OF FIGURES

LIST OF ACRONYMS

aka	also known as
ACIA	Arctic Climate Impact Assessment
ASCII	American Standard Code for Information Interchange
CALM	Circumpolar Active Layer Monitoring
CAVM	Circumpolar Arctic Vegetation Map
DOY	Day Of Year
DEM	Digital Elevation Model
EGP	End of Growing Period
ESRI	Environmental Systems Research Institute
GEM	Greenland Ecosystem Monitoring
GIS	Geographic Information Systems
GPR	Ground Penetrating Radar
IDE	Integrated Development Environment
IPCC	Intergovernmental Panel on Climate Change
LGP	Length of Growing Period
LIDAR	LIght Detection And Ranging
MODIS	MODerate-resolution Imaging Spectroradiometer
N	North
NAO	North Atlantic Oscillation
NASA	National Aeronautics and Space Administration
NDVI	Normalized Difference Vegetation Index
NIR	Near Infra-Red
PAR	Photosynthetically Active Radiation
PDF	Probability Density Function
PGP	Peak of Growing Period
SGP	Start of Growing Period
R	Reflectance
RGB	Red Green Blue
RSE	Residual Standard Error
SWIPA	Snow, Water, Ice and Permafrost in the Arctic
TIN	Triangulated Irregular Network
UTM	Universal Transverse Mercator
USGS	United States Geological Survey
VI	Vegetation Index
vs.	versus
W	West
WGS	World Geodetic System
ZC1	ZeroCalm1
ZC2	ZeroCalm2
ZERO	Zackenberg Ecological Research Operations

1. INTRODUCTION

1.1. OVERVIEW

During the last thirty years, scientific community is concerned that the world's climate is changing due to human activities (Houghton et al. 1990; ACIA 2005; Letcher 2009; Cowie 2013). Arctic regions will not remain intact from such a scenario (Maxwell 1992; IPCC 2007, 2013). According to IPCC (2007)*"such change will take the form of a significant global warming, which is expected to be most pronounced at the polar latitudes"*. The drastic changes that arctic climate has suffered during the last century have led in changes in meteorological aspects, namely temperature and precipitation, and these changes are highly likely to lead to alteration in snow cover and sea/ ice coverage (Rasch et al. 2012). The 2014 Arctic report card stresses that temperature in the arctic is rising rapidly compared to the rest of the earth and this will lead to continuing changes in arctic regions (Jeffries et al. 2014).

Targeting in monitoring and studying the expected changes and their influence on the ecosystems, a large number of continuously monitoring research programs have been established in various stations located in polar region areas and researchers are constantly or periodically gathering information about climate and atmospheric variables (Huettmann 2009). Ground measurements of climate variables, as well as satellite data can provide a measure of environmental variables that can assist researchers, scientists and stakeholders to conclude whether the climate system and photosynthetic activity are stable or changing with time.

According to Hansen et al. (2008) the extreme climate of the arctic is one of the most crucial components of the world's climate system, while according to 2014 Arctic report card the snow cover extent in Eurasia was the lowest in the last fifty years and almost 40% of Greenland's ice sheet experienced melting conditions (Jeffries et al. 2014).

Snow is a main characteristic of arctic landscape and one of the factors affecting the climate and the ecosystems in the Arctic zone, as the majority of the precipitation in the arctic zone falls as snow (Buus-Hinkler et al. 2006; Callaghan et al. 2011). It affects not only the photosynthetic activity of the plants, hence the net plant production (Walker et al. 1993; Høye et al. 2007), but also the length of the growing period within the year (Walker et al. 1999; Post et al. 2009; Elmendorf et al. 2012; Bosiö et al. 2014). In addition, apart from being the significant characteristic of the areas around the Arctic Circle like Greenland, snow cover is also important for the hydrological system of these areas as it is the main regulating natural force of the arctic ecosystems (Jones 1999; Gacitúa et al. 2013; Bosiö et al. 2014).

The “state of the art” in the research, as will be more thoroughly presented in the “Background” chapter, is the recognition of variation in photosynthetic activity in Greenland and more in particularly in the area of Zackenberg research center as well as possible changes and trends in the relations between the results of research activities in the island of Greenland and arctic areas regarding snow, active layer thickness and vegetation growth properties.

The motivation for the use of these parameters is to contribute to the knowledge and findings of previous studies conducted in Zackenberg and other arctic areas (Meltofte and Rasch 2008; Elberling et al. 2008a; Gacitúa et al. 2013; Gangodagamage et al. 2014), that emphasize on the interaction between snow and active layer with vegetation.

1.2. OBJECTIVES- RESEARCH QUESTIONS

This master thesis has two main objectives, which are the investigation of variation in photosynthetic activity in Zackenberg, northeastern Greenland during the last ten years and the detection of possible correlation between the photosynthetic activity that can be monitored by available satellite imagery and properties of snow and top permafrost (active layer) as measured in the research station for this ten-year period.

The first objective will be to look at trends in the photosynthetic activity between years and within the growing period (late spring- early fall) with the help and use of NDVI, an index used to detect variations in photosynthetic activities from observations of satellite images, as well as the detection of inter-annual and intra-annual variations in the photosynthetic activity, in order to derive conclusion about the growing seasons (starting, peak and end of growing season, length of growing season).

The first research question is: *How does NDVI in Zackenberg, Greenland vary between the years 2005-2014 and what changes can be detected in the growing period based on the NDVI observations?*

The second objective will be the detection of possible relations between photosynthetic activity and snow and active layer from secondary data that are provided by the Greenland monitoring program.

The second research question is the following: *Is there a relationship between NDVI and snow and the active layer variation in Zackenberg, Greenland; do snow depth and snow cover in the beginning of the growing season affect photosynthetic activity throughout the growing season and does photosynthetic activity affect the thickness of active layer?*

2. BACKGROUND

2.1. GREENLAND

Greenland is the world's largest non-continental island, covering an area of more than two million km^2, lying between two oceans, Arctic and Atlantic. According to Meltofte and Rasch (2008) the biggest part of the island (about 82%) is covered by a permanent ice pack, surrounded by an area free of ice, forming valleys and fjord systems. The population of the island is approximately 56000 inhabitants that mainly live on the southwest coast, towards Canada (Perdersen et al. 2006; Kjærgaard 2015).

Global climate is mainly described by the large scale climatic patterns, namely the El Nino Southern Oscillation, the North Atlantic Oscillation (NAO) and the North pacific Oscillation (Forchhammer et al. 2008). According to Hurrell (1995) Greenland´s climatic variables can be highly associated with NAO and Bamzai (2003) stresses the correlation between the inter annual variability of the snow properties in the northern hemisphere, such as the number of free-of-snow days per year and snow-melt and the NAO parameters' variance.

The most common division of the arctic climate is between high and low arctic and is based on the mean temperature of the warmest month, with $+6^o$ C being the division limit (Meltofte and Rasch 2008). Furthermore, according to CAVMTeam (2003) this division is usually based on floristic characteristics. Central and southern Greenland is characterized by low arctic climate, while the climate in northern part of the island is high arctic.

Tundra is the common biome type in the ice-free areas of the arctic landscapes; high arctic lowland areas of Greenland are in generally much more sparsely vegetated, covered with short vegetation that does not exceed 20 cm. Large non-vegetated barren areas are present in the northern part of the island. On the contrary, in low arctic Greenland the vegetation is more shrubby and it can even reach 50 cm of height (Meltofte and Rasch 2008).

2.2. STUDY AREA OF ZACKENBERG RESEARCH STATION

Meteorological research stations are settled across the globe in order to assist in studies associated with climate changes. According to ACIA (2005) meteorological stations network across the Arctic -hence in Greenland- is quite sparse and Mernild et al. (2007) point out that snow distribution, snow depletion and glacier melt measurements are not extensive due to the terrain, hard weather conditions and remote locations of the arctic catchments.

Zackenberg research station is located within the Zackenberg valley[1], 74^o 28' N, 20^o 34' W, within the Northeast Greenland national park, in high arctic northeast Greenland. It is located approximately 25 km north of the branch research facilities in Daneborg. It was established in 1995, with the main mission to facilitate ecosystem research in the high arctic (Zackenbergsecretariat 2013). It is been run under the authority of the government of Greenland and operated by Aarhus University (Department of Bioscience). The study area of the research center includes the valley and the Zackenberg river drainage basin (Zackenbergsecretariat 2013). Zackenberg drainage basin has an extent of 512 km^2, of which approximately 20% is covered by ice and glaciers (Rysgaard et al. 2003). Climate, soil, hydrology, geomorphology and flux parameters have been measured since the establishment of the research station. The map in Figure 1 shows the location of Zackenberg within Greenland as well as the Zackenberg drainage basin and Musk ox study area, where most of the research is carried out.

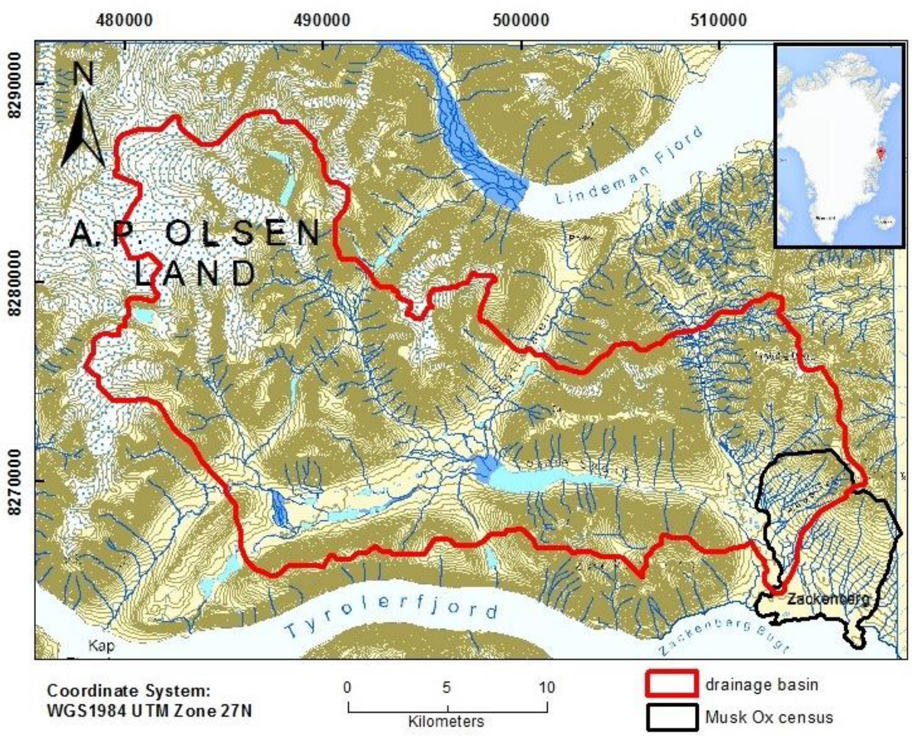

Figure 1: *Zackenberg research station study area and drainage basin (base map adopted from ZERO webpage-http://zackenberg.dk/; Greenland's map downloaded from Google maps https://www.google.se/maps/).*

[1] Zackenbergdalen in Danish.

In accordance with the topography of non-glaciated Greenland, the study area of Zackenberg is characterized by intense topography with mountains and valleys, whereas some peaks can reach up to 1500 m. Fjords are also a significant geomorphological characteristic of the area.

According to Meltofte and Rasch (2008) the climate is high arctic. Like most high arctic regions, Zackenberg is covered with snow during most of the year, so only a limited time-window allows a free of snow surface, when vegetation can grow.

The annual mean temperature has a slight increasing trend during the years 1996-2013. Figure 2 shows the mean annual air temperature in Zackenberg, based on the statistics from ZERO's 2014 annual report (Jensen et al. 2014).

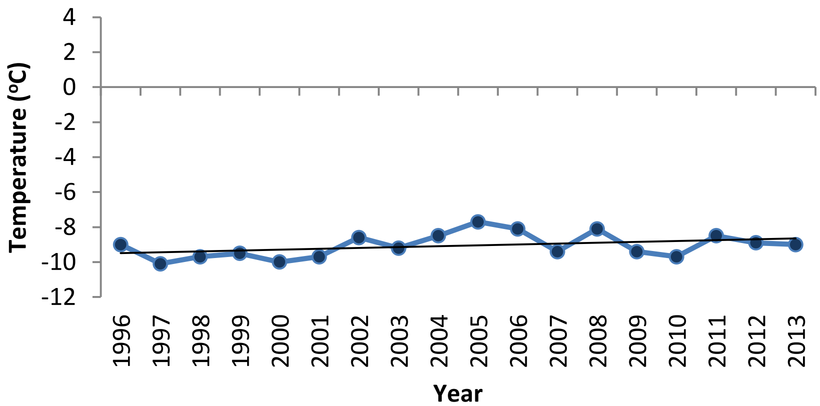

Figure 2: *Mean annual temperature in Zackenberg (graph created using data from Jensen et al. 2014).*

According to CAVMTeam (2003) Circumpolar arctic vegetation map, the area is characterized by a combination of tundra and mountainous flora environment; the vegetation in the coastal part of Zackenberg is mainly described as prostrate and hemi-prostrate dwarf-shrub tundra, a relatively dry environment with very low bushes, which can develop up to 15 cm tall, while inlands mountainous vegetation prevails. Vegetation types that are met in the study area are mostly fens, grasslands and shrubs, as well as vascular and low vascular plants (Bay 1998; Elberling et al. 2008b; Gacitúa et al. 2013). Figure 3 is a land cover map that shows the vegetation distribution in the study area.

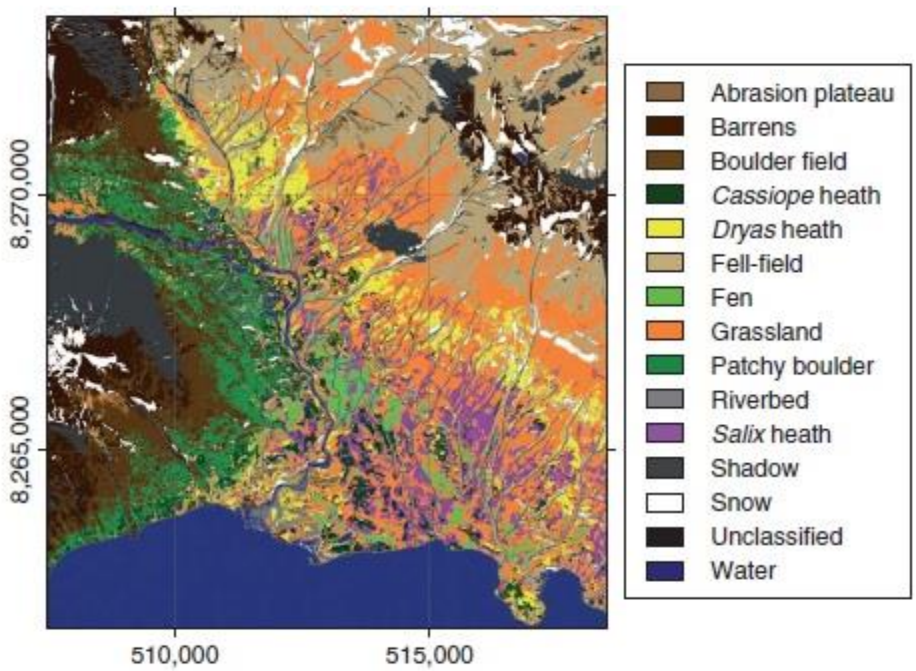

Figure 3: *Land cover map describing the vegetation in the study area (Elberling et al. 2008b).*

Most scientific missions and studies in the area are carried out within the valley of Zackenbergdalen, in the area shown in Figure 1, where the research station is situated. *GeoBasis* is a sub-program of Zackenberg Basic program, established in 1995 and running under the umbrella of Greenland Ecosystem Monitoring (GEM) program, which is an integrated monitoring and long-term research on ecosystems and climate change effects and feedbacks in the arctic consisting of five different sub-programs (Rasch et al. 2012; Zackenbergsecretariat 2013). GeoBasis' mission is the collection of meteorological, hydrological and terrestrial data, such as snow and permafrost, precipitation, geomorphological data, and flux monitoring (Jensen et al. 2014). The main study period begins in late May or early June and finishes in late August or early September, though there are occasions when the study period was extended (Sigsgaard et al. 2014). All the ground measurements of snow and active layer properties used in this thesis were collected for the purposes of GeoBasis monitoring program.

The main research area (and study area of this thesis "Musk ox census") is divided in regions numbered from 1 to 12, which are presented in Figure 4. Measurements of snow properties -namely snow cover- are available for zones 10 and 11, as well as for the central area and for the whole study area of Musk ox census[2]. Snow cover is measured with the use of digital cameras, as it will be thoroughly discussed in chapter 2.5. The dark grey colored part in the image depicts the area that is covered by digital cameras

[2] Only the measurements that refer to the whole study area were used in this thesis.

(approximately 86% of the study area), while the gapped areas in the map are the ones not covered by the cameras.

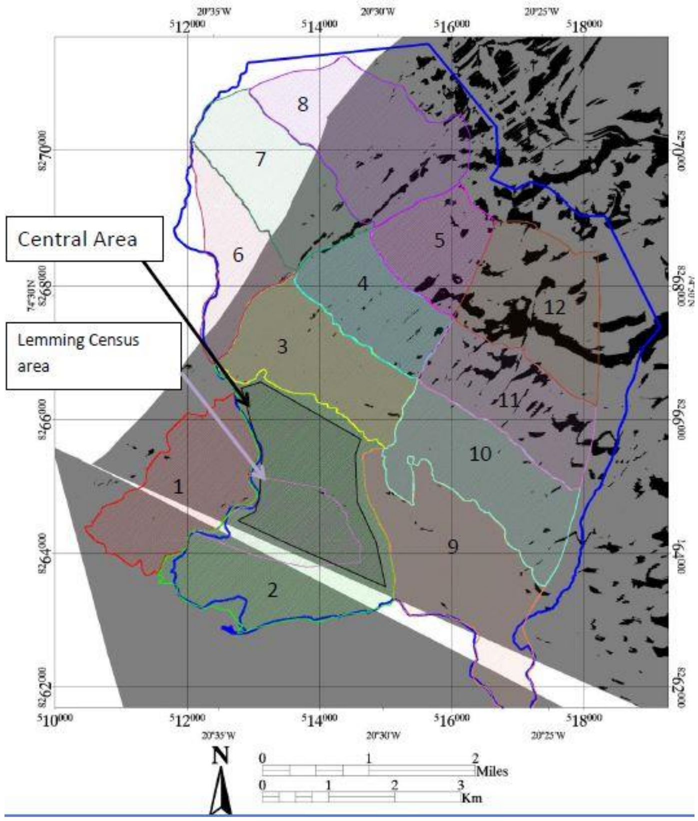

Figure 4: *Musk ox census main study area showing the delimited regions and the part of the study area that is covered by the digital cameras (from GEM database http://data.g-e-m.dk).*

2.3. NDVI

NDVI - Normalized Difference Vegetation Index (Kriegler et al. 1969; Tucker 1979) is an index, that helps monitoring the photosynthetic potential of vegetation, with the use of remote sensing data and satellite image interpretation.

The use of the index for detecting vegetation lies in the significant property of well-developed, healthy vegetation to reflect highly within the near- infrared. NDVI relates the visible and the near-infrared reflectance of the different features on the earth's surface and helps in the assessment of the (non)/existence of vegetation in the area of interest.

The NDVI is defined as follows:

$$NDVI = \frac{R(NIR) - R(red)}{R(NIR) + R(red)}$$

where:

R(NIR) is the spectral reflectance[3] that is measured in the near-infrared part of the electromagnetic spectrum and R(red) the spectral reflectance measured in the visible (and more in particularly in the red part) of the electromagnetic spectrum.

NDVI value varies from -1 to 1. Values that are close to 0 (positive or negative) indicate surfaces that are rocky or covered with sand and snow and negative or zero NDVI indicates that there is no vegetation (Lillesand et al. 2004; Crawford 2008).

According to Lillesand et al. (2004) *"the normalized difference vegetation index is preferred to the simple index[4] for global vegetation monitoring because the NDVI helps compensate for changing illumination conditions, surface slope, aspect, and other extraneous factors"*.

NDVI data are strongly correlated with the fraction of photosynthetically active radiation (wavelength 0.4 – 0.7 μm) absorbed by vegetation (Asrar et al. 1984). Very often, NDVI is used in comparison with ground measurements to derive useful vegetation properties, such as the biomass, the leaf area index (LAI), accumulated rainfall, etc.

2.4. SNOW AND THE RELATION WITH VEGETATION AND NDVI

Arctic ecosystems are characterized by low air and soil temperatures, permafrost, short growing season and limited vegetation productivity (Stow et al. 2004) and they are extremely sensitive to disturbances, therefore respond rapidly to climate changes (Reynolds and Tenhunen 1996).

According to Hinkler et al. (2008) snow is the main cryospheric parameter, due to its spatial extent, while in the same time, as SWIPA report signalizes, it is the component of cryosphere that is changing more rapidly, hence is more difficult for its properties to be measured (Callaghan et al. 2011). Groisman et al. (1994) stress out the importance of snow to the heat balance of the earth's surface, as it affects the earth's albedo and the out-going long-wave radiation.

Snow is characterized by its ability to reflect the incoming solar radiation, and due to this high reflectance, particularly in the visible and the near infra-red wavelengths of the electromagnetic spectrum, it can be easily detected in satellite images. Jönsson et al. (2010) state that snow changes the surface reflectance, while according to Hinkler et al.

[3] Spectral reflectance is the ratio (normalization) of the radiance by the irradiance in order to compensate for the different amount of incoming light and to have comparable measurements.
[4] Simple index VI = R(NIR) - R(red)

(2008) totally snow covered areas can reflect up to 80-90 percent of the incoming solar radiation[5], while snow-free surfaces have the ability to reflect only around 10-20 percent. Hansen et al. (2008) stress out that albedo in Zackenberg decreases rapidly from 80 to 10 percent, when the snow disappears, while during the summer period, when the land in tundra vegetated areas becomes dry, a small increase to 15% is been observed.

According to Hinkler et al. (2008) and Groisman et al. (1994) snow has two main properties, namely high emissivity (especially of long wave radiation) and high insulation, therefore the surface temperature is strongly correlated with snow cover. These two properties of snow are very important, since emissivity may cause low temperature in the surface of snow, but on the other hand high insulation acts like a shield protecting the flora and fauna that is lying beneath the layer of snow.

Analysis and estimation of NDVI in higher latitudes is without doubt complicated due to the almost permanent presence of snow. Snow cover affects the growing season and hence NDVI, since according to Belzile et al. (2001) *"the effects of ice and snow cover on radiative transfer also regulate biological productivity by controlling PAR"*.

There is controversy on the scientific outcomes about NDVI fluctuation in the northern high latitudes. Myneni et al. (1997) suggest that the changes in NDVI are not significant in the Arctic. However, most studies based on satellite data agree that photosynthetic activity in large areas of the northern hemisphere and in latitudes between 45^o and 70^o has generally been increased (Tucker et al. 2001; Zhou et al. 2001; Xu et al. 2013). According to Tucker et al. (2001) the increase was only interrupted during the period 1991-1992, due to the volcanic eruption of Pinatubo.

Another parameter that is also worthy to be mentioned is that there is a fundamental problem in remote sensing analysis in high latitudes, since the reflectance of snow and ice covered areas in the visible wavelength bands of the electromagnetic spectrum is the same as the reflectance of clouds. For this reason Hansen et al. (2008) stress that the discrimination between clouds and ice/snow through satellite images can be rather cumbersome.

Vegetation strength in the high arctic is highly dependent on the duration of the snow-free period as well as the magnitude of the snow cover. Seasons with more extensive snow-free period and less snow cover lead to more vigorous vegetation and vice versa. In fact, as Buus-Hinkler et al. (2006) state, this dependence seems to be more significant than the influence of temperature to the vegetation. According to other studies vegetation vigor in the arctic regions is not only dependent on the snow cover of the same growing season, but also on the previous year's conditions (Bliss and Gold 1999). This means

[5] Reflected solar radiation is also known as albedo.

that a winter with low snowfall can have an impact not only on the vegetation strength and therefore NDVI of the upcoming summer period, but also on the next summer period, one year later.

2.5. SNOW MONITORING IN ZACKENBERG

Precipitation varies significantly in Greenland, from around 25 mm/year in the interior arctic desert to around 2500 mm/year in the southernmost part. According to Jensen et al. (2014) annual mean precipitation in Zackenberg varied from 93 to 254 mm/year for the period between 2005 and 2013. Snow is the main precipitation carrier in the arctic areas and especially the properties of snow depth and snow cover are very important for the arctic ecosystem (Gacitúa et al. 2013; Bosiö et al. 2014; Sigsgaard et al. 2014).

Zackenberg area is covered with snow most of the year. Snowfall starts in early September and the melting will only start in late May, so that by August the least snow-cover can be observed (Hinkler et al. 2008). Since the research station is open only during the summer period, measurements of snow start after May and there have not been any studies regarding snow accumulation.

The meteorological station is located in the remnants of a meltwater plain. There are five permanent automatic weather stations that continuously give information about snow depth by measuring the distance to the snow/soil surface from a fixed point using a Sonic Ranging Sensor (Sigsgaard et al. 2014). Snow depth is also measured manually in two grid nets and along two transects, with the help of a MagnaProbe or a Ground Penetrating Radar (GPR)[6].

Snow cover is monitored with the help of digital images and models of depletion curves as well as snow cover statistics, produced with the help of a specially designed algorithm (Hinkler et al. 2002; Hinkler et al. 2008). Three digital cameras are placed permanently since 1998 on three platforms at the top of Nanseblokken, a rock at the eastern part of Zackenberg, approximately in an elevation of 500 m above sea level (Hinkler et al. 2008; Jensen et al. 2014). The cameras are placed in waterproof boxes. Two of them are conventional RGB cameras, while the third one is multispectral (R,G,NIR). The covering of the main study area is daily and only around 14% of the Musk ox census study area is not covered by the cameras, as mentioned earlier.

Images taken by the camera have been mosaicked and orthographically rectified and transformed in digital orthophotos with a 10*10 m resolution, from which binary snow-cover maps are created with the help of a specially developed algorithm (Hinkler et al.

[6] GPR portrays what lies beneath the surface using radar pulses from the microwave part of the electromagnetic radiation.

2002; Hinkler et al. 2008). Figure 5 is an example of a mosaic from which the orthophotos are been created.[7]

Figure 5: *Mosaic of the photos from which orthophotos are created (Sigsgaard et al. 2014).*

2.6. ACTIVE LAYER MONITORING IN ZACKENBERG

Most studies agree that active layer changes in areas of high latitude are significant indicators of climate change (Christiansen et al. 2008). Permafrost (also known as cryotic soil) is defined in geology as soil, where the ground temperature remains below 0^{o} C, continuously for two years or more and the thickness of the permafrost layer is a function of the internal heat from the ground and the loss of heat from the ground (French 2007).

According to the categorization map for the circumpolar permafrost (Brown et al. 1998, revised February 2001) Zackenberg belongs to the continuous permafrost zone. Christiansen et al. (2008) state that the permafrost condition in Greenland has not been thoroughly investigated, however the depth of permafrost in Zackenberg is estimated to be 400 m thick.

Active layer is also a subject of scientific research for the GeoBasis project. Active layer refers to the upper layer of soil, on top of permafrost, that thaws in the summer and only when the surface is free of snow and the temperature in the air is above 0^{o} C and freezes again when summer ends (Christiansen et al. 2008; Jensen et al. 2014). The thickness of active layers depends on various parameters, meteorological, geomorphological, physical and thermal properties of the surface and vegetation cover (Gangodagamage et al. 2014; Oht 2003). Two monitoring sites of active layer are situated in the lowest part of Zackenberg valley study area, in close distance from the sea.

Research on the monitoring of active layer in Zackenberg and active layer models has shown that active layer's thickness is generally increasing. According to Christiansen et

[7] GeoBasis' orthophotos and snow cover maps were not used in this study.

al. (2008) the results of active layer measurements from the two ZeroCALM stations show an increase in the active layer within the time period 1996-2005 of 19 cm in ZeroCALM 1 and 8 cm in ZeroCALM 2, respectively. Furthermore, Elberling et al. (2013) conclude that within the period 1996-2012, the active layer thickness in Zackenberg has been increasing between 0.8 cm per year in the mountainous part and 1.5 cm per year in the valley.

Furthermore, a model that was run in the period September 1996- August 1997 (model Virtual World for Windows - VW4W) showed that permafrost was between 200 and 300 m in the Zackenberg valley and between 300 and 500 m thick in the mountainous areas around the valley (Christiansen et al. 2008). As for the active layer thickness, it was estimated between 0,40 and 0,65 m in the valley and between 0,3 and 0,5 m in the mountainsides (Christiansen et al. 2008). Finally, a scenario developed by Killsholm predicts an increase between 8 to 30 cm in the thickness of the active layer for Zackenberg area during the 21st century (Kiilsholm et al. 2003).

3. METHODS

3.1. STUDY AREA

The study area for this master thesis covers the “Musk Ox census” site. Musk ox census is located in the southernmost part of Zackenberg valley with vicinity to the sea and a total area of approximately 47 km^2. The area consists of part of the Zackenberg valley and extents up to the slope of mountain Aucella to the north. The topography is quite intense, ranging from the sea level up to 900 m elevation.

The choice of the study area is based on the fact that Zackenberg is one of the few high arctic sites for which research infrastructure exists and data are available. All the ground measurements of snow properties and active layer depth, performed by the Zackenberg research center for the GeoBasis monitoring program, are carried out within the boundaries of Musk Ox census. Moreover, this is the area covered by the digital cameras. Figure 6 shows a close view of Musk Ox census with 25 m contour lines.

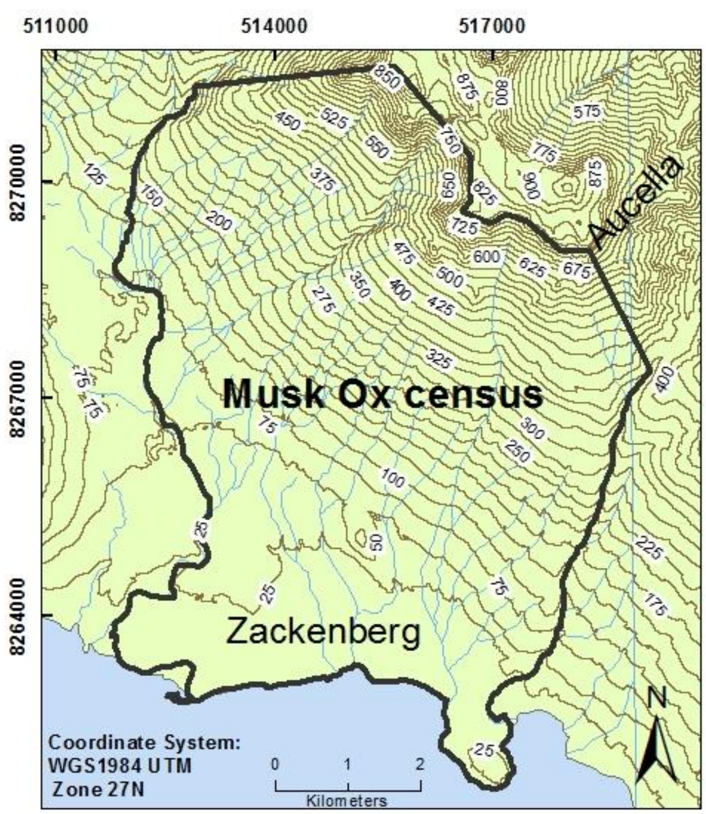

Figure 6: *Thesis’ study area (Musk Ox census)*

3.2. AVAILABLE DATA

The data that were used for the analysis can be separated into three main categories:

- Ground truth data from Zackenberg research center
- Geographical data of the study area
- Satellite imagery data

3.2.1. Geographical data

The geographical data consist of data that were either available for downloading from GeoBasis webpage (zackenberg.dk/monitoring/geobasis/) or asked from and retrieved by the Department of Bioscience, Aarhus University. They are shapefiles depicting the main geographical features of the area as well as shapefiles of the boundaries of the Musk ox census study area. Table 1 lists the available geographical data for this study.

Table 1: *List of geographical data*

No	Description	Source	Data format
1	coastline	ZERO GeoBasis	shapefile
2	rivers	ZERO GeoBasis	shapefile
3	lakes	ZERO GeoBasis	shapefile
4	25 meters contours	ZERO GeoBasis	shapefile
5	Musk Ox census area *(thesis study area)*	Aarhus University	shapefile

3.2.2. Ground truth data

The ground truth data used in this study were found available for downloading from the GEM online database (g-e-m.dk) and contain the following datasets:

Active layer: The active layer depth monitoring is carried out in two sites located in the southwestern part of the study area situated in well-drained heath, named ZeroCalm1 and ZeroCalm2 (Jensen et al. 2014). The two sites are rectangular grid nets and measurements are taken in the grid points of these nets. ZC1 covers an area of 100 by 100 meters, while ZC2 covers an area of 120 by 150 meters (Sigsgaard et al. 2014). Measurements are performed manually using a metal rod and they start when the grid points are free of snow. Measurements are conducted weekly. The location of the two CALM stations and their grid structure can be seen in Figure 7.

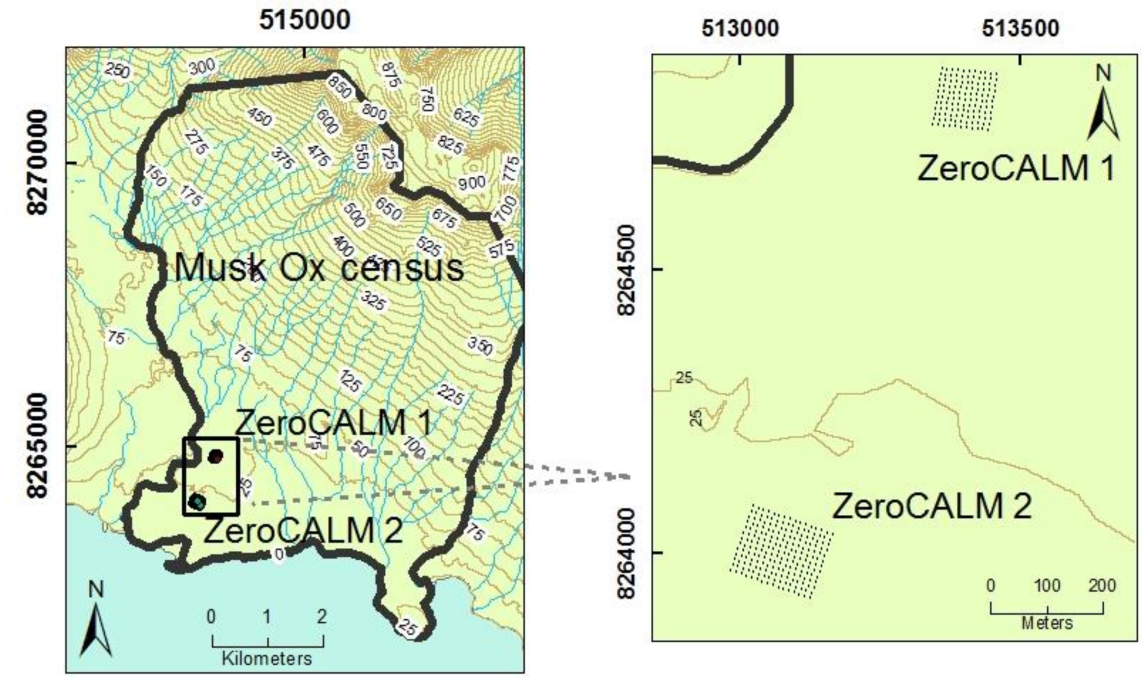

Figure 7: *Location and structure of the active layer thickness monitoring (ZeroCALM 1 & 2).*

Snow cover: Snow cover is computed using the photographs taken by the three automatic cameras that are placed in the Zackenberg slope. The photos are orthorectified and mosaicked, and the snow cover is computed based on these images using a classification algorithm for the whole study area of Musk Ox census, which is visible by the cameras, but also for sub-areas. The data contain total snow cover percentage for the study area, measured approximately two or three times per week and they are provided in excel tables.

Snow depth: Snow depth is measured daily during the snow cover period in late spring and early summer. The measurements are performed mainly along two transects located within the study area of Musk Ox census. SNZ transect that stretches from the coastline to the top of Aucella slope with south-west to north-east direction and SNM transect, which is located in the central part of Zackenberg valley with direction from South to North. Measurements are taken also in the ZeroCALM plots. In addition, measurements are also carried out automatically from the five snow depth masts. However, two of the stations are located far outside the boundaries of the study area. The measurements are provided in excel tables in the GEM database webpage and the coordinates of the points where snow depth is measured are provided in geographic coordinates. Figure 8 shows the two transects where snow depth has been measured as well as the locations of the three masts, which are within the study area boundaries.

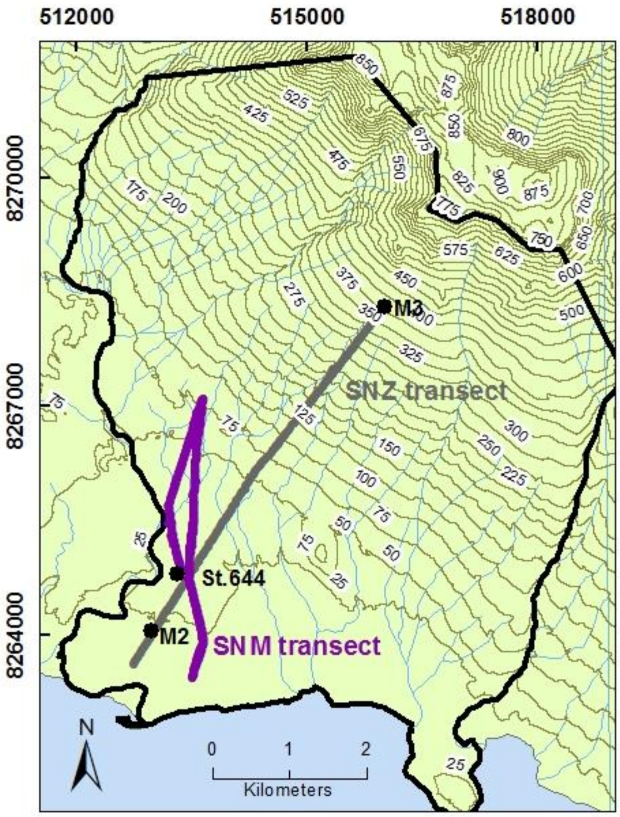

Figure 8: *Transects and meteorological stations where snow depth is measured.*

Table 2 lists the ground-truth datasets that were employed in this study.

Table 2: *List of ground truth data from Zackenberg research station*

No	Dataset	Source	Data format	Temporal resolution
1	Active layer	GEM online database	Excel tables	Weekly
2	Snow cover	GEM online database	Excel tables	Almost daily
3	Snow depth	GEM online database	Excel tables	Daily

The temporal extent of the ground truth data is presented in Table 3 and as it can be seen they are not harmonized.

__Table 3__: Temporal extent of the ground truth data from Zackenberg research station

Year	Active layer		Snow cover	Snow depth
	ZeroCalm 1	**ZeroCalm 2**	**Musk ox census**	**Transects and masts**
1996	Jun 22 - Aug 16	X	X	X
1997	Jun 8 - Aug 21	X	X	X
1998	Jun 13 - Aug	X	X	X
1999	Jul 4 - Sep 8	X	X	X
2000	Jun 4 - Jun 28	Jun 4 – Jun 28	X	X
2001	Jun 25 - Aug 29	Jun 9 - Aug 22	X	X
2002	Jun 24 - Aug 30	Jun 1 - Aug 30	X	X
2003	Jun 11- Aug 30	Jun 4 - Aug 30	X	X
2004	Jun 8 - Aug 29	Jun 3 - Aug 29	X	Jun 1 – Jun 6
2005	Jun 1 - Aug 27	May 20- Aug 28	X	May 19 - Jun 2
2006	Jun 20 - Aug 28	May 20 - Aug 28	X	May 26 – Jun 26
2007	Jun 9 - Sep 4	May 26 - Sep 5	X	May 26 - Jun 9
2008	Jun 23 - Sep 1	Jun 1 - Sep 1	May 4 - Jul 29	Jun 1, 2008 -
2009	May 17 - Sep 1	May 14 - Sep 1	X[9]	Oct 22, 2009[8]
2010	Jun 20 - Sep 4	May 9 - Sep 4	May 7 - Jul 15	May 9 - Jun 13 Oct 13 – Oct31
2011	Jun 10 - Sep 13	May 1 - Sep 13	May 1 - Jul 19	May 2 - Jun 9
2012	Jun 26 - Sep 5	Jun 5 - Sep 8	Apr 30 - Aug 17	May 6 - May 29
2013	Jun 1 - Sep 7	May 15 - Sep 9	May 7 - Jul 1	Apr 27 - Jun 2
2014	Jun 24 - Sep 1	X	May 2 - Jul 26	Apr 23 - Jul 1

3.2.3. Satellite imagery

The satellite imagery data used for the purpose of this thesis are images from the MODIS payload NASA instrument. More specifically, the datasets used are the MODIS Level 3 dataset products MOD13Q1 from the Terra platform satellite, which provide vegetation indices like NDVI in tiles rastertype, with spatial resolution of approximately 231 meters. The images are composites of 16 days. The MODIS images were downloaded from the USGS webpage (earthexplorer.usgs.gov) and are courtesy of NASA.

The selection of MODIS images -apart from the obvious advantage of the free distribution by NASA- is justified due to the fact that they provide satisfying temporal resolution for the purpose of this study to detect changes and variation of vegetation.

An additional reason for this choice is that NASA provides datasets with already calculated- ready to use NDVI measurements, diminishing the significant amount of time that would be needed to perform geometric and radiometric corrections and calculate

[8] For this period measurements of snow depth were taken throughout the whole year between the summers of 2008 and 2009.
[9] Due to not many cloud-free days during the snow melting period.

NDVI for a large number of images, if for example an alternative satellite product like Landsat images was chosen instead.

Last but not least, the selection of MODIS images instead of Landsat TM is justified due to the fact that the use of Landsat data for the current study, in which a pixel by pixel raster analysis was performed -as will be presented in a later chapter- would require the correction of the data gaps in Landsat images as well as corrections due to cloud cover contamination, processes which would be time consuming, due to the significant number of images that were used.

The satellite images that were used cover the study period 2005-2014 and more specifically the months between early May and late September, which was decided to be the study "time-window" for each summer in order to be harmonized with the temporal extent of the ground-truth data and at the same time to help answering the thesis' research questions, specifically the first research question (investigation of NDVI variation as well as detection of changes in the growing season). Ten satellite images were used for every spring-summer within this ten year interval, with the first image from May 9-25 composite period and the last from September 30-October 15 composite period, respectively. One hundred images were used in total to cover the study period.

Table 4 lists the temporal extent of the 16-day composite MODIS images that were employed in this study. The first column refers to the day of the year as referenced by NASA and the second to the period that each composite covers. A list of all the images that were used can be found in Table 16 of Appendix A.

Table 4: *Temporal extent of the 16 day composites*

16-day composite DOY	**Temporal extent[10]**
129	May 9-May 24
145	May 25-June 9
161	June 10-June 25
177	June 26-July 11
193	July 12-July 27
209	July 28-August 12
225	August 13-August 28
241	August 29-September 13
257	September 14- September 29
273	September 30-October 15

[10] For the leap years 2008 and 2012 the 16 day composite periods vary by one day before, e.g. May 8- May 23.

3.3. MATERIAL

The following software was used for the purposes of this thesis:

a) ESRI ArcGIS 10.2: All the geographical data manipulations as well as manipulations-computations on the satellite images were performed using ESRI's ArcGIS platform. The same software was also used for the mapping.

b) R version 3.2.1: R open source environment was used to perform statistical computations and produce graphs. The computations were performed in R Studio IDE (integrated development environment), which includes the console, the editor as well support for direct execution of the code and moreover helping tools for plotting, debugging and management of the working interface.

c) Microsoft Office Excel: Additional statistical computations and data analysis were performed using Microsoft's Office Excel spreadsheet application.

3.4. METHODOLOGY

3.4.1. Geographical data manipulations

a) All the geographical data were projected to the same coordinate system: WGS84 UTM 27N.

b) A DEM was created for the study area, with interpolation of the 25 m contour lines that were downloaded from ZERO GeoBasis webpage. The cell size of the DEM was decided to be 25 m for reasons of sufficient representation of the topography and comfort in ArcGIS computations. Figure 9 presents the created DEM.

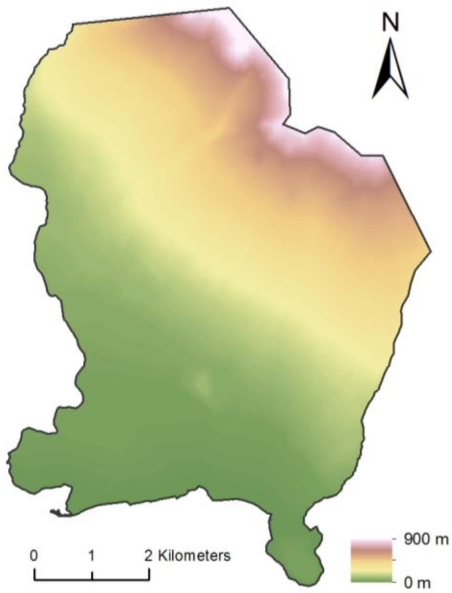

Figure 9: *Digital Elevation Model of the study area.*

3.4.2. Satellite images manipulations

The following manipulations were performed for all the satellite images with the help of ArcGIS's appropriate tools:

a) Projection to the same coordinate system as the geographical data: Many of the MODIS products -including the 16 day NDVI composites- use the global sinusoidal projection, which is basically a projection that uses a spherical projection ellipsoid, but a WGS84 datum ellipsoid. All images were projected to the same projected coordinate system as the geographical data; WGS84 UTM Zone 27N projected coordinate system.

b) Homogenization of all satellite images to the spatial extent of the study area (Musk ox census).

3.4.3. NDVI computations- Growing season

Statistical computations were performed on the satellite images of the ten year study period in order to detect variations and trends in the NDVI. Computations were performed in ArcGIS using the appropriate tools to retrieve the raster properties and in Microsoft Excel.

According to White et al. (1997) the determination of the exact beginning and ending of the growing season by satellite observation is a rather subjective and cumbersome procedure. However, several approaches have been proposed to define the length of growing period (Vrieling et al. 2013). Due to time limitations for this study and the use of 16-day composite NDVI images and not daily, which make the observations more generalized, a more subjective and simplistic yet functional approach was adopted. The start of the growing season was decided to be the day when average NDVI reaches positive values (since negative values employ the presence of snow) and the end of the growing season was decided to be the day when the average NDVI falls below 0.1.

3.4.4. Ground-truth data manipulations

The ground truth data (namely snow cover, snow depth and active layer depth measurements) were initially harmonized and categorized per year and date within the year. The measurements for each year (summer) were then separated and sorted using the time extent of the satellite images, so 16-day measurements periods were created. The result was to have the ground truth data timely consistent with the NDVI composites.

Regarding the snow depth measurements, points of low accuracy in measurement (e.g. measurements denoted as “over 200 cm”) were not included in the analysis, because they would add a level of inaccuracy and would not be manageable by the employed software.

3.4.5. Snow depth mapping

The next step was the creation of snow map rasters using the measurements of snow depth from GeoBasis data; the created maps correspond to the same 16 day periods along the 10 year study period between 2005 and 2014.

Spatial interpolation of the measurements was not possible, because of the non-uniform distribution of the points within the study area, since almost all the measurements were performed along the two transects and the ZeroCALM stations. Due to that, spatial extrapolation of the measurements was performed instead.

Figure 10 shows the spatial distribution of the snow depth measurements for DOY 145 (May 25-June 9) of each year of the study period. The particular time period was chosen, because it was the only sub-period matching with the NDVI 16-day composites, for which adequate measurements of snow depth were performed. Nevertheless, as seen in the figure, years 2005, 2012 and 2013 measurements’ spatial extent is not representative for the whole study area -covering only minor areas within Musk ox census- compared to the other years, for which at least there were measurements of snow depth along one or both transects covering different elevations. Therefore, years 2005, 2012 and 2013 were excluded from the analysis of snow depth.

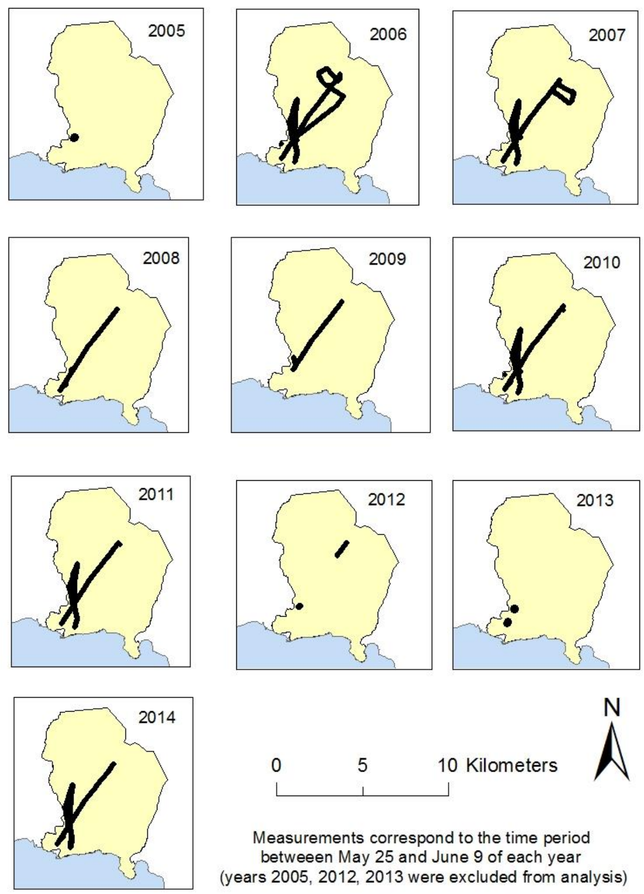

Figure 10: *The snow depth measurements spatial extent (2005-2014).*

The main idea of the snow depth mapping was to correlate the variables of snow depth (from the GeoBasis data) and elevation (from the created DEM) and create 16-day composite raster snow depth maps, harmonized with the 16-day NDVI composites from the satellite imagery.

The initial idea was to find a regression equation between snow depth and the elevation. However, the regression between the snow depth and the elevation with the fit of a 2nd order polynomial trendline showed low correlation (very low values of coefficient of determination). Same results were derived for the correlation between snow depth and other parameters of the geomorphology, such as slope, aspect and curvature.

Figure 11 is an example to show the low level of correlation between geomorphological parameters (elevation, slope, aspect and curvature) and snow depth. The scatterplots correspond to the snow depth measurements between May 9 and May 25 (harmonized with DOY 129 MODIS NDVI composite) of the year 2005 and they depict the general picture, since the correlation values were found to be similar or even lower for other years within the study period.

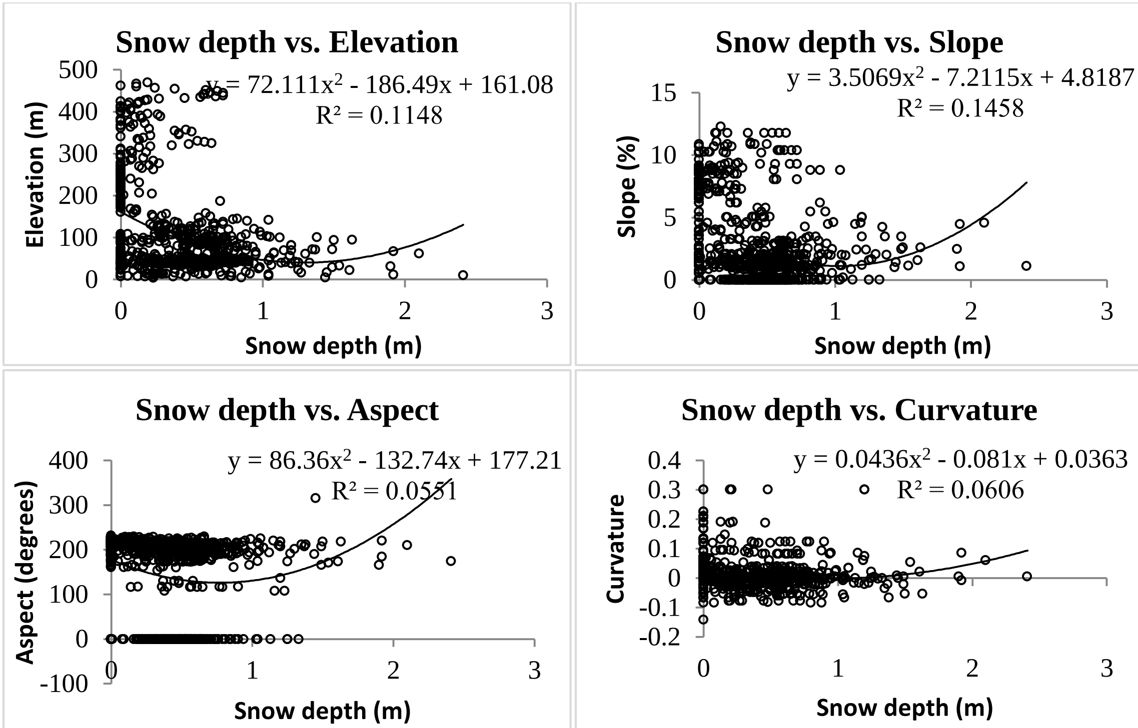

Figure 11: *Scatterplots of geomorphological factors vs. snow depth.*

To overcome this obstacle, analysis was performed based on the principles of the *Probability Density Function* (aka density of a continuous random variable), a function used in probability theory, that aims to describe the relative likelihood of a variable to be assigned with a value within a particular interval, regarding that the variable is continuous (Colla et al. 2015; Devore 2015). PDF is defined as following:

If x is a continuous random variable, the PDF of x is a function f(x), for which $P(a \leq x \leq b) = \int_a^b f(x)dx$. This means the probability that x takes on a value in the interval [a,b] is the area between this interval and under the graph of the density function (Devore 2015). Figure 12 is a random example that explains PDF's mathematical concept. According to the definition above, PDF equals with the shaded area of the graph.

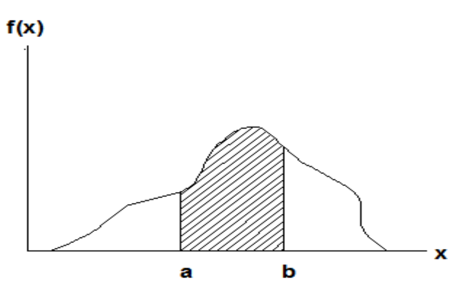

Figure 12: *Probability density function mathematical concept.*

The process that was followed to produce the snow depth maps consists of the following steps:

a) Elevation zones of 25 m were created from the DEM, using the tool of raster reclassification and maintaining the same cell size of 25*25 m. The areas with elevation between 500-900 m were reclassified in one class, since there were not adequate measurements of snow depth above this elevation in order to be treated separately. Figure 13 portrays the created reclassified DEM.

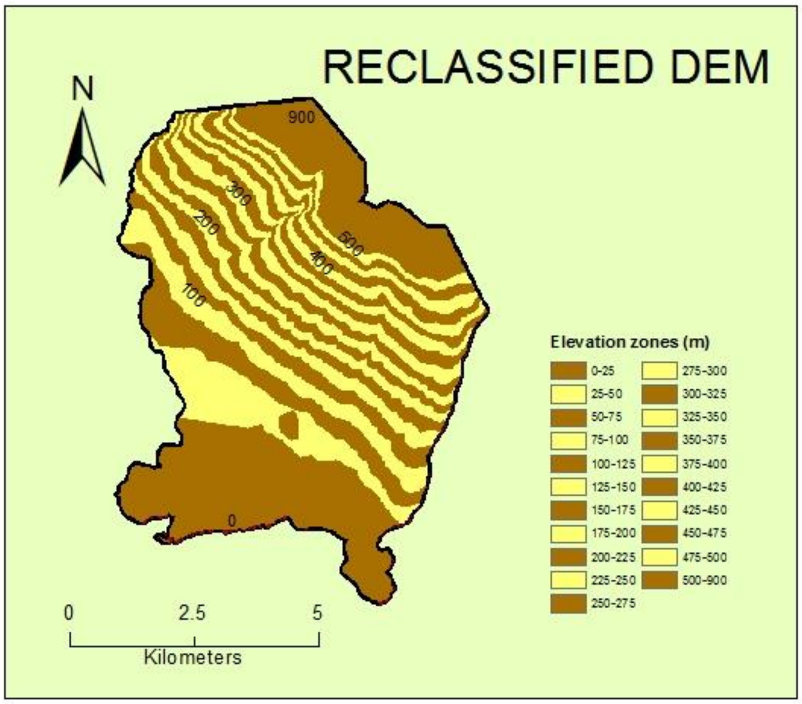

Figure 13: *Reclassified 25 m elevation zones DEM.*

b) Rasters of the 25 m elevation zones were converted to vectors of elevation zones; hence, each raster cell was represented by a point.
c) The ground-truth data of snow depth measurements of each 16 day time integral were sorted by 25 m elevation zones.
d) Histograms were created with ranges of snow depth for each one of the 25 m zone Ranges: 0, 0-0.5, 0.5-1, 1-1.5, 1.5-2, 2-2.5, 2.5+.
e) The principles of Probability Density Function were used and random values within the ranges mentioned in d) were given to each point representing the DEM cell within every 25 m zone based on the histogram and statistics.
f) Snow depth values were joined with the Table of Attributes of the shapefiles of each one of the 25 m elevation zones.

g) The 25 m elevation zones were merged into a single vector, covering the whole study area and including the snow depth values.
h) The merged vector was converted back to a 25m cell size raster.
i) Snow map rasters of 25*25 m cell size were produced, corresponding to the snow depth between May 25 and June 9 for each year of the study period, except years 2005, 2012, 2013 for reasons explained before.

The above process was performed for the whole study period of the research (2005-2014) and for the same time-interval that corresponds to the late spring-early summer NDVI 16-day composite, namely DOY 145 (composite May 25-June9). Microsoft Excel was employed for the statistical computations while the geographical manipulations were performed with the help of ArcGIS.

The workflow of the above procedure is presented in Figure 14.

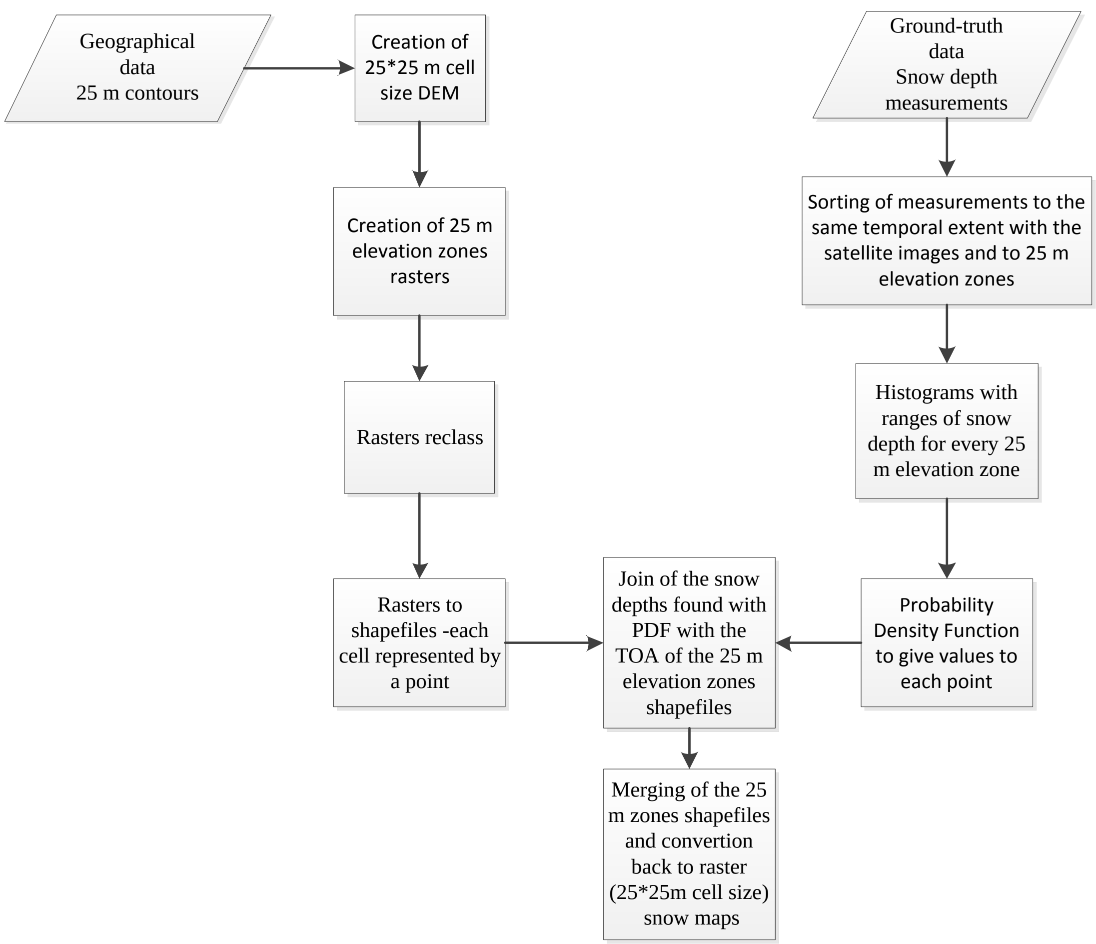

Figure 14: *Workflow of the process of the snow depth mapping.*

3.4.6. Snow depth analysis

The next step was to perform statistical analysis (including linear regression modeling and statistical significance test as will be more thoroughly explained below) between the rasters of the NDVI and the created snow depth raster maps (corresponding to the relative DOY NDVI raster) in order to detect possible correlation between them.

To perform this analysis, it was first necessary to upscale the snow depth rasters to the same spatial resolution as the NDVI rasters (approximately 231*231 m cell size). The 25m cell snow depth rasters were first aggregated by a scale factor of 8, to 200*200m cell size, using the aggregation technique of average (the average value of the input cells was used to compute the value of the new cells). The produced raster was then resampled to the resolution of the NDVI rasters. Bilinear resampling technique was chosen in order to maintain the range of the input rasters and the processing extent was chosen to be the same with the NDVI raster to avoid spatial mismatch of the two rasters.

Figure 15 is an example showing the above mentioned procedure for the snow depth raster of the period May 25- June 9 of the year 2006.

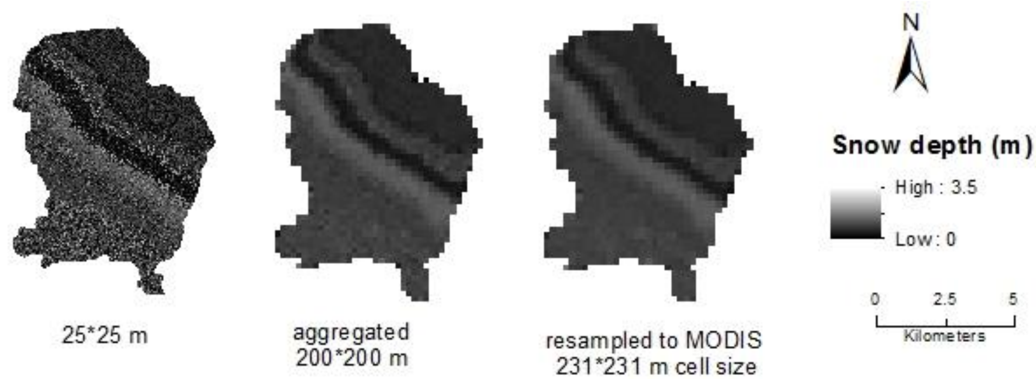

Figure 15: *Aggregation and resampling of snow depth rasters to the same cell size as the satellite images.*

Furthermore, it was necessary to homogenize the geoprocessing environment between the two rasters representing the snow depth composite and the NDVI composite, so that there would not be any “NoData” cells that would affect the pixel by pixel statistical analysis. The ArcGIS tool of Raster calculator was employed to achieve that; the two rasters were multiplied and the raster that was produced was used as a mask to clip them both to the same spatial extent. Figure 16 shows the workflow of the manipulations that were performed to be able to perform the statistical analysis between NDVI and snow depth.

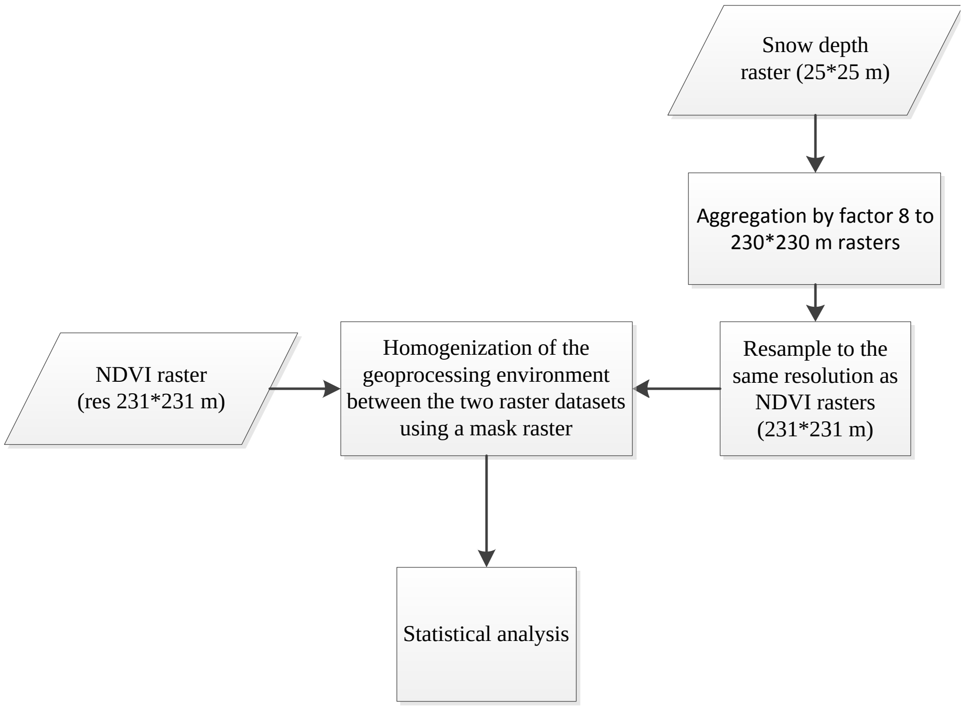

Figure 16: *Workflow of the snow depth statistical analysis.*

The NDVI and snow depth raster datasets were then converted into ASCII files and regression analysis was performed in order to detect possible relation between the NDVI values of DOY145 and the corresponding snow depth values of the same time period. A linear regression model was fitted to the dataset to explain the relationship between the two variables (NDVI and snow depth). A statistical significance test was performed to identify how significant is snow depth to explain changes in NDVI. This test is used in statistical theory in order to decide if a null hypothesis can be rejected (Moore et al. 2009). The null hypothesis for this study was that the two variables are not related and the alternative hypothesis was that they are related. Statistical parameters that were evaluated were the following:

- coefficient of determination (R^2), which measures the goodness of the fit of a dataset to the regression line that was chosen to depict the trend of the data
- residual standard error, which refers to the error in the estimated values of the dependent variable in a regression model
- p-value (ranging from 0 to 1), that indicates the level of confidence in rejecting the null hypothesis. P-value is the probability of the statistical test to take extreme values, regarding that the null hypothesis is true, therefore the lower the p-value the more sure one can be to reject the null hypothesis (Moore et al. 2009; Shaw and Wheeler 1994)

Analysis was performed with the use of R studio for each one of the years between 2005 and 2014 with the exception of the years 2005, 2012 and 2013 due to reasons already mentioned. The code that was developed for this procedure is available in Appendix F, which shows the 2006 linear regression model statistical analysis.

The correlation between the two variables was also studied for the whole study period by calculating the mean values of the two variables for DOY 145. A significance test was performed as well in order to investigate the overall relationship within the two variables. The code that was developed in R studio is included as an example in Appendix F.

Correlation analysis with the fit of linear regression models and tests of statistical significance was also performed between the values of the mean snow depth in DOY 145 and the mean seasonal NDVI, maximum seasonal NDVI and length and peak of growing period calculated from the satellite images. The null hypothesis was that mean snow depth is not related to each of the other variables. The aim was to detect if and to which extent pre-growing season snow depth may affect the growing season photosynthetic activity.

3.4.7. Snow cover analysis

The first approach was the study of snow depletion for each of the summers and the creation of snow depletion curves by averaging the data from GEM data tables to a monthly level. The time expand of the depletion was chosen to be the period between months May, June and July of the years 2008- 2014, period for which adequate data exist[11].

The next step was to perform statistical analysis with the fit of linear regression models and use of statistical significance test between the NDVI values and snow cover to detect the level of correlation between these variables. Values of snow cover retrieved by the GEM Excel tables -which in some cases had daily temporal extent-, were averaged in 16-day mean values, consistent to the 16-day NDVI composites.

As with snow depth, correlation analysis was also performed between the averaged values of the snow cover in the end of winter-beginning of growing period of each year (early May DOY 129) and the mean and maximum seasonal NDVI values as well as the length and peak of growing period calculated from the satellite images, in order to detect how the early season snow cover (as observed before snow starts to melt) may affect the photosynthetic activity within the growing season. Linear regression models were fitted and tests of statistical significance were performed, with the null hypothesis being that snow cover is not related to each of the other variables.

[11] Year 2009 was not included, as there were no data for this year.

Snow cover percentage within the study area was also calculated using the created rasters of the snow depth mapping process (for DOY 145). The results were compared to the results provided by the GEM database, as an evaluation of the snow mapping. To perform this comparison, snow depth rasters created with the procedure explained in chapter 3.4.5 were reclassified in snow-covered and snow-free pixels using ArcGIS.

3.4.8. Active layer thickness analysis

Active layer thickness data retrieved from GEM were first sorted per year and separated into 16-day period measurements according to the MODIS NDVI 16-day composites. The values of all the grid-points measurements were then averaged for each of the 16-day period. This procedure was performed for both CALM stations, in order to find the active layer's inter-annual variation and trend for the study period and to perform correlation statistical analysis between the NDVI values and the averaged active layer values in both the stations by fitting a linear model to the dataset and with the use of a test of statistical significance. It is necessary to be stated that the NDVI values that were used are the mean NDVI values retrieved from the satellite images, corresponding to the whole study area and not just to the areas where CALM stations are located.

Temporal break-up correlation analysis was also performed in order to detect whether and how the late season active layer depth condition is affected by the early photosynthetic activity and the overall seasonal photosynthetic activity. Analysis was conducted with the fit of linear regression models and statistical significance test between the value of active layer depth in late August and the values of early season (late May) NDVI and seasonal mean NDVI.

4. RESULTS

The results obtained from the analysis of the available data of satellite imagery and ground-truth data from the GEM database above using the previously described methods are presented below in terms of photosynthetic activity variation and the relation with the measured snow and permafrost properties.

4.1. NDVI VARIATION- GROWING SEASON

Maps of the 16-day composites NDVI values for the period between early May and late September of the years 2005 and 2013 are included in Appendix B (Figures 38 to 47) and they show variations among the same periods within the 10 year study period, with some years showing higher NDVI value, hence higher photosynthetic activity. Year 2005 appears to be the year with the higher NDVI values, while year 2013 seems to be the less photosynthetically active year of the study period.

By using the statistical values found from the satellite images raster computation and analysis, useful graphs were created in order to investigate the inter-annual and intra-annual variation in the photosynthetic activity in Zackenberg. The NDVI rasters statistics are included in Table 17 of Appendix C.

Figures 17 & 18 show the intra-annual and inter-annual variation of the average NDVI values between May and September throughout the study period.

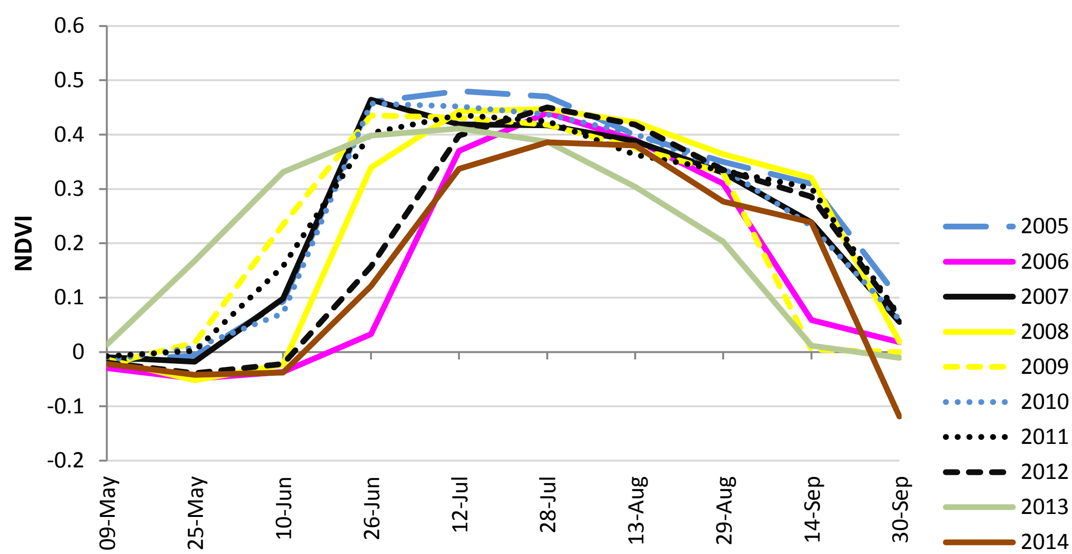

Figure 17*: 16-day composite average NDVI intra-annual variation.*

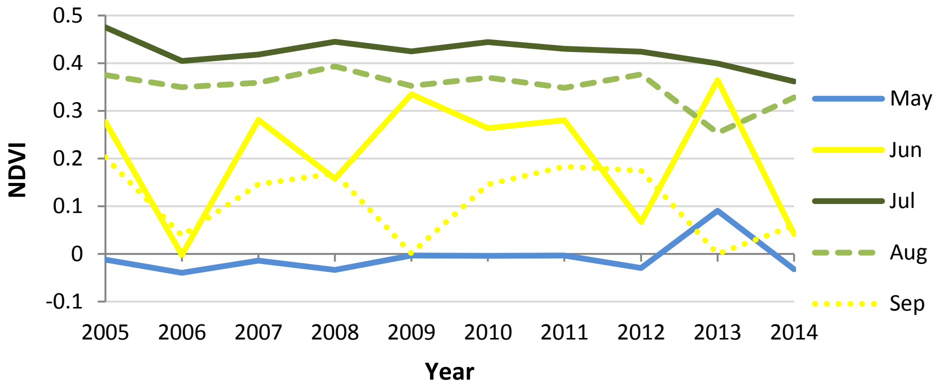

Figure 18: *Monthly average NDVI inter-annual variation.*

The two graphs show significant variation between the average NDVI values within the study period. The variation is more intense in the starting and ending of the growing season, hence during June and September, where the NDVI values are generally unpredictable, not following a particular trend. However, a trend can be detected in the peak of the growing season, which is during July (mainly) and August. Moreover, graph in Figure 18 shows a decreasing tendency of the average NDVI values during July, the peak season of the photosynthetic activity. Finally, the graph shows negative values of NDVI for May, something that can be explained since the snow has not yet started to melt, with the exception of year 2013, when growing season appeared to start earlier.

The general trend for a decreasing NDVI is verified also by the computation of the seasonal average NDVI values[12], as it can be seen in Figure 19.

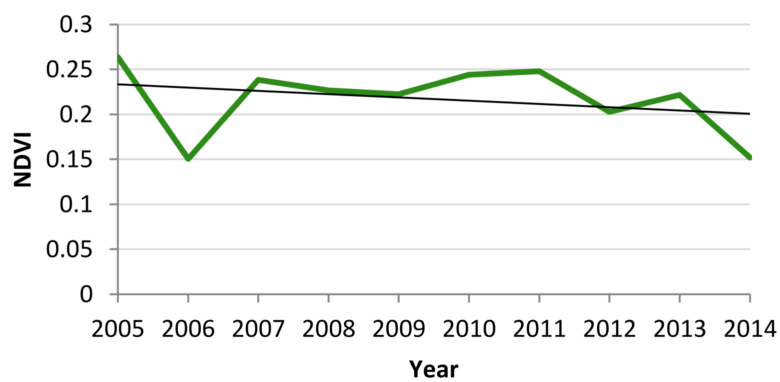

Figure 19: *Seasonal (May to September) average NDVI variation and trendline (2005-2014).*

[12] Term seasonal refers to the period between early May to late September

The first year of the study period, year 2005 is the year with the highest average NDVI, while the next year (2006) shows a rapid decrease of the NDVI value. NDVI increases the next years, being quite stable between years 2007 and 2011 and then decreasing again to reach the lowest value in 2014 (equivalent to the study period minimum of 2006).

The trend however can be different if particular years with "extreme" NDVI values are excluded. For instance, if the first and last year of the study period (years 2005 and 2014) are excluded, the NDVI trendline is slightly increasing, as seen in Figure 20.

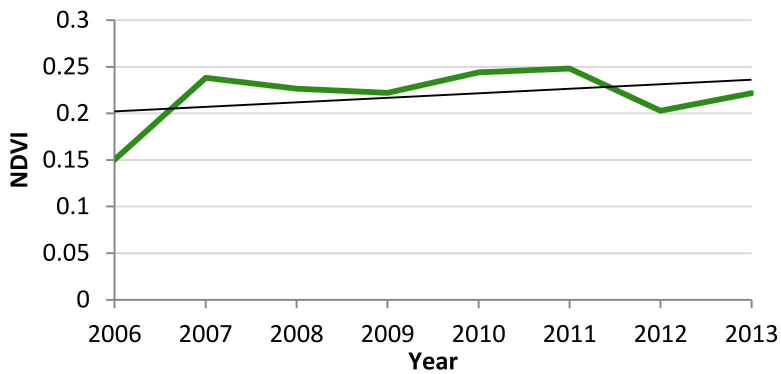

Figure 20: *The impact of two years' measurements on the overall trend of the seasonal average NDVI variation (2006-2013).*

Statistics calculated from the raster analysis provided results on the variation of the growing seasons. The graph in Figure 17 was used to detect the characteristics of the growing period for each year and significant variations between the starting, peak and ending of growing period can be detected. Growing season in Zackenberg usually starts between late May- mid June; nevertheless, the beginning of the growing season can be shifted quite sooner or quite later, as it happened for example the year 2013, when the NDVI started increasing in early May or the year 2006, when growing season was delayed as the NDVI started to reach positive values only in late June. The ending of the growing season usually occurs in late September, although it can be shifted earlier to early or mid-September, like in year 2013, while the peak of the growing period also varies between late June and late July.

Table 5 presents the growing period for each of the years between 2005 and 2014, derived from Figure 17. The columns of the table represent the starting, peak and ending of the growing period (SGP, PGP, EGP), as well as the length of the growing period (LGP).

__Table 5:__ Growing period

Year	SGP	PGP	EGP	LGP
2005	May 25	July 12	September 30	129
2006	June 18	July 28	September 10	85
2007	May 28	June 24	September 27	123
2008	June 11	July 28	September 26	108
2009	May 18	June 25	September 10	116
2010	May 18	June 26	September 25	131
2011	May 25	July 12	September 26	125
2012	June 12	July 28	September 25	106
2013	May 7	July 12	September 8	125
2014	June 13	July 25	September 21	101

The length of the growing period is usually over 100 days per year varying between 100 and 130 days, with the exception of the year 2006 where it was significantly lower. Figure 21 shows the trend in the length of the growing period throughout the period of study.

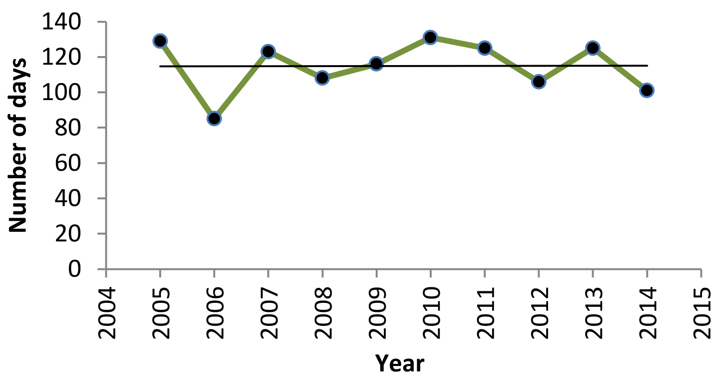

***Figure 21:** Length of the growing period and trendline.*

4.2. NDVI - SNOW AND PERMAFROST PROPERTIES

4.2.1. Snow depth and NDVI

The results of snow depth analysis were mapped and Figure 22 presents the snow depth mapping for early summer, DOY 145, which refers to the 16-day period between May 25 and June 9. The maps in Figure 22 are the 25m resolution rasters, resulted from the extrapolation analysis. The maps show the variations in the depth of snow both between the years as well as between the elevation zones.

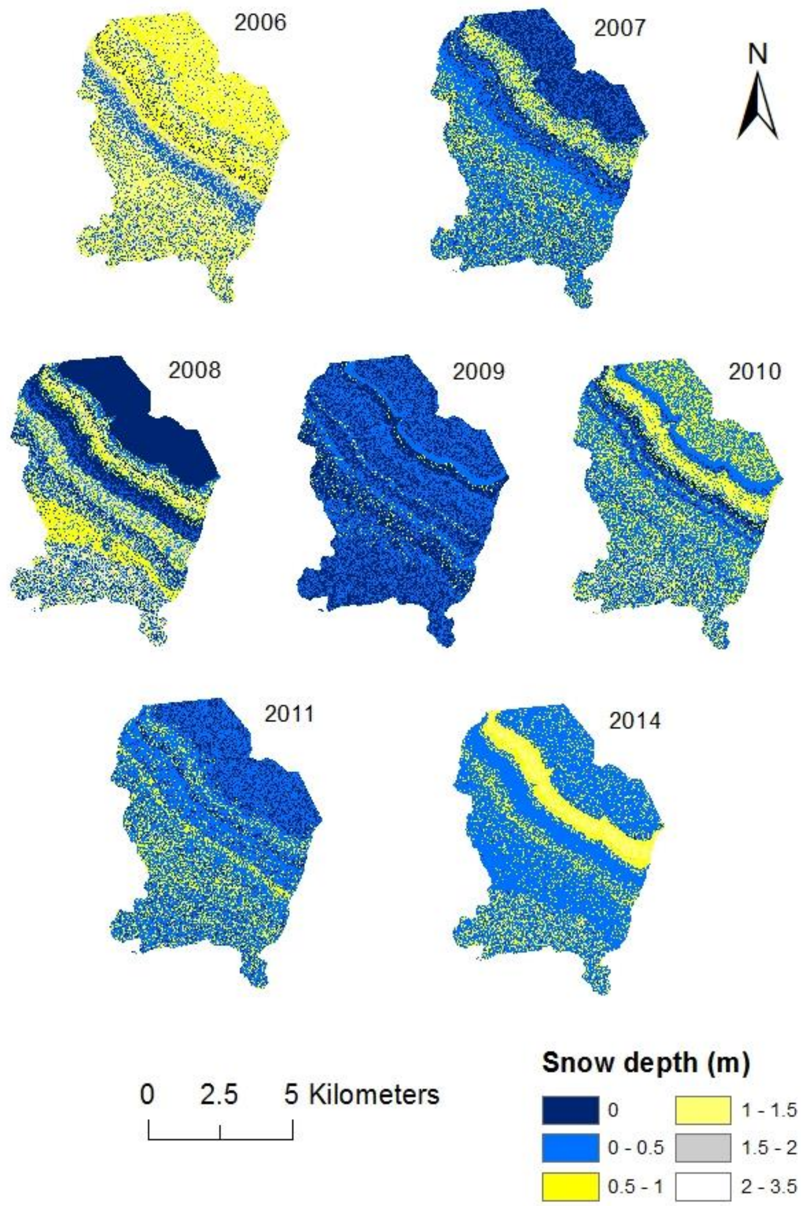

Figure 22: *Snow depth composite mapping (DOY145 May 25-June 9).*

The first outcome is that years 2007 and 2009 seem to have a thinner layer of snow in the beginning of summer compared to the other years.

As explained in the Methodology chapter, the 25 m resolution snow depth rasters were scaled up to the same spatial resolution with the MODIS satellite images in order to be able to compare the ground data with the satellite observations by performing a cell by cell regression analysis between them. Figure 23 is a comparative mapping of the MODIS satellite 16-day composites of DOY 145 with the scaled up snow depth rasters, both 231*231 m resolution.

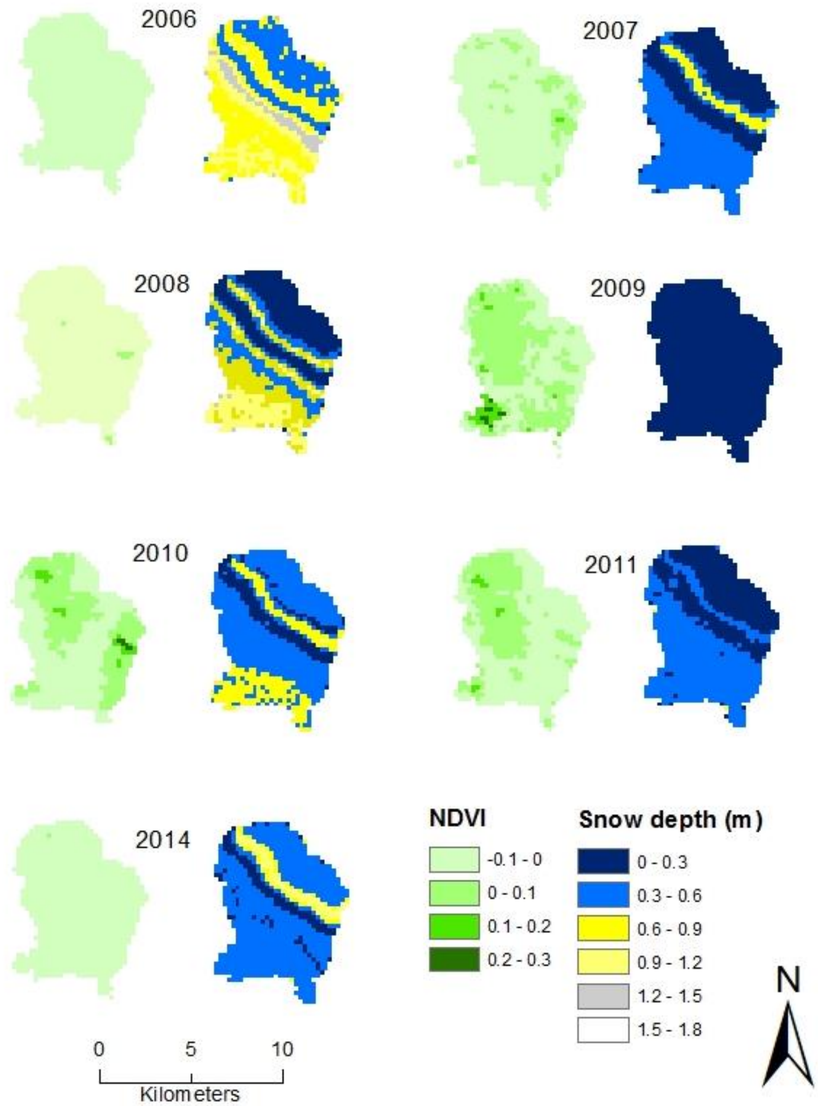

Figure 23: *NDVI and Snow depth for DAY145 (May 25-June 9).*

At a first glance, the logical assumption that for years with lower snow depth (resulted from a winter with less snowfall), NDVI values are higher and vice versa is been confirmed. This can be seen for example in the year 2009 where low snow depth and higher NDVI can be observed.

The **per pixel** regression analysis between the rasters of the satellite images and snow depth is presented in Figure 24. All scatterplots refer to the snow depth and NDVI pixel values for DOY 145 (May 25-June 9) of each year. NDVI pixel values are generally -and in some cases totally- negative since they refer to the early season before the start of the growing period when there is still a lot of snow.

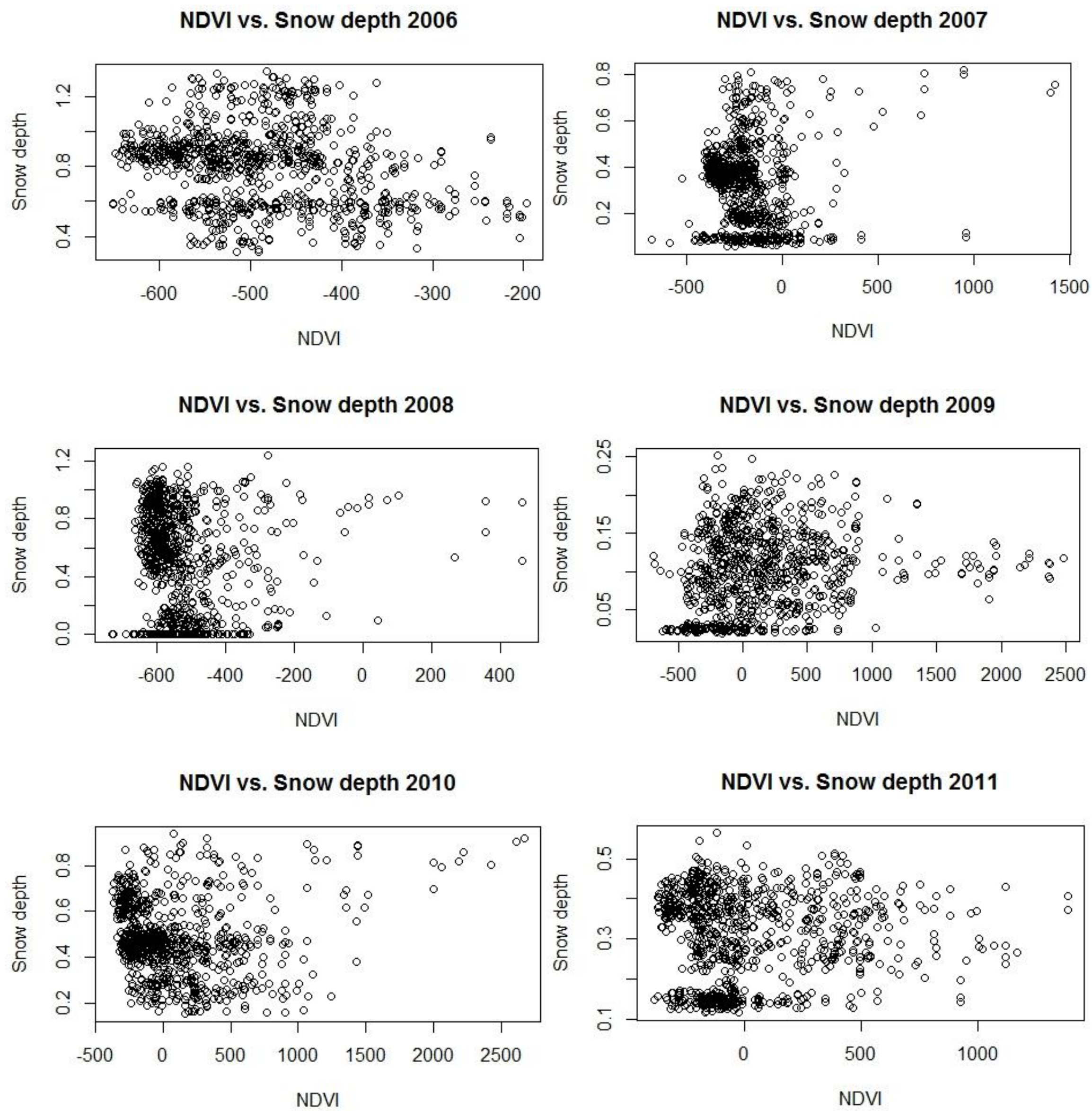

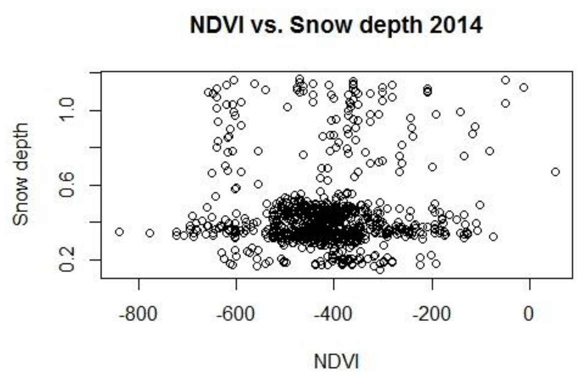

*** Due to the MODIS representation of NDVI within range -10000 to +10000, divide NDVI values by 10000 to get NDVI range between -1 and +1*

Figure 24: *Scatterplots of NDVI vs. snow depth -DOY 145 (May 25-June 9).*

Table 6 shows the results of the statistical significance test for the per pixel regression analysis between NDVI and snow depth.

Table 6: *NDVI vs. snow depth statistics and test of significance results*

Year	**Linear regression equation (x: NDVI, y: snow depth)**	R^2	**Residual standard error**	**p-value**
2006	y = -0.0006x+0.5069	0.0553	0.2225	$1.666*10^{-12}$
2007	y = 0.000025x+0.3332	0.0007	0.1762	0.426
2008	y = -0.00026x+0.3692	0.0090	0.3573	0.0049
2009	y = 0.000016x+0.1012	0.0227	0.0525	$9.812*10^{-6}$
2010	y = 0.000006x+0.479	0.0002	0.1589	0.6463
2011	y = -0.000004x+0.3121	0.0001	0.1093	0.7578
2014	y = -0.00008x+0.4801	0.0018	0.2145	0.210

The R^2 values are low, indicating poor fitness of the linear model to the dataset. Significance test showed low p-values for years 2006, 2008 and 2009, but high p-values for years 2007, 2010. However, the combination of low coefficient of determination and p-values indicate that the variables are not highly related.

A linear regression model was also fitted to explain the relation between the averaged snow depth values for DOY 145 (May 25- June 9) as they were calculated from the snow depth rasters and the corresponding mean NDVI value of the same period, calculated from the satellite images. Figure 25 presents the scatterplot of the two variables as well as the regression equation and the coefficient of determination. Table 7 shows the results of the statistical significance test.

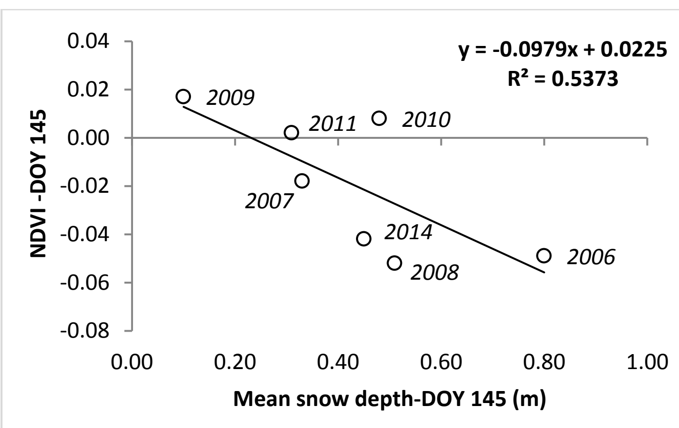

Figure 25: *Scatterplot of mean NDVI vs. mean snow depth values for DOY 145.*

Table 7: *NDVI vs. snow depth statistical significance test results*

R^2	**Residual standard error**	**p-value**
0.5373	0.1608	0.0609

The scatterplot in Figure 25 shows that there is correlation between the two variables with low snow depth leading to high NDVI and vice versa, with a coefficient of determination approximately 0.54 meaning that the chosen linear model fits quite well to the dataset, and low RSE that adds accuracy to the obtained results. The test of statistical significance gave a low p-value equal to 0.06.

A linear regression equation was also used to explain the relation between the average snow depth values for DOY 145 and the seasonal mean and seasonal maximum NDVI. Figure 26 shows the scatterplots and the regression equations. Table 8 shows the results of the statistical significance tests.

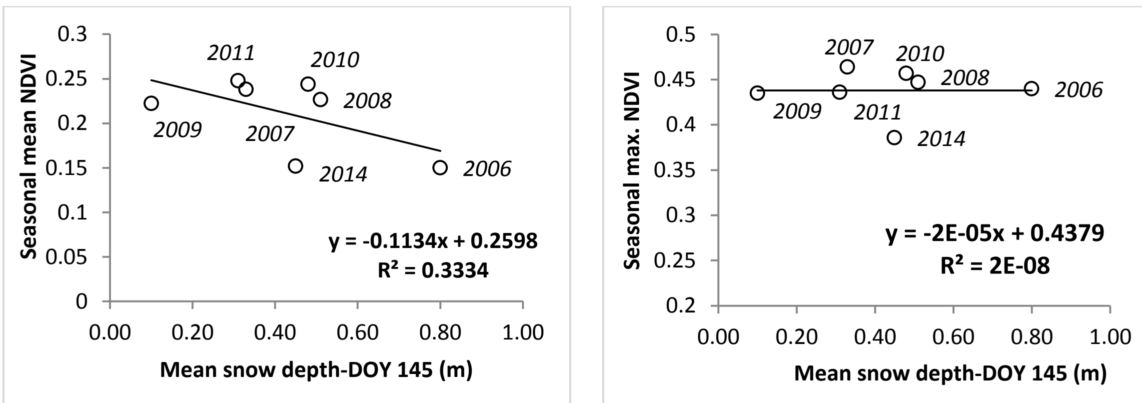

Figure 26*: Scatterplots of mean snow depth (DOY 145) vs. seasonal mean NDVI and seasonal maximum NDVI.*

Table 8: *Snow depth vs. seasonal mean and seasonal maximum NDVI statistical significance test results*

	R^2	Residual standard error	p-value
mean snow depth (DOY145) vs. seasonal mean NDVI	0.3334	0.193	0.1746
mean snow depth (DOY145) vs. seasonal maximum NDVI	$1.71*10^{-8}$	0.2364	0.9998

Seasonal mean NDVI seems to be related to snow depth to some extent, as seen in the left scatterplot (Figure 26). The linear model explains 33% of the dataset (R^2=0.33) and the p-value of 0.17 tells us that one cannot be sure to reject the null hypothesis. Seasonal maximum NDVI appears not to be related with the early season snow depth. Observation of the right scatterplot in Figure 26, coefficient of determination R^2 value ($1.71*10^{-8}$) and the test of statistical significance results with p-value=0.999 suggest that the null hypothesis of non-related variables is verified.

Moreover, linear regression models were also fitted to the relative datasets in order to detect the relation between the average snow depth values for DOY 145 and the length and peak of the growing period (LGP, PGP), as they were computed in Chapter 4.1. The scatterplots and the statistical significance test results are presented in Figure 27 and Table 9.

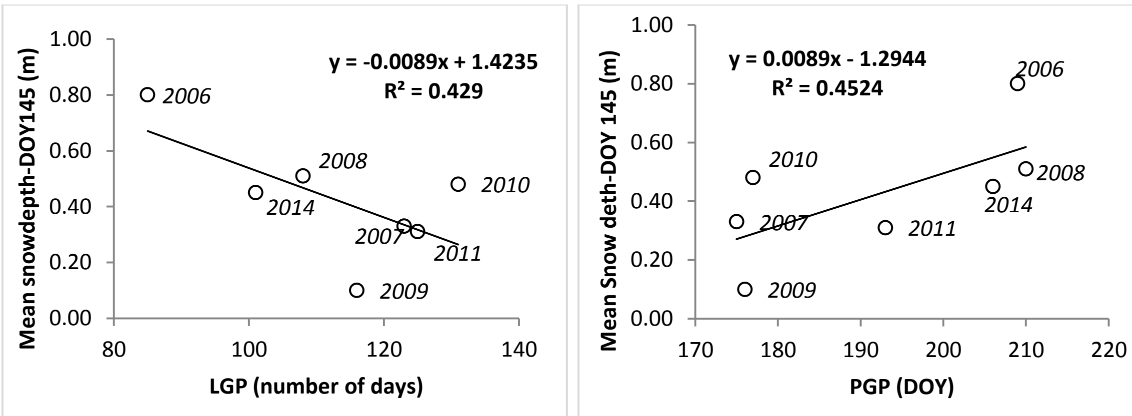

Figure 27: *Scatterplots of mean snow depth (DOY 145) vs. length and peak of growing period.*

Table 9: *Snow depth vs. length and peak of growing period statistical significance test results*

	R^2	Residual standard error	p-value
mean snow depth (DOY 145) vs. LGP	0.429	0.1786	0.1103
mean snow depth (DOY 145) vs. PGP	0.4524	0.1749	0.0978

Both scatterplots show that the variables are correlated and that mean snow depth in early season affects the growing period. In both cases, models explain more than 40% of the datasets, while the RSE are low. According to the obtained p-values there is indication that the null hypothesis can be rejected for both datasets.

4.2.2. Snow cover and NDVI

The graph in Figure 28 presents the created snow depletion curves for the period 2008-2014[13]. The values refer to the monthly averaged snow cover percentage in Musk Ox census study area.

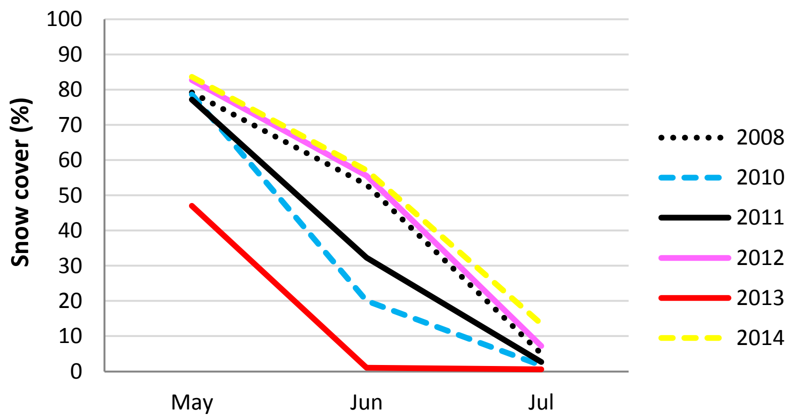

Figure 28: *Snow depletion in Musk ox census (2008-2014).*

The graph shows three different trends in the snowmelt. In the years 2008, 2012 and 2014 snow melt occurred gradually from May to July. On the contrary 2010 and 2011 had a quite more rapid snowmelt and snow cover was below 50% already from May. Year 2013 is an interesting year with significantly less total snow cover in the end of the winter snow season compared to the other years (less than 50%). At a first glance, one could say that this finding is in accordance with the outcomes in Figure 17, when NDVI for May is increased compared to the other years. However, the lower snowfall of winter of 2013 does not seem to significantly affect the seasonal NDVI of this year, which seems to be relative low compared to other years.

Analysis between snow cover and NDVI showed correlation between them. Photosynthetic activity is higher for years with less total snow cover in Musk ox study area as it can be seen in the graphs of Figure 29, which represents the monthly trend in both variables for the period 2008-2014. This is evident especially for the years 2008 and 2013, where low snow cover in June 2013 reflects to a high NDVI, while the high snow cover of years 2008, 2012, 2014 led to low NDVI in June. One can see from the graphs that the negative trend in snow cover during May causes a positive trend in the values of NDVI for this month. The opposite happens for July, where there is a positive trend for snow cover and a negative trend in NDVI values.

---

[13] Year 2009 not included due to the lack of data

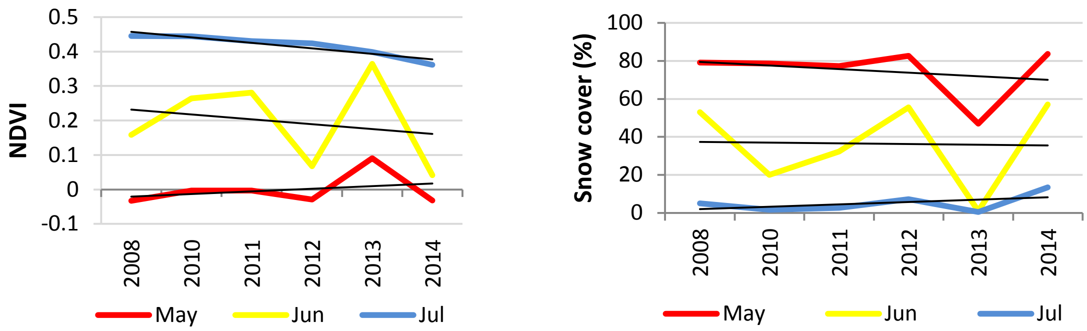

Figure 29: *Monthly trend in NDVI and snow cover (2008-2014).*

The following regression analysis results aim to show more relations between snow cover and photosynthetic activity in the growing season. Figure 30 shows the overall fitness of total snow cover in Musk ox census against the mean NDVI values for same time intervals (16 day composites) of the period 2008-2014, with exception of 2009 due to lack of data. The time intervals of the points in the dataset and the regression analysis for each one of the years are presented in Figure 48 of Appendix D. Table 10 presents the test of statistical significance results.

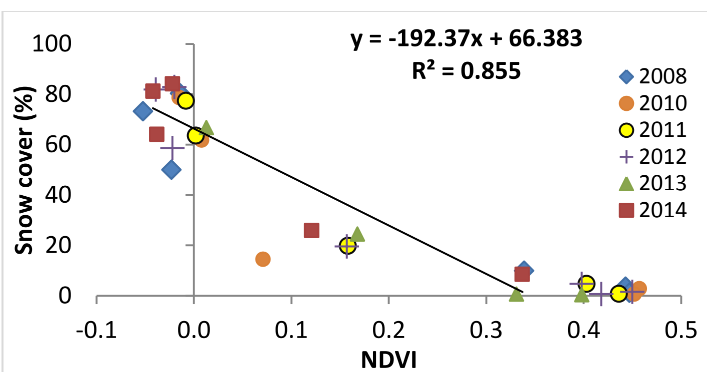

Figure 30: *Overall goodness of fit of NDVI against Snow cover (2008-2014).*

Table 10: *NDVI vs. snow cover test of statistical significance results*

R^2	Residual standard error	p-value
0.8548	12.99	$4.182*10^{-14}$

The chosen linear model describes sufficiently the overall relation between the two variables as indicated by the scatterplot of Figure 30 and the value of R^2 (0.85), which means that the chosen model explains about 85% of the dataset. Moreover, the low p-value ($4.182*10^{-14}$) indicates a high level of confidence in rejecting the null hypothesis.

The scatterplots of the linear regression models used to explain the relation between snow cover in the beginning of snow melting (early May) and photosynthetic activity of the growing period are presented in Figure 31. The first scatterplot explains the correlation between snow cover and seasonal mean NDVI and the second the correlation between snow cover and seasonal averaged maximum NDVI. Both scatterplots refer to the years between 2008 and 2014, years for which snow cover data from GEM are available.

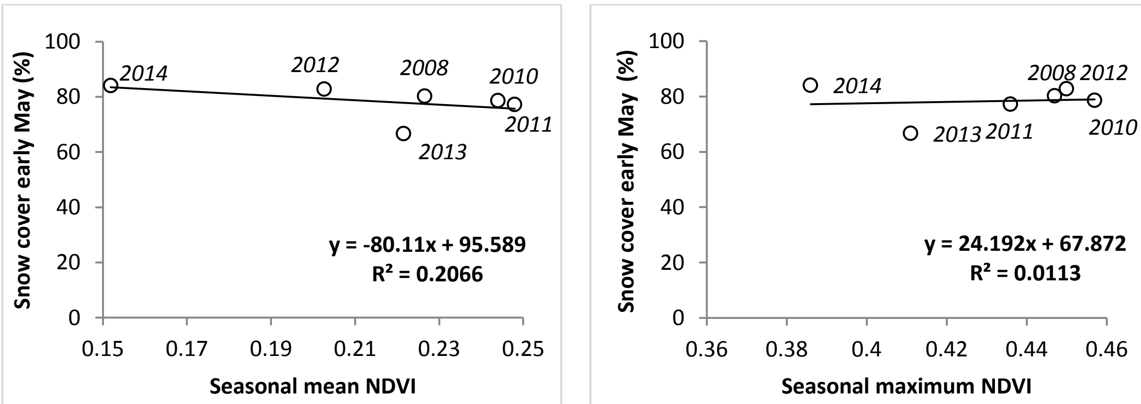

Figure 31: *Scatterplots of snow cover (DOY 129) vs. seasonal mean NDVI and seasonal maximum NDVI.*

Table 11 shows the results of the test of statistical significance that was performed to evaluate the relationship between the variables and to check whether the null hypothesis of the variables not being related to each other can be rejected.

Table 11: *Snow cover (DOY 129) vs. seasonal mean and seasonal maximum NDVI statistical significance test results*

	R^2	Residual standard error	p-value
snow cover (DOY129) vs. seasonal mean NDVI	0.2066	6.191	0.3622
Snow cover (DOY129) vs. seasonal maximum NDVI	0.0113	6.921	0.8414

Snow cover seems to have low influence on the seasonal mean NDVI, as shown by the values of coefficient of determination and p-value. Seasonal maximum NDVI appears not to be related with the early season snow depth. The scatterplot of the two variables and the test of statistical significance, showed relatively small p-value and coefficient of determination.

In addition, linear regression equations were also fitted to the models that explain the relation between the snow cover in DOY 129 and the length and the peak of the growing period (LGP, PGP). The scatterplots and statistical significance tests results are presented in Figure 32 and Table 12.

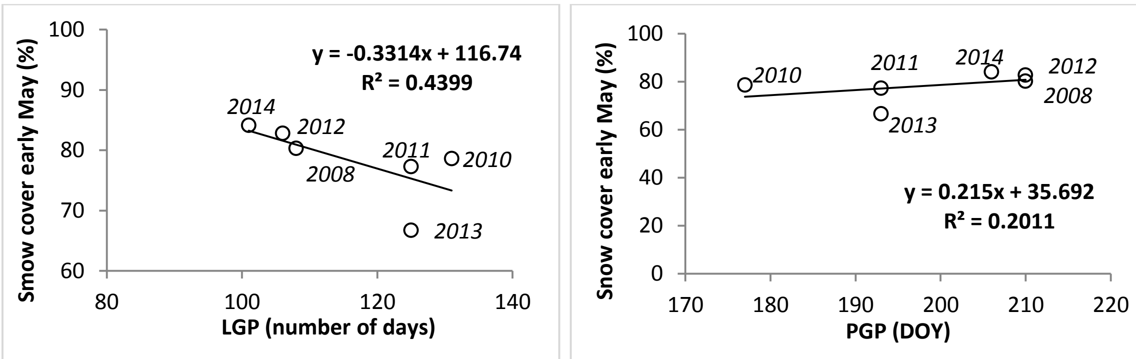

Figure 32: *Scatterplot of snow cover (DOY 129) vs. length and peak of growing period.*

Table 12: *Snow cover vs. length and peak of growing period statistical significance test results*

	R^2	Residual standard error	p-value
snow cover (DOY 129) vs. LGP	0.4399	5.209	0.151
snow cover (DOY 129) vs. PGP	0.2012	6.221	0.3723

Both scatterplots show that the variables are correlated to some point and that snow cover in early season affects the growing period. According to the coefficients of determination for the linear regression models, around 44% of the dataset fits well to the model explaining the relationship between snow cover and length of the growing period (R^2=0.44), while the chosen model is less able to explain the relationship between the snow cover and the peak of the growing period (R^2=0.2). The statistical test showed indication that one can reject the null hypothesis of non-correlation between snow cover and LGP. However, the p-value of 0.37 indicates that the correlation between snow cover and PGP cannot be confirmed.

4.2.3. Active layer thickness and NDVI

Figure 33 depicts the inter-annual variation in the thickness of the active layer at both CALM stations.

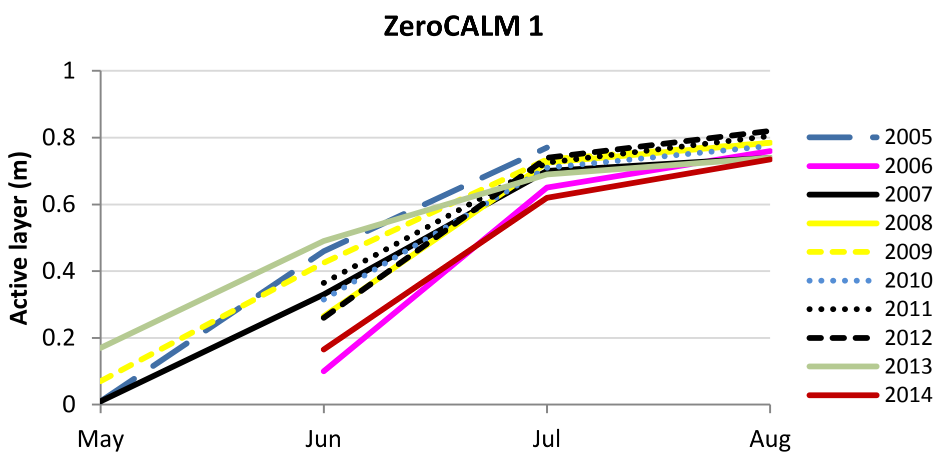

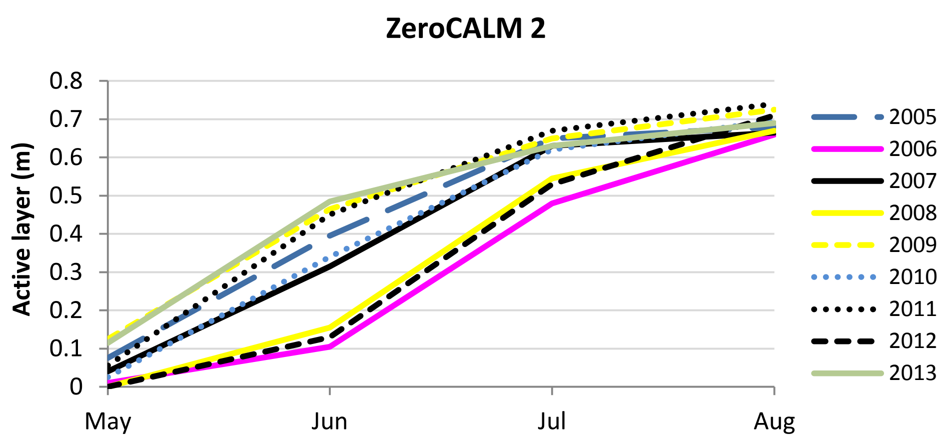

Figure 33: *Active layer variation at the two monitoring stations ZeroCALM1 and ZeroCALM2 for years 2005-2014 (updated from Christiansen et al. 2008 and Elberling et al. 2013).*

Figure 34 shows the increasing trend for the mean annual thickness of active layer in both stations, where active layer is measured. The increase seems to be higher in ZeroCALM 1 station (around 15 cm) while in ZeroCALM 2 is around 10 cm.

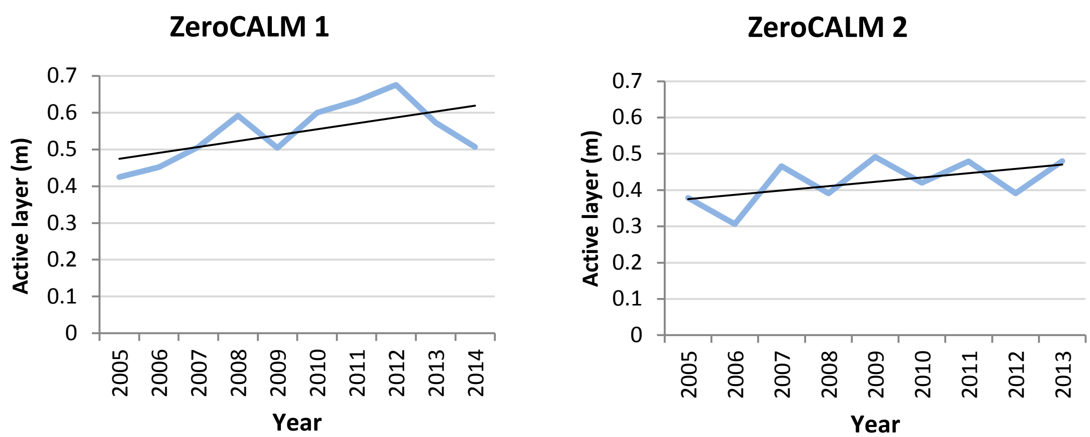

Figure 34: *Mean annual active layer depth (updated from Christiansen et al. 2008 and Elberling et al. 2013).*

The relation between average NDVI retrieved for the whole study area from the satellite observations and depth of active layer in both CALM stations was studied and a regression analysis was performed, fitting a linear model between the two variables. Scatterplots of NDVI values against active layer depth values for both CALM stations in Figure 35 depict the overall goodness of fit of the linear model that was chosen to explain the relationship between the two variables for measurements of active layer depth and the mean NDVI for the same time intervals (16-day composites).

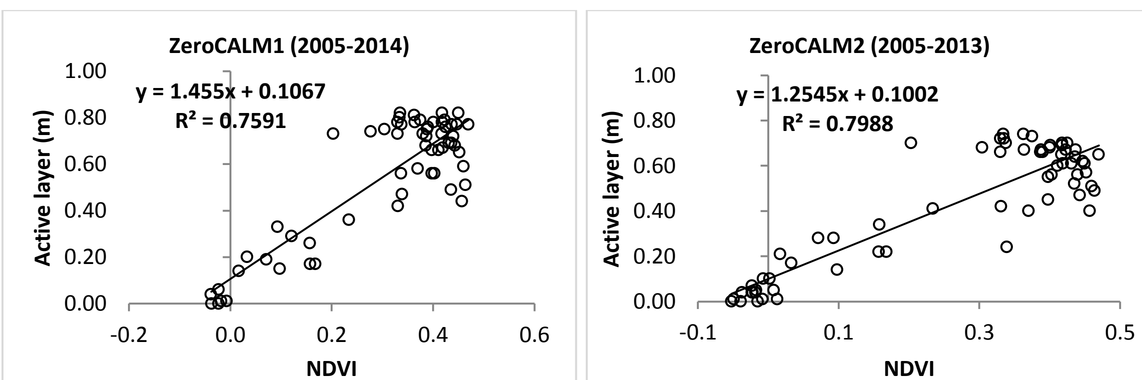

Figure 35: *Overall goodness of fit of NDVI against active layer (ZeroCALM 1 and 2).*

A test of statistical significance was performed and the results can be seen in Table 13.

Table 13: *NDVI vs. active layer test of statistical significance results*

	ZeroCALM 1	**ZeroCALM 2**
$\mathbf{R^2}$	0.7591	0.7988
Residual standard error	0.1324	0.1198
p-value	$2.2*10^{-16}$	$2.2*10^{-16}$

Scatterplots and R^2 values show that the chosen linear models fit well to the datasets and obtained p-value of $2.2*10^{-16}$ indicates that the null hypothesis of no-relation between the variables can be rejected. Figures 36, 37 and Table 14 present the scatterplots and statistical significance test results of the temporal break-up regression analysis between the averaged values of active layer thickness in later season (end of August) and the early season (late May) NDVI and seasonal mean NDVI. Analysis was performed separately for the two CALM stations.

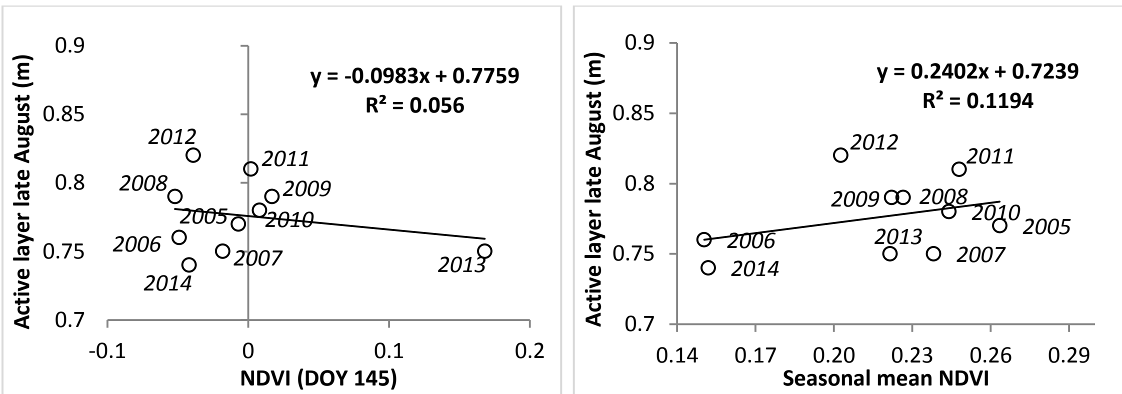

Figure 36: *Scatterplots of early season and seasonal mean NDVI vs. late season active layer (ZeroCALM 1).*

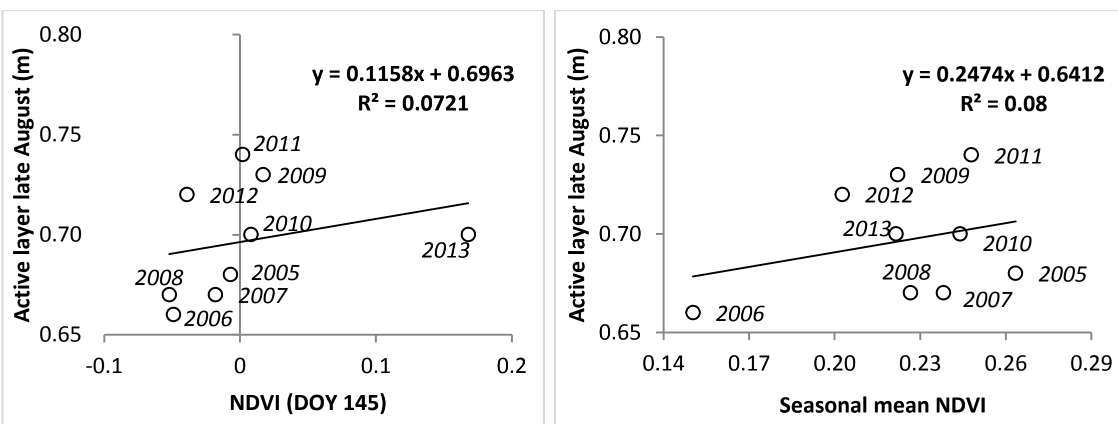

Figure 37: *Scatterplots of early season and seasonal mean NDVI vs. late season active layer (ZeroCALM 2).*

Table 14: *Late season active layer depth vs. early season and seasonal mean NDVI statistical significance test results*

		R^2	**Residual standard error**	**p-value**
ZeroCALM 1	late season active layer depth vs. early season NDVI	0.056	0.02757	0.5105
	late season active layer depth vs. seasonal mean NDVI	0.1194	0.02662	0.3281
ZeroCALM 2	late season active layer depth vs. early season NDVI	0.072	0.02958	0.4847
	late season active layer depth vs. seasonal mean NDVI	0.08	0.02946	0.4624

The scatterplots and the correlation coefficients (R^2) show poor goodness of fit of the linear models to the datasets. Moreover, the p-values ranging from 0.33 to 0.51 indicate uncertainty whether the variables are related to each other and to which extent.

5. DISCUSSION

5.1. NDVI VARIATION – GROWING SEASON

Mean seasonal NDVI in Zackenberg Musk ox census (from beginning of May to end of September) seems to have a slight negative trend, decreasing from 0.23 to 0.20 throughout the last ten years as seen in Figure 19. The decreasing trend is also evident for the monthly NDVI variation, as seen in Figure 18. However, it is necessary to mention that the vegetation index is not decreasing steadily and there is fluctuation throughout this 10 year period (Figure 19), which makes the conclusion of a decreasing NDVI disputed as seen in Figure 20, where the exclusion of two years led to a different outcome on the NDVI trend.

The outcome of decreasing NDVI is somehow contrary to the findings of scientific studies that show increasing NDVI trend in the high latitudes (Zhou et al. 2001; Xu et al. 2013). But, as mentioned in the Background chapter there is controversy among scientists on this issue (Myneni et al. 1997; Tucker et al. 2001; Zhou et al. 2001). However, the result is in agreement with the Zackenberg research operations findings (Jensen et al. 2014), also showing decreasing NDVI trend throughout the period 1995-2013.

The fluctuation in NDVI is more intense in the start and end of the growing season, as May and September show higher intra-annual seasonal variation compared to the peak of growing season (July and August). This finding agrees with previous studies performed for Zackenberg and other arctic environments (Ellebjerg et al. 2008; Karlsen et al. 2014).

In this study NDVI computations from satellite images were used to define the growing season, method that was used by other studies before (Chen and Pan 2002; Vrieling et al. 2013; Karlsen et al. 2014). Growing season can alternatively be defined by the time of snowmelt and/or the air temperature (Rixen et al. 2008; Luus et al. 2013; Bosiö et al. 2014). The variation in the start of the growing season is quite significant, as according to the results in Table 5 photosynthetic activity may start in any day between May 7 and June 18, meaning that there is a 41-day time interval within which growing season started the last ten summers. Moreover, there is variation in the rapidness of the beginning of photosynthetic activity, as one can see in the graph of Figure 17, with some years showing a more rapid increase in NDVI (for example year 2007) compared to years when the starting of growing season is more gradual, like year 2012 for example. The variation in the end of growing season is not so intense, usually occurring in late September, with recorded time interval of 22 days (between September 8 and September 30). The peak of growing season also varies, occurring between a 35-day time interval, June 24 and July 28. Regarding the length of the growing period, although there seems to be an inter-annual variation of around 30 days, no increasing or decreasing trend can be detected.

Figure 17 shows a shift in the growing season within the ten year study period. Years with early start of NDVI increase, hence early onset of the growing season tend to also have an early offset of growing season, like for example year 2013, while on the other hand the late starting of the growing season in years 2012 or 2014 led to a later offset of the growing season.

5.2. SNOW DEPTH AND PHOTOSYNTHETIC ACTIVITY

Per pixel statistical analysis for DOY 145 (period May 25-June 9) between the rasters of NDVI satellite observations and snow depth revealed a relation between the values of the two variables, although the results of the analysis are ambiguous. The scatterplots between the two variables (Figure 24) and the values of the coefficient of determination (R^2) in Table 6 of the results chapter clearly show poor goodness of fit of the linear regression model that was chosen to explain the relationship between the two variables. This means that the linear model cannot adequately explain the relationship between them. Moreover, the performed significance test showed controversial p-values, meaning that the non-relation between the two variables cannot be rejected for all the years of the study.

In this content, it can be said that the per-pixel statistical analysis of the correlation between ground truth measurements of snow depth and satellite observations of NDVI was not very successful mainly due to the following reasons:

a) Spatial resolution of the rasters used: The spatial resolution of both raster datasets was chosen to be the resolution of the available satellite images. The created snow depth rasters were scaled up by a factor of 8 from 25*25 m to 231*231 m cell size, which proved to be weak in order to depict such a complex phenomenon that varies constantly in space, as seen in the per pixel regression analysis between snow depth and NDVI.
b) Ground measurements collection method: Snow depth was measured along two transects in the study area, this means along a small area and a particular aspect range and they cannot be truly representative for the whole study area. In addition, the manual measurement may add a level of non- confidence.
c) Extrapolation method: The values of the snow depth in this project were calculated-extrapolated as a function of the elevation using the principles of the probability density function. However, elevation and geomorphology in general is clearly not the only parameter affecting snow depth. Other geomorphological parameters that affect snow accumulation are aspect, slope, physical obstacles like rocks and they should also be considered. In addition, meteorological microclimate parameters (temperature, wind, etc.) should be taken into consideration.

Despite the fact that per pixel raster analysis was not considered very successful in explaining the relation between snow depth and vegetation growth, analysis of the yearly mean values between them showed that there is correlation and this is agreement with previous studies that stress the importance of snow depth for vegetation in arctic regions (Buus-Hinkler et al. 2006; Gacitúa et al. 2013). The graph in Figure 25 shows that for years with less snow in the beginning of the summer period, the vegetation index is higher and vice versa. Additionally, the linear regression model that was fitted to the datasets has an adequate goodness of fit (coefficient of determination value R^2=0.53) and the statistical significance test showed indication that null hypothesis can be rejected.

Regarding the effect of early season snow depth to the seasonal vegetation strength, it appears that snow depth in the beginning of the growing period is more likely to affect the seasonal mean NDVI, while on the other hand is not related to the seasonal maximum NDVI.

Moreover, early season snow depth affects the growing season both in terms of the length of the growing season as well as the day when vegetation reaches the seasonal peak. Deeper snow depth in late May- early June seems to lead to a smaller growing period and to a delay in the day when vegetation growth reaches its seasonal peak.

5.3. SNOW COVER AND PHOTOSYNTHETIC ACTIVITY

The study showed that snow cover is related to the photosynthetic activity and this conclusion can be supported by other scientific studies, like the study performed by Ellebjerg et al. (2008) stating that photosynthetic activity starts by the time that snow melts.

Statistical analysis between the two variables showed a strong relation between them for datasets measured in the same period of time, a result that was expected. Moreover, analysis showed that snow cover is related with the length of the growing period, while there is indication that there is a correlation between snow cover and the seasonal mean NDVI. These findings agree with previous studies that stress out the importance of snow cover for the strength of vegetation (Belzile et al. 2001; Buus-Hinkler et al. 2006) and the length of the growing season (Myneni et al. 1997; Zhou et al. 2001; Xu et al. 2013). However, the seasonal maximum NDVI and the peak of growing period seem not highly related to the early season snow cover.

Snow cover was also calculated by the created snow depth rasters in order to evaluate the suggested method in comparison to the GEM data. Table 15 shows the comparison between the method used to compute the total snow cover percentage of the study area computed by this study (by resampling the snow depth rasters) and the snow cover statistics as they were estimated by GEM using rectified orthophotos as discussed in chapter 3.2.2. (Hinkler et al. 2008; Jensen et al. 2014). The evaluation refers to the period May 25-June 9 (DOY 145), period for which the results can be compared.

Table 15: *Snow cover for DOY 145*

Year	**Snow cover (GEM database)**	**Snow cover (calculated)**	**Difference**
2008	73%	61%	-12%
2010	62%	90%	+28%
2011	63%	80%	+17%
2014	81%	97%	+16%

The method that was adopted by this study to compute the snow cover gives in general higher values than the ones estimated by GEM. Differences can be explained by the fact that the orthophotos do not cover part of the study area (around 14%) as well by the weaknesses of the method proposed in this study, as they were discussed in chapter 5.2. The snow cover maps created with the resampling method are included in Figure 49 of Appendix E.

5.4. ACTIVE LAYER THICKNESS AND PHOTOSYNTHETIC ACTIVITY

The increasing trend in active layer thickness that has been detecting at both monitoring sites in previous studies (Christiansen et al. 2008; Elberling et al. 2013) has continued also during the last years.

The temporal break-up regression analysis between the variables of early season and seasonal mean NDVI vs. the depth of active layer in late season showed no correlation between them. However, this finding is in accordance with previous studies that agree on the fact that active layer thickness is dependent on a number of different factors (Gangodagamage et al. 2014) and that air temperature is the factor that mainly affects the thickness of active layer (Christiansen et al. 2008; Oht 2003).

5.5. METHODOLOGY DISCUSSION AND FUTURE PROSPECTS

Apart from corroborating the existing scientific bibliography on climatic changes in the arctic regions and more in particular in Greenland, this study's innovation and main strength is the attempt to associate crucial climatic parameters of the far northern latitude areas with the vegetation changes. This attempt is characterized as successful, regarding the interesting results found, facilitating the explanation of vegetation variation by the properties of snow and permafrost, crucial climatic factors of the arctic regions.

Moreover, the methodology that was followed is believed to have taken into consideration different aspects of the studied phenomena and is supported by theories of statistics and statistical analysis (Shaw and Wheeler 1994; Moore et al. 2009; Devore 2015). Regression analysis performed in this study provided linear equations that explain the level of relation between the studied datasets and could potentially be used in modeling snow and permafrost properties from vegetation indices, like NDVI.

The spatial and temporal resolution of the satellite images proved to be a weakness in the per-pixel regression statistical analysis. The spatial resolution of MODIS seems rather coarse to detect changes in a phenomenon that is radically changing in time and cells of 231*231 m are too big to be able to explain the changes. However, the selected satellite images were adequate for obtaining statistical mean values from them.

The per pixel snow depth regression statistical analysis was only performed for a time period of 16 days between May 25 and June 9, due to lack of ground truth data expanding throughout the whole early summer period. Moreover, there were not adequate data for three of the years of the study period and therefore snow depth could not be analyzed for the whole of the study period. Finally, parameters other than geomorphological were not taken into consideration for the extrapolation of the snow depth due to lack of data in such a small scale and time limitation.

Regression analysis on active layer thickness contains a level of uncertainty due to the fact that active layer depth monitoring is limited to the two ZeroCALM stations, with measurements covering an area of 2.8 km^2, which is relatively small compared to the study area. Moreover, the measurements are not evenly distributed across Musk Ox census study area. However, extrapolation of the values of active layer depth was not feasible regarding the poor spatial distribution of the data.

Linear models were chosen for the performed statistical analysis for reasons of adequate goodness of fit to the datasets after primary visual inspection. Moreover, linear models are easier to be understood, presented and especially manipulated in R studio. However, use of other types of models might have been able to explain better the behavior of particular datasets (for instance active layer thickness in late season vs. early season NDVI) and a comparison between the results of different models would be an interesting future research.

Considering the drawbacks and limitations of this study as they were stressed above, possible further research on this topic should take into account the following:

The measuring technique for snow depth could be enhanced with the use of airborne laser altimetry (LIDAR technology), which would add accuracy and above all spatial continuity in the measuring of snow depth. In addition, harmonization and /or expansion of the length of snow depth measuring period to one and a half month time-window (between early May and late June) in order to be able to perform statistical analysis for a larger period could add accuracy to the results. Furthermore, satellite images of higher spatial and temporal resolution compared to MODIS would help to analyze the phenomena in time periods smaller than 16 days and in more detailed spatial extent than 231*231 m.

Apart from elevation, which was the only geomorphological parameter that was taken into consideration in this study in order to predict the values of snow depth, analysis of more geomorphological parameters that may affect snow properties and especially snow accumulation and therefore snow depth, namely slope, aspect, curvature could enhance the results. Moreover, measurement and analysis of non-geomorphological parameters that may affect snow accumulation and active layer thickness, such as local temperatures, local wind conditions and microclimate parameters could also be studied.

In this study simple linear regression was used to detect correlations between two variables at each time. A future research prospect could be the use of multiple regression analysis that would take into consideration more than two variables at a time, such as the parameters mentioned above (geomorphological and non-geomorphological). Furthermore, models other than linear could be used, like polynomial or logarithmic.

6. CONCLUSIONS

This study showed that snow is a parameter that affects the photosynthetic activity in Zackenberg study area and added up to the scientific findings that snow is a factor of high importance for the climate ecosystem dynamics in and around the arctic regions.

The results of the study answering the first research question show a slight decreasing trend in the inter-annual average values of the vegetation index. The variation seems more intense for the start and the end of the growing season, where more intense fluctuation in NDVI was observed. Differences between the duration (length) of growing season also were detected, not showing a particular increasing/ decreasing trend though.

Regarding the second research question stated, this study showed that there is correlation between snow depth and snow cover expressed by the ground measured data and photosynthetic activity expressed by NDVI and that snow affects the seasonal vegetation. On the other hand the role of photosynthetic activity to the thickness of active layer seems to be rather secondary.

Without any doubt, snow depth is a cumbersome parameter to be explained as it seems to depend on many factors not considered in this study due to limitations in time and data; hence the method followed in this study can only to some extent explain snow depth and its relation to photosynthetic activity.

However, the overall results of the study are believed to be confident at some extent to be used in estimation and modeling of snow properties from remote sensing and the use of satellite imagery as well as in the prediction of the influence of early season snow conditions to the later seasonal vegetation activity.

REFERENCES

ACIA. 2005. Arctic climate impact assessment. 1042. Cambridge: Cambridge University Press.

Asrar, G., M. Fuchs, E. T. Kanemasu, and J. L. Hatfield. 1984. Estimating Absorbed Photosynthetic Radiation and Leaf Area Index from Spectral Reflectance in Wheat1. *Agron. J.,* 76**:** 300-306.

Bamzai, A. S. 2003. Relationship between snow cover variability and arctic pscillation index on a hierarchy of time scales. *Internationla Journal on climatology,* 23**:** 131-142. DOI: 10.1002/joc.854

Bay, C., 1998. Vegetation mapping of Zackenberg valley, northeast Greenland. Report. [in Swedish, English summary]

Belzile, C., W. F. Vincent, J. A. E. Gibson, and P. Van Hove. 2001. Bio-optical characteristics of the snow, ice, and water column of an perennially ice-covered lake in the High Arctic. *Canadian Journal of Fisheries & Aquatic Sciences,* 58**:** 2405.

Bliss, L., and W. Gold. 1999. Vascular plant reproduction, establishment, and growth and the effects of cryptogamic crusts within a polar desert ecosystem, Devon Island, NWT, Canada. *Canadian Journal of Botany,* 77**:** 623-636.

Bosiö, J., C. Stiegler, M. Johansson, H. Mbufong, and T. Christensen. 2014. Increased photosynthesis compensates for shorter growing season in subarctic tundra—8 years of snow accumulation manipulations. *Climatic Change,* 127**:** 321-334. DOI: 10.1007/s10584-014-1247-4

Brown, J., O. Ferrians, J. A. Hegingbottom, and E. Melnikov. 1998, revised February 2001. Circum-Arctic Map of Permafrost and Ground-Ice Conditions. Colorado, USA: National snow and ice data center.

Buus-Hinkler, J., B. U. Hansen, M. P. Tamstorf, and S. B. Pedersen. 2006. Snow-vegetation relations in a High Arctic ecosystem: Inter-annual variability inferred from new monitoring and modeling concepts. *Remote Sensing of Environment,* 105**:** 237-247.

Callaghan, T., M. Johansson, T. Prowse, M. Olsen, and L.-O. Reiersen. 2011. Arctic cryosphere: changes and impacts. *Ambio,* 40**:** 3-5.

CAVMTeam. 2003. Circumpolar Arctic Vegetation Map. In *Conservation of Arctic Flora and Fauna (CAFF) Map No. 1*. Anchorage, Alaska: U.S Fish and Wildlife Service.

Chen, X., and W. Pan. 2002. Relationships among phenological growing season, time-integrated normalized difference vegetation index and climate forcing in the temperate region of eastern China. *International Journal of Climatology,* 22**:** 1781-1792. DOI: 10.1002/joc.823

Christiansen, H. H., C. Sigsgaard, O. Humlum, M. Rasch, and B. U. Hansen. 2008. Permafrost and Periglacial Geomorphology at Zackenberg. In *Advances in Ecological Research,* eds. T. R. C. B. E. M. C. F. Hans Meltofte, and R. Morten, 151-174 pp.: Academic Press.

Colla, V., M. Vannucci, and L. M. Reyneri. 2015. Artificial neural networks applied for estimating a probability density function. *Intelligent Data Analysis,* 19**:** 29-41.

Cowie, J. 2013. *Climate change : biological and human aspects*. Cambridge : Cambridge University Press, 2013 2nd ed.
Crawford, R. M. M. 2008. *Plants at the margin : ecological limits and climate change*. Cambridge : Cambridge Univ. Press, 2008.
Devore, J. 2015. *Probability and Statistics for Engineering and the Sciences*. Cengage Learning.
Elberling, B., A. Michelsen, C. Schadel, E. A. G. Schuur, H. H. Christiansen, L. Berg, M. P. Tamstorf, and C. Sigsgaard. 2013. Long-term CO2 production following permafrost thaw. *Nature Clim. Change,* 3**:** 890-894. DOI: 10.1038/nclimate1955
Elberling, B., C. Nordstrøm, L. Grøndahl, H. Søgaard, T. Friborg, T. R. Christensen, L. Ström, F. Marchand, et al. 2008a. High-Arctic Soil CO2 and CH4 Production Controlled by Temperature, Water, Freezing and Snow. In *Advances in Ecological Research,* eds. T. R. C. B. E. M. C. F. Hans Meltofte, and R. Morten, 441-472 pp.: Academic Press.
Elberling, B., M. P. Tamstorf, A. Michelsen, M. F. Arndal, C. Sigsgaard, L. Illeris, C. Bay, B. U. Hansen, et al. 2008b. Soil and Plant Community-Characteristics and Dynamics at Zackenberg. In *Advances in Ecological Research,* eds. T. R. C. B. E. M. C. F. Hans Meltofte, and R. Morten, 223-248 pp.: Academic Press.
Ellebjerg, S. M., M. P. Tamstorf, L. Illeris, A. Michelsen, and B. U. Hansen. 2008. Inter-Annual Variability and Controls of Plant Phenology and Productivity at Zackenberg. In *Advances in Ecological Research,* eds. T. R. C. B. E. M. C. F. Hans Meltofte, and R. Morten, 249-273 pp.: Academic Press.
Elmendorf, S. C., G. H. Henry, R. D. Hollister, R. G. Björk, A. D. Bjorkman, T. V. Callaghan, L. S. Collier, E. J. Cooper, et al. 2012. Global assessment of experimental climate warming on tundra vegetation: heterogeneity over space and time. *Ecology Letters,* 15**:** 164-175.
Forchhammer, M. C., T. R. Christensen, B. U. Hansen, M. P. Tamstorf, N. M. Schmidt, T. T. Høye, J. Nabe-Nielsen, M. Rasch, et al. 2008. Zackenberg in a Circumpolar Context. In *Advances in Ecological Research,* eds. T. R. C. B. E. M. C. F. Hans Meltofte, and R. Morten, 499-544 pp.: Academic Press.
French, H. 2007. *The periglacial environment*. England: John Wiley and Sons.
Gacitúa, G., C. Bay, M. R. Pedersen, and M. P. Tamstorf. 2013. Quantifying snow and vegetation interactions in the high arctic based on ground penetrating radar (GPR). *Arctic, Antarctic, and Alpine Research,* 45**:** 201-210.
Gangodagamage, C., J. C. Rowland, S. S. Hubbard, S. P. Brumby, A. K. Liljedahl, H. Wainwright, C. J. Wilson, G. L. Altmann, et al. 2014. Extrapolating active layer thickness measurements across Arctic polygonal terrain using LiDAR and NDVI data sets. *Water resources research,* 50**:** 6339-6357.
Groisman, P. Y., T. R. Karl, and R. W. Knight. 1994. Observed Impact of Snow Cover on the Heat Balance and the Rise of Continental Spring Temperatures. *Science,* 263**:** 198-200. DOI: 10.2307/2882373
Hansen, B. U., C. Sigsgaard, L. Rasmussen, J. Cappelen, J. Hinkler, S. H. Mernild, D. Petersen, M. P. Tamstorf, et al. 2008. Present-Day Climate at Zackenberg. In *Advances in Ecological Research,* eds. T. R. C. B. E. M. C. F. Hans Meltofte, and R. Morten, 111-149 pp.: Academic Press.

Hinkler, J., B. U. Hansen, M. P. Tamstorf, C. Sigsgaard, and D. Petersen. 2008. Snow and Snow-Cover in Central Northeast Greenland. In *Advances in Ecological Research,* eds. T. R. C. B. E. M. C. F. Hans Meltofte, and R. Morten, 175-195 pp.: Academic Press.

Hinkler, J., S. B. Pedersen, M. Rasch, and B. U. Hansen. 2002. Automatic snow cover monitoring at high temporal and spatial resolution, using images taken by a standard digital camera. *International Journal of Remote Sensing,* 23**:** 4669-4682. DOI: 10.1080/01431160110113881

Houghton, J. T., G. J. Jenkins, and J. J. Ephraums. 1990. *Climate change : the IPCC scientific assessement*. Cambridge : Published for the Intergovernmental Panel on Climate Change [by] Cambridge University Press, 1990.

Høye, T. T., E. Post, H. Meltofte, N. M. Schmidt, and M. C. Forchhammer. 2007. Rapid advancement of spring in the High Arctic. *Current Biology,* 17**:** R449-R451.

Huettmann, F. 2009. " High-Arctic Ecosystem Dynamics in a Changing Climate: Ten Years of Monitoring and Research at Zackenberg Research Station, Northeast Greenland. Advances in Ecological Research (Volume 40)" edited by H. Meltofte et al. 2008.[book review]. *The Canadian Field-Naturalist,* 123**:** 88-89.

Hurrell, J. W. 1995. Decadal Trends in the North Atlantic Oscillation: Regional Temperatures and Precipitation. *Science,* 269**:** 676-679. DOI: 10.2307/2888966

IPCC. 2007. *Climate Change 2007: the physical science basis*. USA: Cambridge Univeristy Press, Cambridge, United Kingdom and New York.

IPCC. 2013. *Climate Change 2013: The Physical Science Basis. Contribution of Working Group I to the Fifth Assessment Report of the Intergovernmental Panel on Climate Change* USA: Cambridge Univeristy Press, Cambridge, United Kingdom and New York.

Jeffries, M. O., J. Richter-Menge, and J. E. Overlands, Eds. 2014. Arctic Report Card 2014. Retrieved, from. http://www.arctic.noaa.gov/reportcard

Jensen, L. M., T. R. Christensen, and N. M. Schmidt. 2014. Zackenberg ecological research operations 19th annual report 2013. 130. Aarhus University, DCE-Danish Centre for Environment and Energy.

Jones, H. 1999. The ecology of snow-covered systems: a brief overview of nutrient cycling and life in the cold. *Hydrological processes,* 13**:** 2135-2147.

Karlsen, S., A. Elvebakk, K. Høgda, and T. Grydeland. 2014. Spatial and Temporal Variability in the Onset of the Growing Season on Svalbard, Arctic Norway — Measured by MODIS-NDVI Satellite Data. *Remote Sensing,* 6**:** 8088.

Kiilsholm, S., J. H. Christensen, K. Dethloff, and A. Rinke. 2003. Net accumulation of the Greenland ice sheet: High resolution modeling of climate changes. *Geophysical Research Letters,* 30**:** n/a.

Kjærgaard, K. 2015. Religious Education, Identity and Nation Building–the Case of Greenland. *Nordidactica: Journal of Humanities and Social Science Education***:** 114-130.

Kriegler, F. J., W. A. Malila, R. F. Nalepka, and W. Richardson. 1969. Preprocessing Transformations and Their Effects on Multispectral Recognition. In *Sixth International Symposium on Remote Sensing of Environment,*. Infrared and Optics Laboratory, Willow Run Laboratories, Environmental Research Institute of Michigan.

Letcher, T. M. 2009. *Climate change. [Elektronisk resurs] : observed impacts on planet Earth*. Amsterdam : Elsevier, 2009.
Lillesand, T. M., R. W. Kiefer, and J. W. Chipman. 2004. *Remote sensing and image interpretation* New York: Wiley, cop.
Luus, K., Y. Gel, J. Lin, R. Kelly, and C. Duguay. 2013. Pan-Arctic linkages between snow accumulation and growing-season air temperature, soil moisture and vegetation. *Biogeosciences,* 10**:** 7575-7597.
Maxwell, B. 1992. 2 - Arctic Climate: Potential for Change under Global Warming. In *Arctic Ecosystems in a Changing Climate,* ed. F. S. C. L. J. F. R. R. S. S. W. Chu, 11-34 pp. San Diego: Academic Press.
Meltofte, H., and M. Rasch. 2008. The Study Area at Zackenberg. In *Advances in Ecological Research,* eds. T. R. C. B. E. M. C. F. Hans Meltofte, and R. Morten, 101-110 pp.: Academic Press.
Mernild, S. H., G. E. Liston, and B. Hasholt. 2007. Snow-distribution and melt modelling for glaciers in Zackenberg river drainage basin, north-eastern Greenland. *Hydrological processings,* 21**:** 3249–3263. DOI: 10.1002/hyp.6500
Moore, D., G. McCabe, and B. Craig. 2009. *Introduction to the practice of statistics*. New York: Bruth Ruth.
Myneni, R. B., C. D. Keeling, C. J. Tucker, G. Asrar, and R. R. Nemani. 1997. Increased plant growth in the northern high latitudes from 1981 to 1991. *Nature,* 386**:** 698-702.
Oht, M. 2003. Impact of meteorological factors on active layer development in Central Spitsbergen. In *Proceedings 8th International Permafrost Conference, Zürich, Switzerland*, 845-850.
Perdersen, C., H. Gotzsche, J. Moller, and P. Mortensen. 2006. The Danish Civil Registration System. A cohort of eight million persons. *Danish Medical Bulletin,* 53**:** 441-449.
Post, E., M. C. Forchhammer, M. S. Bret-Harte, T. V. Callaghan, T. R. Christensen, B. Elberling, A. D. Fox, O. Gilg, et al. 2009. Ecological dynamics across the Arctic associated with recent climate change. *Science,* 325**:** 1355-1358.
Rasch, M., N. M. Schmidt, and T. Juul-Pedersen. 2012. Greenland Ecosystem Monitoring Strategy and working programme 2011-2015. 82. Aarhus University, DCE – Danish Centre for Environment and Energy.
Reynolds, J. F., and J. D. Tenhunen. 1996. Ecosystem Response, Resistance, Resilience, and Recovery in Arctic Landscapes: Introduction. *Landscape Function and Disturbance in Arctic Tundra. Ecological studies,* 120**:** 3-18.
Rixen, C., M. Freppaz, V. Stoeckli, C. Huovinen, K. Huovinen, and S. Wipf. 2008. Altered snow density and chemistry change soil nitrogen mineralization and plant growth. *Arctic, Antarctic, and Alpine Research,* 40**:** 568-575.
Rysgaard, S., T. Vang, M. Stjernholm, B. Rasmussen, A. Windelin, and S. Kiilsholm. 2003. Physical Conditions, Carbon Transport, and Climate Change Impacts in a Northeast Greenland Fjord. *Arctic, Antarctic, and Alpine Research,* 35**:** 301-312.
Shaw, G., and D. Wheeler. 1994. *Statistical techniques in Geographical Analysis*. London: David Fulton Publishers Ltd.
Sigsgaard, C., M. R. Mylius, and K. Skov. 2014. Zackenberg Ecological Research Operations GeoBasis Guidelines and sampling procedures for the geographical

monitoring programme of Zackenberg Basic. Department of Bioscience, Aarhus University & Department of Geosciences and Natural Resource Management, University of Copenhagen.

Stow, D. A., A. Hope, D. McGuire, D. Verbyla, J. Gamon, F. Huemmrich, S. Houston, C. Racine, et al. 2004. Remote sensing of vegetation and land-cover change in Arctic Tundra Ecosystems. *Remote Sensing of Environment*, 89**:** 281-308.

Tucker, C. J. 1979. Red and photographic infrared linear combinations for monitoring vegetation. *Remote Sensing of Environment,* 8**:** 127-150.

Tucker, C. J., D. A. Slayback, J. E. Pinzon, S. O. Los, R. B. Myneni, and R. B. Myneni. 2001. Higher northern latitude normalized difference vegetation index and growing season trends from 1982 to 1999. *International Journal of Biometeorology* 45**:** 184-190. DOI: 10.1007/s00484-001-0109-8

Vrieling, A., J. de Leeuw, and M. Said. 2013. Length of Growing Period over Africa: Variability and Trends from 30 Years of NDVI Time Series. *Remote Sensing,* 5**:** 982.

Walker, D., J. C. Halfpenny, M. D. Walker, and C. A. Wessman. 1993. Long-term studies of snow-vegetation interactions. *BioScience***:** 287-301.

Walker, M., D. Walker, J. Welker, A. Arft, T. Bardsley, P. Brooks, J. Fahnestock, M. Jones, et al. 1999. Long-term experimental manipulation of winter snow regime and summer temperature in arctic and alpine tundra. *Hydrological processes,* 13**:** 2315-2330.

White, M., P. Thorton, and S. Running. 1997. A continental phenology model for monitoring vegetation responses to interannual climatic variability. *Global Biogeochemical Cycles,* 11. DOI: 10.1029/97GB00330

Xu, L., R. Myneni, F. Chapin Iii, T. Callaghan, J. Pinzon, C. Tucker, Z. Zhu, J. Bi, et al. 2013. Temperature and vegetation seasonality diminishment over northern lands. *Nature Climate Change,* 3**:** 581-586.

Zackenbergsecretariat. 2013. ZERO site manual Zackenberg Ecological Research Operations. Department of Bioscience Aarhus University.

Zhou, L., C. J. Tucker, R. K. Kaufmann, D. Slayback, N. V. Shabanov, and R. B. Myneni. 2001. Variations in northern vegetation activity inferred from satellite data of vegetation index during 1981 to 1999. *Journal of geophysic research,* 106**:** 20069-20083.

APPENDICES

APPENDIX A: MODIS employed products

Table 16: *MODIS 16-day composite satellite images*

MOD13Q1.A2005129.h17v01.005.2008033233719.hdf	MOD13Q1.A2010129.h17v01.005.2010147212043.hdf
MOD13Q1.A2005145.h17v01.005.2008233234136.hdf	MOD13Q1.A2010145.h17v01.005.2010165152256.hdf
MOD13Q1.A2005161.h17v01.005.2008044151144.hdf	MOD13Q1.A2010161.h17v01.005.2010179124631.hdf
MOD13Q1.A2005177.h17v01.005.2008204230253.hdf	MOD13Q1.A2010177.h17v01.005.2011018004238.hdf
MOD13Q1.A2005193.h17v01.005.2008216093623.hdf	MOD13Q1.A2010193.h17v01.005.2010212001552.hdf
MOD13Q1.A2005209.h17v01.005.2008060054145.hdf	MOD13Q1.A2010209.h17v01.005.2010238165206.hdf
MOD13Q1.A2005225.h17v01.005.2008214091158.hdf	MOD13Q1.A2010225.h17v01.005.2010251203134.hdf
MOD13Q1.A2005241.h17v01.005.2008066181557.hdf	MOD13Q1.A2010241.h17v01.005.2010259225810.hdf
MOD13Q1.A2005257.h17v01.005.2008218215858.hdf	MOD13Q1.A2010257.h17v01.005.2010283101832.hdf
MOD13Q1.A2005273.h17v01.005.2008074114111.hdf	MOD13Q1.A2010273.h17v01.005.2010291072418.hdf
MOD13Q1.A2006129.h17v01.005.2008321183233.hdf	MOD13Q1.A2011129.h17v01.005.2011154010023.hdf
MOD13Q1.A2006145.h17v01.005.2008122093316.hdf	MOD13Q1.A2011145.h17v01.005.2011164082555.hdf
MOD13Q1.A2006161.h17v01.005.2008234114047.hdf	MOD13Q1.A2011161.h17v01.005.2011179182032.hdf
MOD13Q1.A2006177.h17v01.005.2008133055154.hdf	MOD13Q1.A2011177.h17v01.005.2011213155410.hdf
MOD13Q1.A2006193.h17v01.005.2008138092841.hdf	MOD13Q1.A2011193.h17v01.005.2011210140342.hdf
MOD13Q1.A2006209.h17v01.005.2008100144632.hdf	MOD13Q1.A2011209.h17v01.005.2011226220334.hdf
MOD13Q1.A2006225.h17v01.005.2008104101430.hdf	MOD13Q1.A2011225.h17v01.005.2011242132149.hdf
MOD13Q1.A2006241.h17v01.005.2008105201916.hdf	MOD13Q1.A2011241.h17v01.005.2011258045947.hdf
MOD13Q1.A2006257.h17v01.005.2008112031206.hdf	MOD13Q1.A2011257.h17v01.005.2011274075416.hdf
MOD13Q1.A2006273.h17v01.005.2008273142752.hdf	MOD13Q1.A2011273.h17v01.005.2011292225756.hdf
MOD13Q1.A2007129.h17v01.005.2007154060908.hdf	MOD13Q1.A2012129.h17v01.005.2012146134322.hdf
MOD13Q1.A2007145.h17v01.005.2007182154231.hdf	MOD13Q1.A2012145.h17v01.005.2012166150707.hdf
MOD13Q1.A2007161.h17v01.005.2007186080744.hdf	MOD13Q1.A2012161.h17v01.005.2012178090404.hdf
MOD13Q1.A2007177.h17v01.005.2007207112225.hdf	MOD13Q1.A2012177.h17v01.005.2012209031736.hdf
MOD13Q1.A2007193.h17v01.005.2007217191654.hdf	MOD13Q1.A2012193.h17v01.005.2012212162450.hdf
MOD13Q1.A2007209.h17v01.005.2007233015934.hdf	MOD13Q1.A2012209.h17v01.005.2012228232202.hdf
MOD13Q1.A2007225.h17v01.005.2007247070554.hdf	MOD13Q1.A2012225.h17v01.005.2012242094024.hdf
MOD13Q1.A2007241.h17v01.005.2007263192607.hdf	MOD13Q1.A2012241.h17v01.005.2012258061040.hdf
MOD13Q1.A2007257.h17v01.005.2007279071849.hdf	MOD13Q1.A2012257.h17v01.005.2012275131237.hdf
MOD13Q1.A2007273.h17v01.005.2009165215027.hdf	MOD13Q1.A2012273.h17v01.005.2012299111741.hdf
MOD13Q1.A2008129.h17v01.005.2008149230458.hdf	MOD13Q1.A2013129.h17v01.005.2013146130752.hdf
MOD13Q1.A2008145.h17v01.005.2008163110230.hdf	MOD13Q1.A2013145.h17v01.005.2013162150654.hdf
MOD13Q1.A2008161.h17v01.005.2008179051912.hdf	MOD13Q1.A2013161.h17v01.005.2013178201703.hdf
MOD13Q1.A2008177.h17v01.005.2008195124238.hdf	MOD13Q1.A2013177.h17v01.005.2013194150009.hdf
MOD13Q1.A2008193.h17v01.005.2008211015711.hdf	MOD13Q1.A2013193.h17v01.005.2013213234511.hdf
MOD13Q1.A2008209.h17v01.005.2008237200441.hdf	MOD13Q1.A2013209.h17v01.005.2013226134233.hdf
MOD13Q1.A2008225.h17v01.005.2008244055510.hdf	MOD13Q1.A2013225.h17v01.005.2013242163930.hdf
MOD13Q1.A2008241.h17v01.005.2008264085724.hdf	MOD13Q1.A2013241.h17v01.005.2013261020955.hdf
MOD13Q1.A2008257.h17v01.005.2008277091652.hdf	MOD13Q1.A2013257.h17v01.005.2013277224329.hdf
MOD13Q1.A2008273.h17v01.005.2008292073722.hdf	MOD13Q1.A2013273.h17v01.005.2013303135051.hdf
MOD13Q1.A2009129.h17v01.005.2009151110414.hdf	MOD13Q1.A2014129.h17v01.005.2014148011223.hdf
MOD13Q1.A2009145.h17v01.005.2009168131353.hdf	MOD13Q1.A2014145.h17v01.005.2014162003727.hdf
MOD13Q1.A2009161.h17v01.005.2009182143900.hdf	MOD13Q1.A2014161.h17v01.005.2014178102452.hdf
MOD13Q1.A2009177.h17v01.005.2009201233221.hdf	MOD13Q1.A2014177.h17v01.005.2014194110419.hdf
MOD13Q1.A2009193.h17v01.005.2009212130724.hdf	MOD13Q1.A2014193.h17v01.005.2014210191634.hdf.
MOD13Q1.A2009209.h17v01.005.2009228052157.hdf	MOD13Q1.A2014209.h17v01.005.2014226071652.hdf
MOD13Q1.A2009225.h17v01.005.2009249132309.hdf	MOD13Q1.A2014225.h17v01.005.2014242060919.hdf
MOD13Q1.A2009241.h17v01.005.2009260013850.hdf	MOD13Q1.A2014241.h17v01.005.2014275170254.hdf
MOD13Q1.A2009257.h17v01.005.2009276055131.hdf	MOD13Q1.A2014257.h17v01.005.2014279063302.hdf
MOD13Q1.A2009273.h17v01.005.2009307055845.hdf	MOD13Q1.A2014273.h17v01.005.2014297072608.hdf

APPENDIX B: NDVI 2005-2014

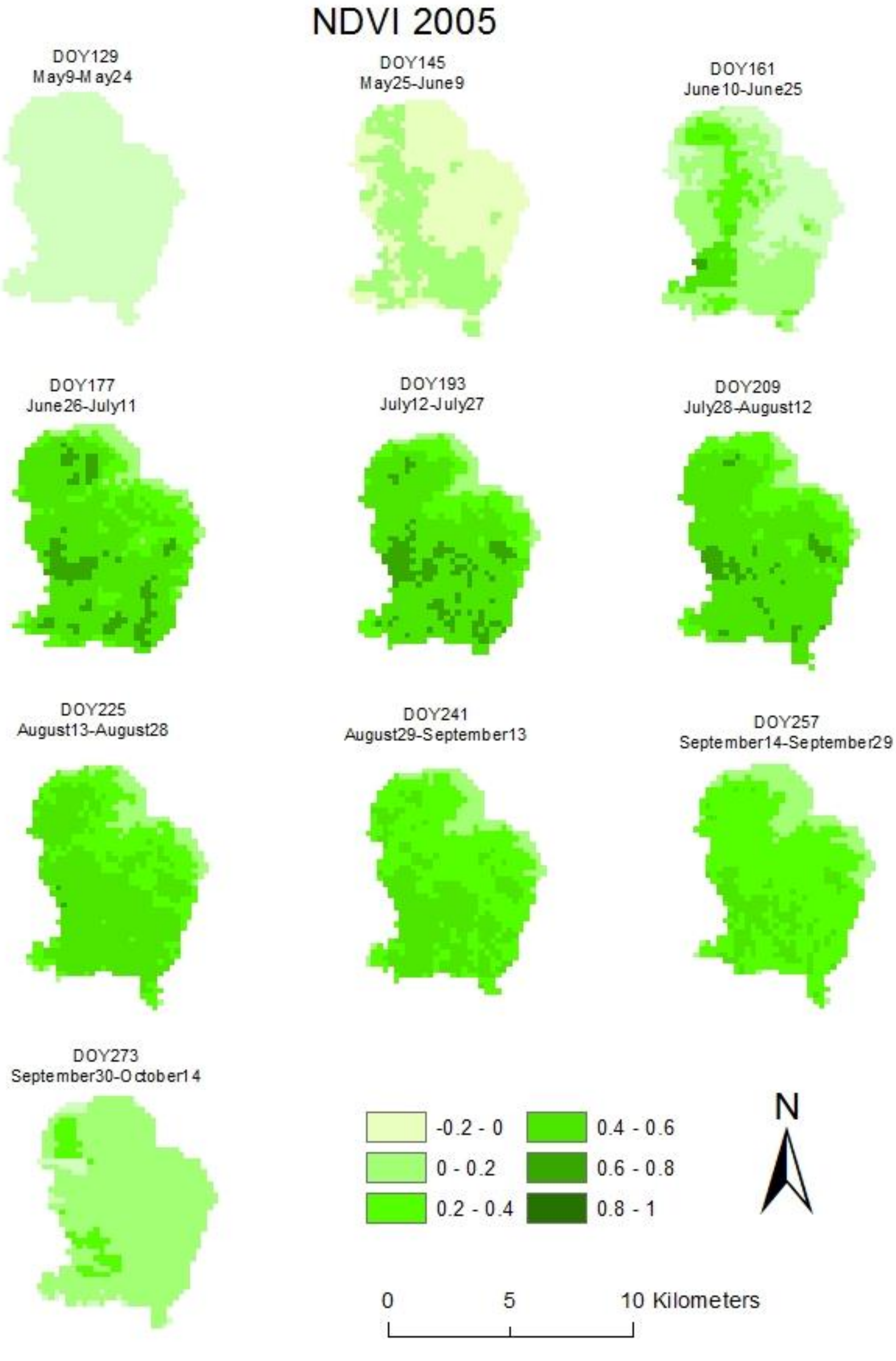

Figure 38: *16 day NDVI composites for year 2005.*

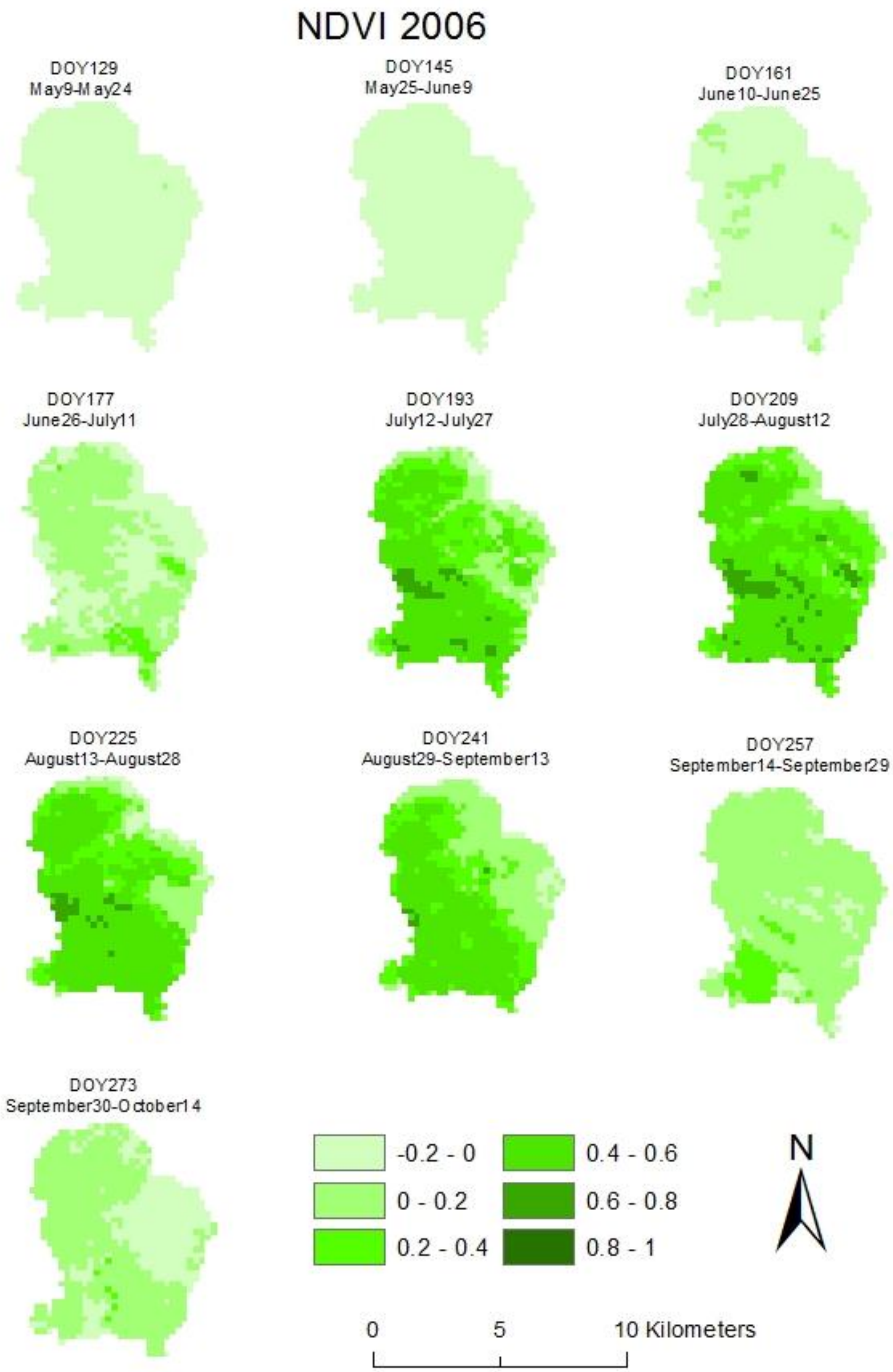

Figure 39: *16 day NDVI composites for year 2006.*

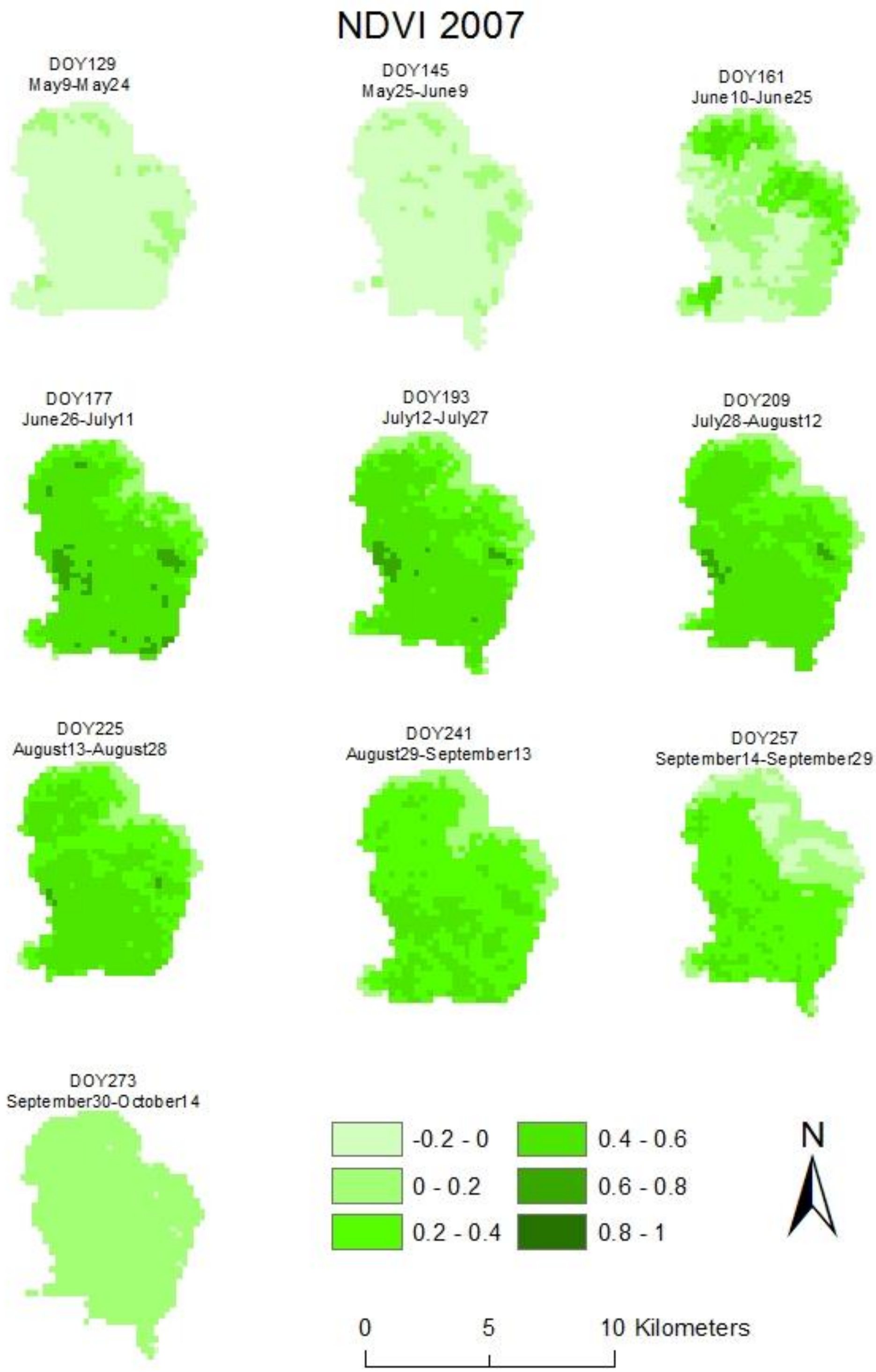

Figure 40: *16 day NDVI composites for year 2007.*

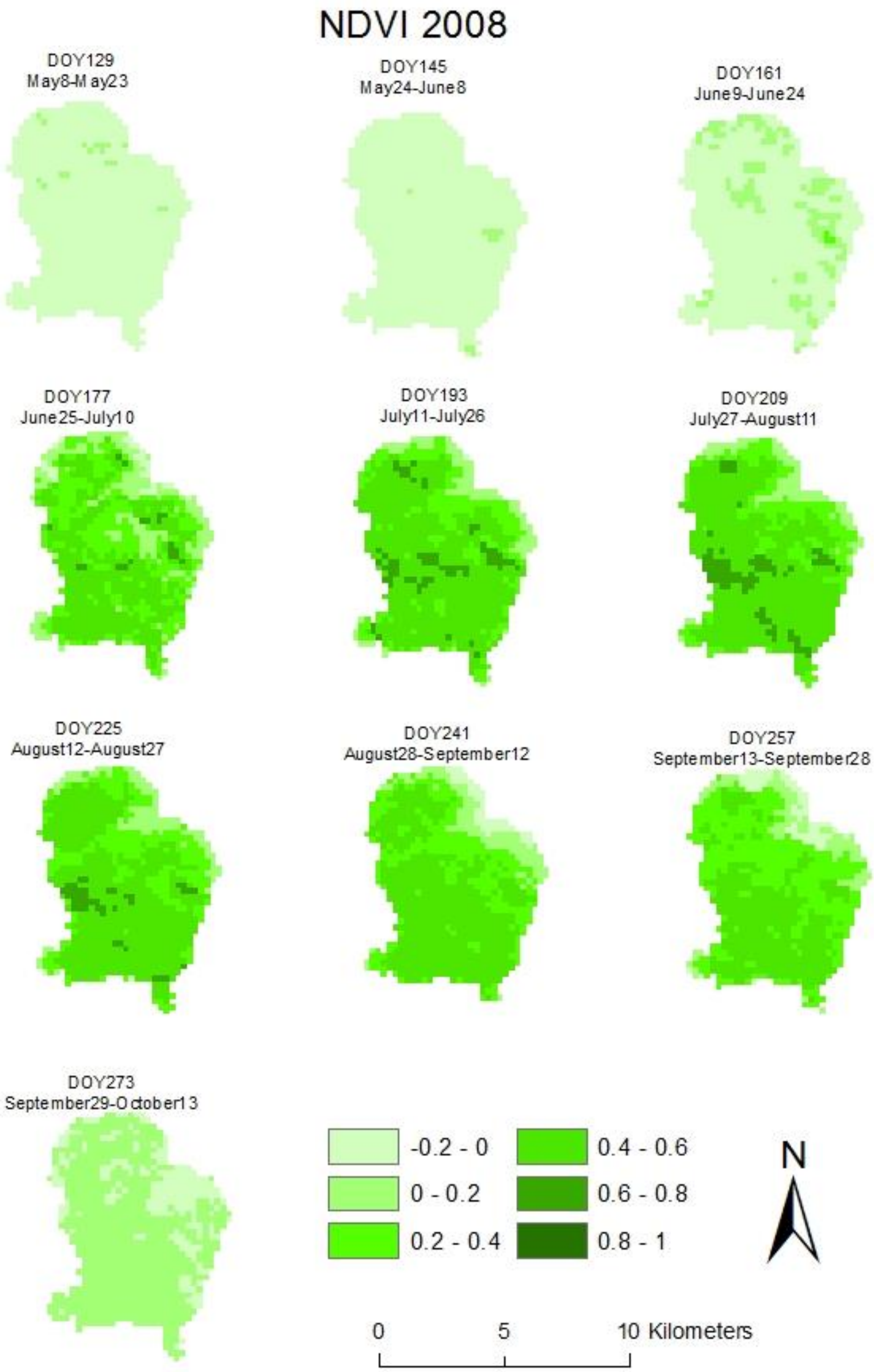

Figure 41: *16 day NDVI composites for year 2008.*

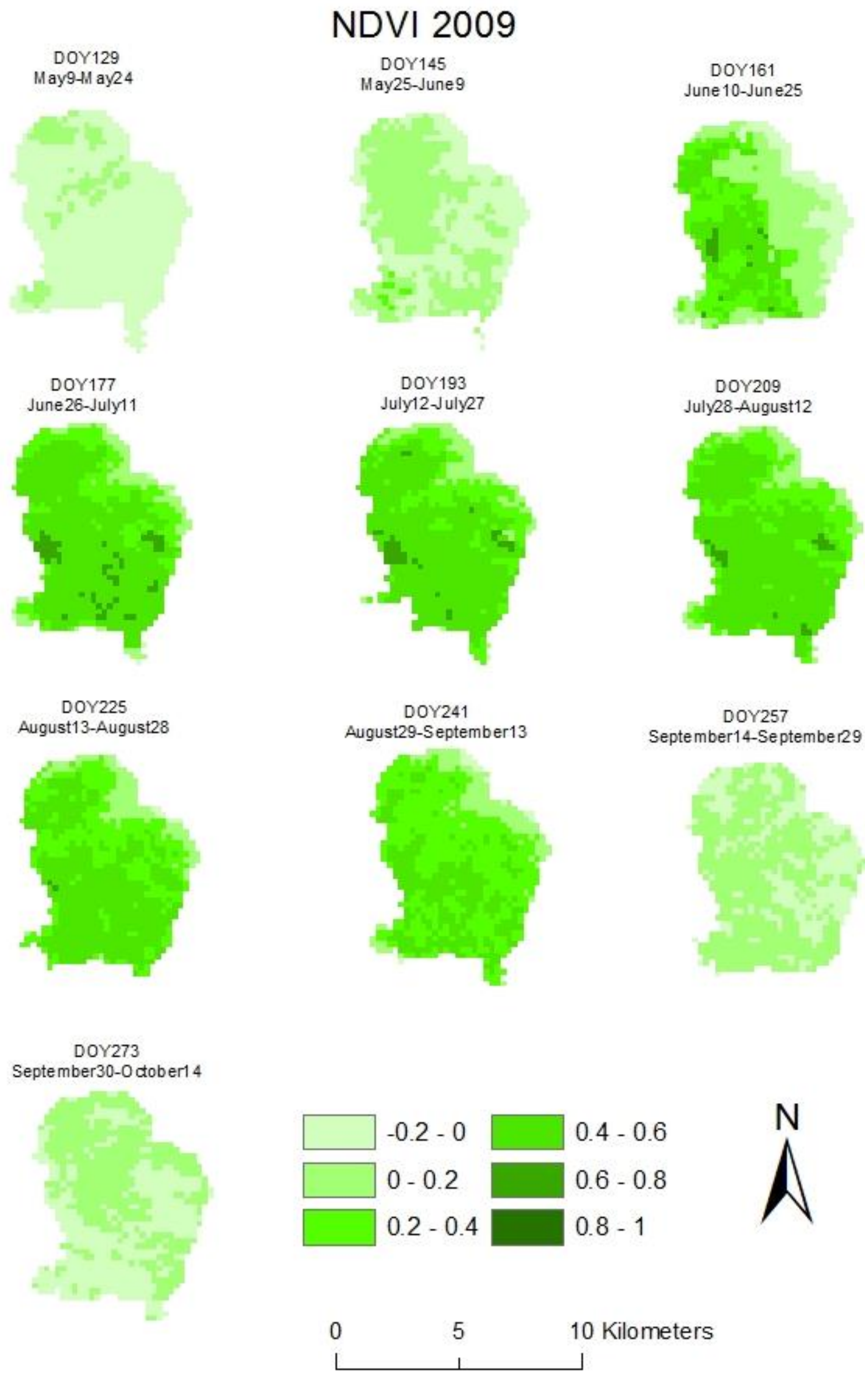

Figure 42: *16 day NDVI composites for year 2009.*

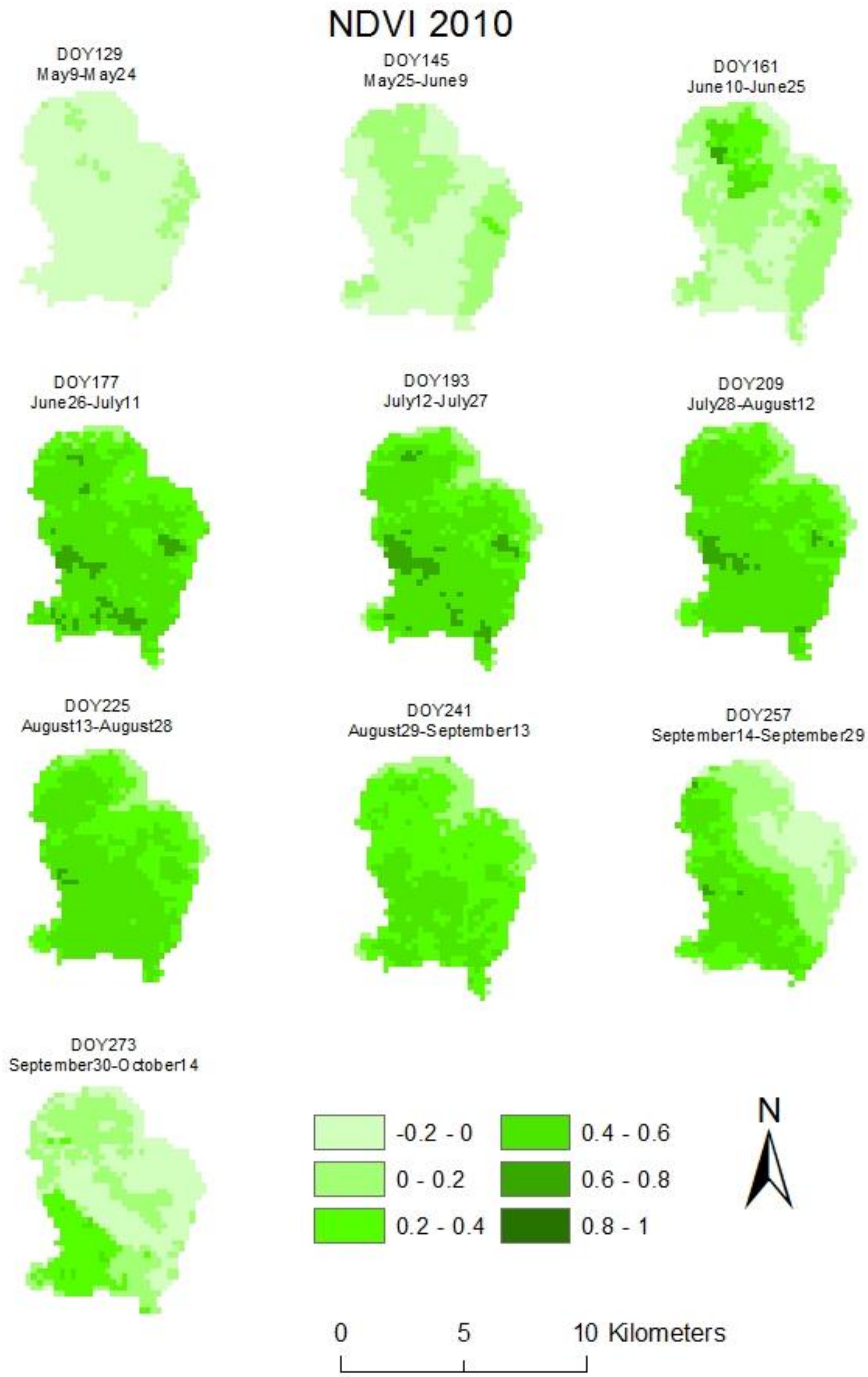

Figure 43: *16 day NDVI composites for year 2010.*

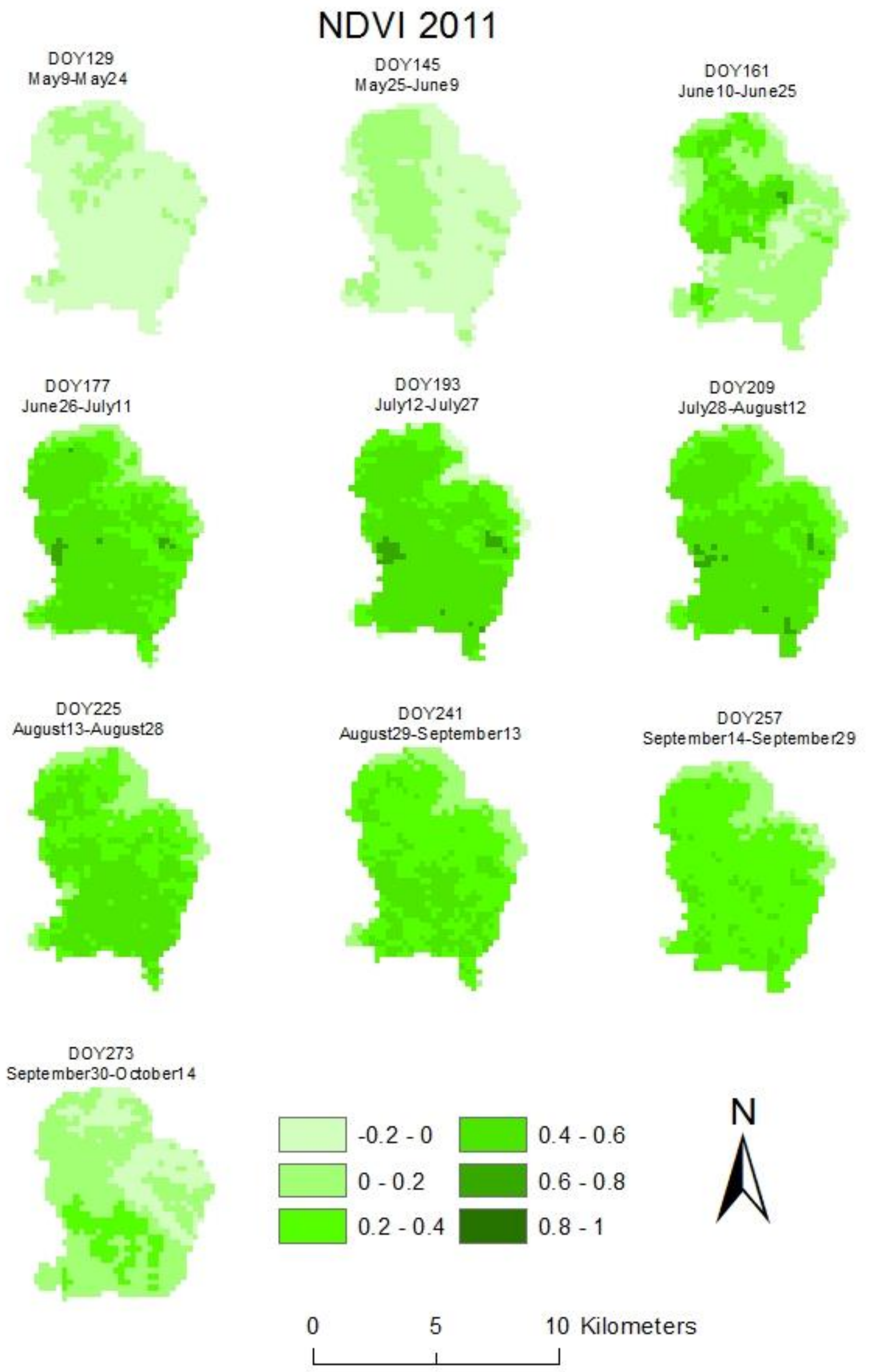

Figure 44: *16 day NDVI composites for year 2011.*

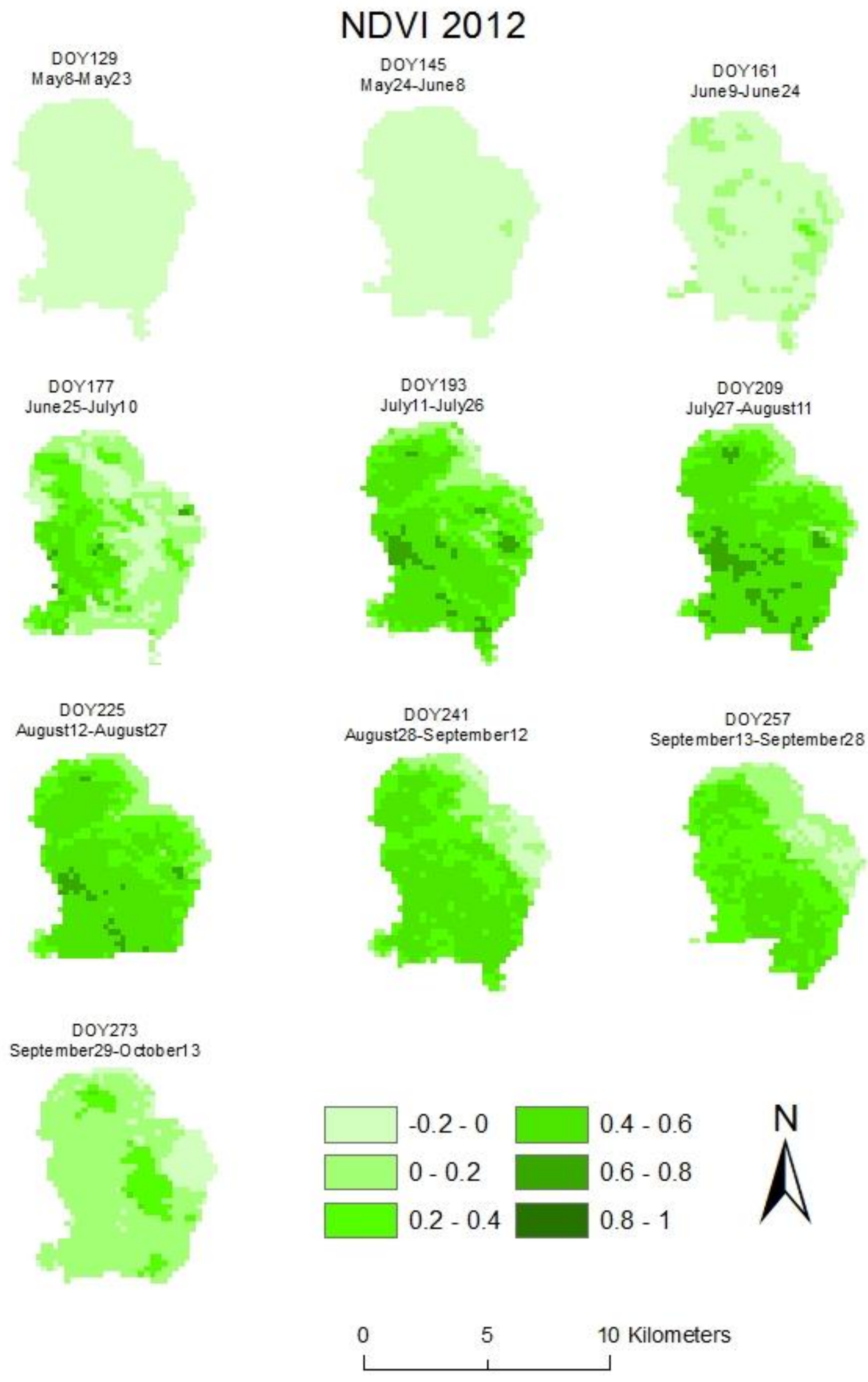

Figure 45: *16 day NDVI composites for year 2012.*

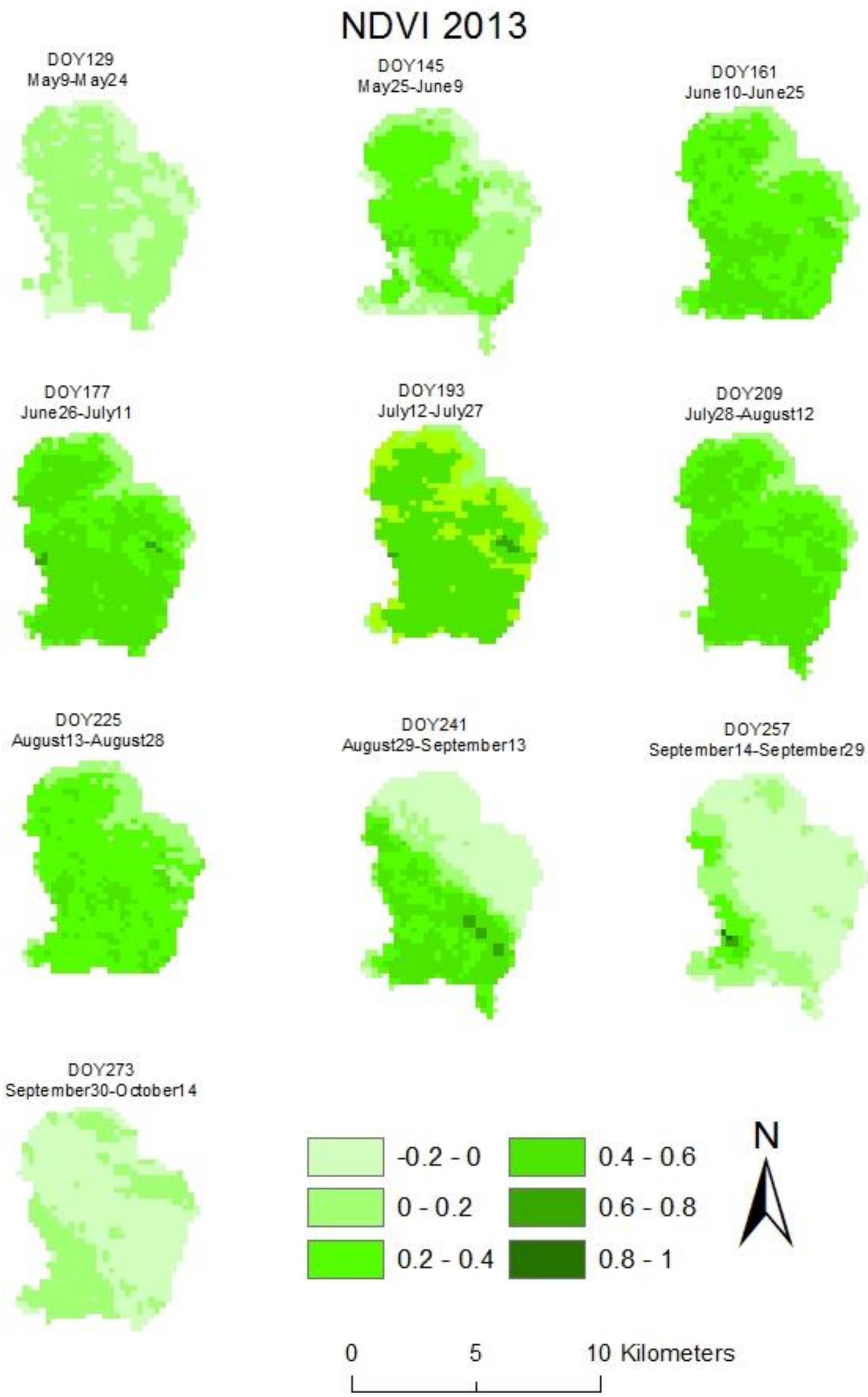

Figure 46: *16 day NDVI composites for year 2013.*

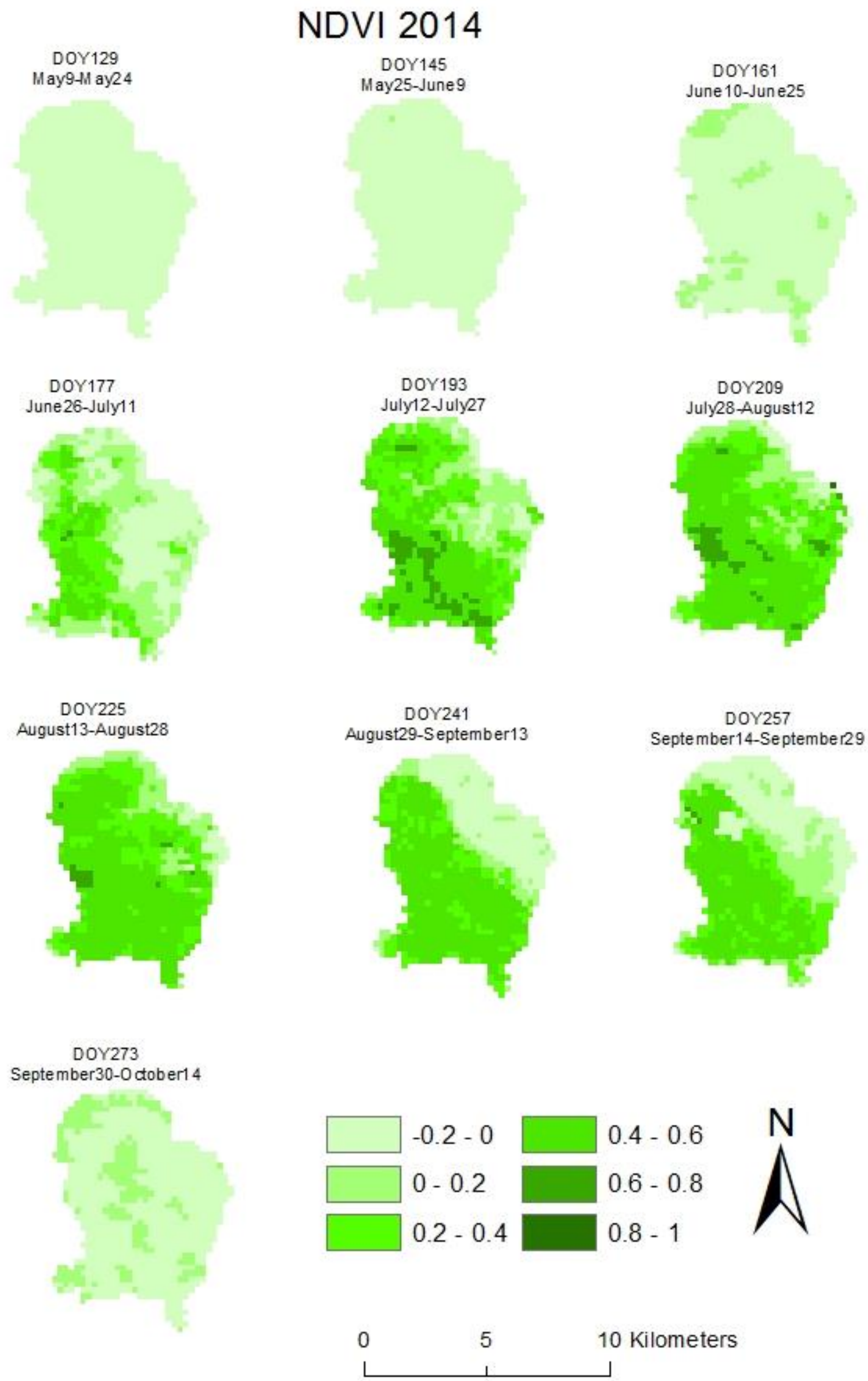

Figure 47: *16 day NDVI composites for year 2014.*

APPENDIX C: NDVI statistics from the satellite imagery

Table 17: *Satellite images statistics*

Year 2005

Date	Mean NDVI value	Seasonal mean NDVI
9-May	-0.017	
25-May	-0.007	0.264
10-Jun	0.093	
26-Jun	0.460	
12-Jul	0.480	**Seasonal**
28-Jul	0.470	**maximum NDVI**
13-Aug	0.400	
29-Aug	0.350	0.480
14-Sep	0.309	
30-Sep	0.097	

Year 2006

Date	Mean NDVI value	Seasonal mean NDVI
9-May	-0.030	
25-May	-0.049	0.150
10-Jun	-0.037	
26-Jun	0.033	
12-Jul	0.370	**Seasonal**
28-Jul	0.440	**maximum NDVI**
13-Aug	0.390	
29-Aug	0.310	0.440
14-Sep	0.059	
30-Sep	0.018	

Year 2007

Date	Mean NDVI value	Seasonal mean NDVI
9-May	-0.010	
25-May	-0.018	0.238
10-Jun	0.098	
26-Jun	0.464	
12-Jul	0.419	**Seasonal**
28-Jul	0.417	**maximum NDVI**
13-Aug	0.388	
29-Aug	0.330	0.464
14-Sep	0.239	
30-Sep	0.055	

Year 2008

Date	Mean NDVI value	Seasonal mean NDVI
8-May	-0.014	
24-May	-0.052	0.227
9-Jun	-0.023	
25-Jun	0.339	
11-Jul	0.443	**Seasonal**
27-Jul	0.447	**maximum NDVI**
12-Aug	0.423	
28-Aug	0.364	0.447
13-Sep	0.320	
29-Sep	0.019	

Year 2009

Date	Mean NDVI value	Seasonal mean NDVI
9-May	-0.023	
25-May	0.017	0.222
10-Jun	0.234	
26-Jun	0.435	
12-Jul	0.431	**Seasonal**
28-Jul	0.418	**maximum NDVI**
13-Aug	0.375	
29-Aug	0.330	0.435
14-Sep	0.004	
30-Sep	-0.001	

Year 2010

Date	Mean NDVI value	Seasonal mean NDVI
9-May	-0.015	
25-May	0.008	0.244
10-Jun	0.071	
26-Jun	0.457	
12-Jul	0.452	**Seasonal**
28-Jul	0.437	**maximum NDVI**
13-Aug	0.401	
29-Aug	0.338	0.457
14-Sep	0.232	
30-Sep	0.060	

Year 2011

Date	Mean NDVI value	Seasonal mean NDVI
9-May	-0.008	
25-May	0.002	0.248
10-Jun	0.158	
26-Jun	0.403	
12-Jul	0.436	**Seasonal maximum NDVI**
28-Jul	0.425	
13-Aug	0.363	
29-Aug	0.334	0.436
14-Sep	0.301	
30-Sep	0.066	

Year 2012

Date	Mean NDVI value	Seasonal mean NDVI
9-May	-0.020	
25-May	-0.039	0.203
10-Jun	-0.022	
26-Jun	0.157	
12-Jul	0.398	**Seasonal maximum NDVI**
28-Jul	0.450	
13-Aug	0.418	
29-Aug	0.335	0.450
14-Sep	0.286	
30-Sep	0.064	

Year 2013

Date	Mean NDVI value	Seasonal mean NDVI
9-May	0.013	
25-May	0.168	0.222
10-Jun	0.331	
26-Jun	0.398	
12-Jul	0.411	**Seasonal maximum NDVI**
28-Jul	0.387	
13-Aug	0.304	
29-Aug	0.203	0.411
14-Sep	0.011	
30-Sep	-0.011	

Year 2014

Date	Mean NDVI value	Seasonal mean NDVI
9-May	-0.022	
25-May	-0.042	0.152
10-Jun	-0.038	
26-Jun	0.121	
12-Jul	0.337	**Seasonal maximum NDVI**
28-Jul	0.386	
13-Aug	0.380	
29-Aug	0.277	0.386
14-Sep	0.238	
30-Sep	-0.119	

APPENDIX D: Snow cover regression analysis

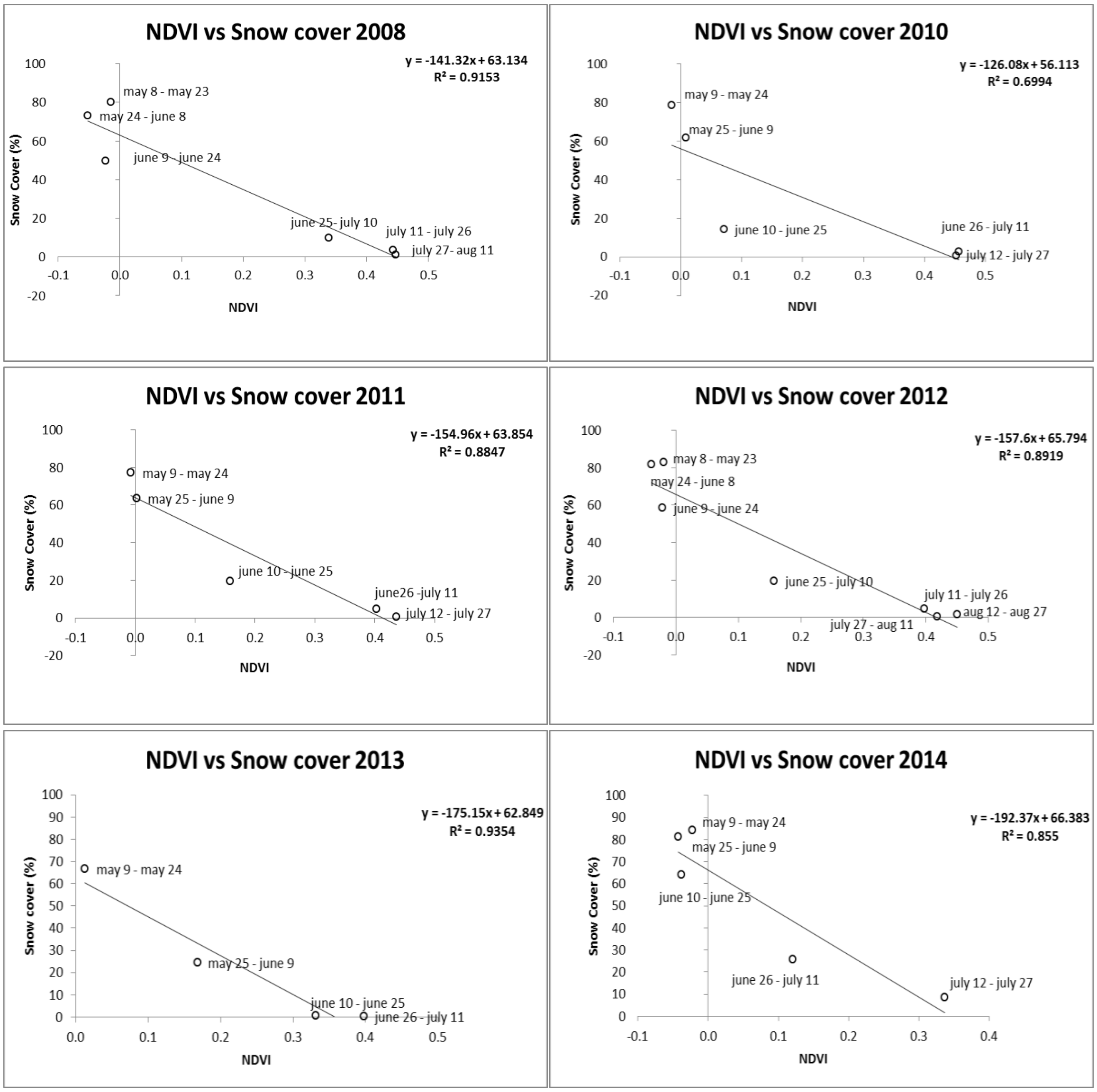

Figure 48: *Scatterplots of snow cover vs. NDVI (2008, 2010, 2011, 2012, 2013, and 2014).*

APPENDIX E: Snow cover 2006-2014 (created with resampling of snow depth rasters)

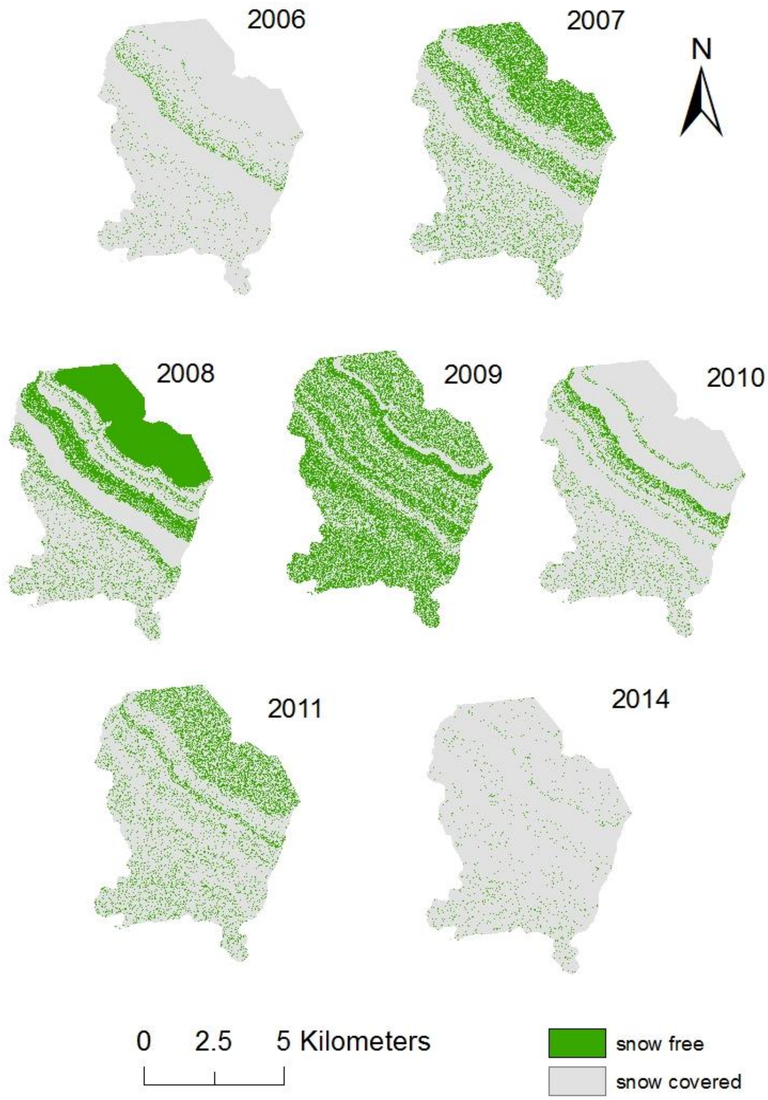

Figure 49: *Snow cover maps DOY145 (May 25- June 9) 2006-2014.*

APPENDIX F: Codes developed for the statistical analysis

Cell by cell regression analysis between NDVI and snow depth rasters DOY 145, year 2006

```
setwd("C:\\Users\\G.K\\Documents\\GEOMATICS\\THESIS\\ANALYSIS\\R\\SNOWDEPTH")
library(raster)

ndvi <- raster("ndvi2006.asc")
ndvi
plot(ndvi)

snowdepth <- raster("snowdepth2006.asc")
snowdepth
plot(snowdepth)

u<- stack(ndvi, snowdepth)
plot(u)

df.ndvi <- as.data.frame(ndvi)
df.ndvi <- na.omit(df.ndvi)
df.ndvi

df.snowdepth <- as.data.frame(snowdepth)
df.snowdepth <- na.omit(df.snowdepth)
df.snowdepth

df <- data.frame(df.ndvi,df.snowdepth)
df
x <- df[,1]
y <- df[,2]
plot (x,y,
    main = "NDVI vs. Snow depth 2006",
    xlab = "NDVI",
    ylab = "Snow depth")
names(df)

regr.model  <-lm(df$snowdepth2006 ~ df$ndvi2006)
summary(regr.model)
```

Regression analysis between mean NDVI and mean snow depth for DOY 145

```
setwd("C:\\Users\\G.K\\Documents\\GEOMATICS\\THESIS\\ANALYSIS\\R\\SNOWDEPTH")

allyears = read.table("doy145allyears.txt", header = TRUE)
allyears

regr.model = lm(snowdepth ~ ndvi,data=allyears)
regr.model
summary(regr.model)
```

LIST OF PUBLICATIONS

Institutionen för naturgeografi och ekosystemvetenskap, Lunds Universitet.

Student examensarbete (Seminarieuppsatser). Uppsatserna finns tillgängliga på institutionens geobibliotek, Sölvegatan 12, 223 62 LUND. Serien startade 1985. Hela listan och själva uppsatserna är även tillgängliga på LUP student papers (https://lup.lub.lu.se/student-papers/search/) och via Geobiblioteket (www.geobib.lu.se)

The student thesis reports are available at the Geo-Library, Department of Physical Geography and Ecosystem Science, University of Lund, Sölvegatan 12, S-223 62 Lund, Sweden. Report series started 1985. The complete list and electronic versions are also electronic available at the LUP student papers (https://lup.lub.lu.se/student-papers/search/) and through the Geo-library (www.geobib.lu.se)

335 Fei Lu (2015) Compute a Crowdedness Index on Historical GIS Data- A Case Study of Hög Parish, Sweden, 1812-1920
336 Lina Allesson (2015) Impact of photo-chemical processing of dissolved organic carbon on the bacterial respiratory quotient in aquatic ecosystems
337 Andreas Kiik (2015) Cartographic design of thematic polygons: a comparison using eye-movement metrics analysis
338 Iain Lednor (2015) Testing the robustness of the Plant Phenology Index to changes in temperature
339 Louise Bradshaw (2015) Submerged Landscapes - Locating Mesolithic settlements in Blekinge, Sweden
340 Elisabeth Maria Farrington (2015) The water crisis in Gaborone: Investigating the underlying factors resulting in the 'failure' of the Gaborone Dam, Botswana
341 Annie Forssblad (2015) Utvärdering av miljöersättning för odlingslandskapets värdefulla träd
342 Iris Behrens, Linn Gardell (2015) Water quality in Apac-, Mbale- & Lira district, Uganda - A field study evaluating problems and suitable solutions
343 Linnéa Larsson (2015) Analys av framtida översvämningsrisker i Malmö - En fallstudie av Castellums fastigheter
344 Ida Pettersson (2015) Comparing Ips Typographus and Dendroctonus ponderosas response to climate change with the use of phenology models
345 Frida Ulfves (2015) Classifying and Localizing Areas of Forest at Risk of Storm Damage in Kronoberg County

346 Alexander Nordström (2015) Förslag på dammar och skyddsområde med hjälp av GIS: En studie om löv- och klockgroda i Ystad kommun, Skåne

347 Samanah Seyedi-Shandiz (2015) Automatic Creation of Schematic Maps - A Case Study of the Railway Network at the Swedish Transport Administration

348 Johanna Andersson (2015) Heat Waves and their Impacts on Outdoor Workers – A Case Study in Northern and Eastern Uganda

349 Jimmie Carpman (2015) Spatially varying parameters in observed new particle formation events

350 Mihaela – Mariana Tudoran (2015) Occurrences of insect outbreaks in Sweden in relation to climatic parameters since 1850

351 Maria Gatzouras (2015) Assessment of trampling impact in Icelandic natural areas in experimental plots with focus on image analysis of digital photographs

352 Gustav Wallner (2015) Estimating and evaluating GPP in the Sahel using MSG/SEVIRI and MODIS satellite data

353 Luisa Teixeira (2015) Exploring the relationships between biodiversity and benthic habitat in the Primeiras and Segundas Protected Area, Mozambique

354 Iris Behrens & Linn Gardell (2015) Water quality in Apac-, Mbale- & Lira district, Uganda - A field study evaluating problems and suitable solutions

355 Viktoria Björklund (2015) Water quality in rivers affected by urbanization: A Case Study in Minas Gerais, Brazil

356 Tara Mellquist (2015) Hållbar dagvattenhantering i Stockholms stad - En riskhanteringsanalys med avseende på långsiktig hållbarhet av Stockholms stads
dagvattenhantering i urban miljö

357 Jenny Hansson (2015) Trafikrelaterade luftföroreningar vid förskolor – En studie om kvävedioxidhalter vid förskolor i Malmö

358 Laura Reinelt (2015) Modelling vegetation dynamics and carbon fluxes in a high Arctic mire

359 Emelie Linnéa Graham (2015) Atmospheric reactivity of cyclic ethers of relevance to biofuel combustion

360 Filippo Gualla (2015) Sun position and PV panels: a model to determine the best orientation

361 Joakim Lindberg (2015) Locating potential flood areas in an urban environment using remote sensing and GIS, case study Lund, Sweden

362 Georgios-Konstantinos Lagkas (2015) Analysis of NDVI variation and snowmelt around Zackenberg station, Greenland with comparison of ground data and remote sensing